开都河流域

Impact of Climate Variability on Hydrological Processes in the Kaidu River Basin (China)

Gonghuan Fang

UNIVERSITEIT GENT

Impact of climate variability on hydrological processes in the Kaidu River Basin (China)

Gonghuan FANG

Faculty of Sciences

Department of Geography

Impact of climate variability on hydrological processes in the Kaidu River Basin (China)

Dissertation submitted in accordance with the requirement for the degree of doctor of science: Geography

Gonghuan Fang (v)

(Joint PhD of Xinjiang Institute of Ecology and Geography, China, and Ghent University, Belgium)

Examination Board:

Prof. dr. M. De Dapper (chair)

Department of Geography, Ghent University

Prof. dr. J. Yang (promotor)

Xinjiang Institute of Ecology and Geography, Chinese Academy of Sciences

Prof. dr. Ph. De Maeyer (promotor)

Department of Geography, Ghent University

Prof. dr. B. Derudder

Department of Geography, Ghent University

Prof. dr. T. Liu

Xinjiang Institute of Ecology and Geography, Chinese Academy of Sciences

Prof. dr. A. Kurban

Xinjiang Institute of Ecology and Geography, Chinese Academy of Sciences

Prof. dr. X. Chen

Xinjiang Institute of Ecology and Geography, Chinese Academy of Sciences

Prof. dr. Y. Chen

Xinjiang Institute of Ecology and Geography, Chinese Academy of Sciences

Prof. dr. C. Zhang

Xinjiang Institute of Ecology and Geography, Chinese Academy of Sciences

Prof. dr. J. Ding

Xinjiang University, China

Table of contents

Table of contents I
List of Figures V
List of Tables IX
Preface XI
1 Introduction 1
1.1 Context 2
1.2 Climate model 3
1.2.1 GCM models 3
1.2.2 RCM models 4
1.3 Hydrological models 5
1.4 Impact of climate change on hydrological processes 6
1.4.1 Downscaling 7
1.4.2 Impact of climate change on hydrological processes 8
1.4.3 Uncertainties in the projection of future hydrological processes 8
1.4.4 Water resources related decision-making 9
1.5 Rationale and synopsis 10
1.5.1 Research objectives and questions 10
1.5.2 Outline of the dissertation 12
1.5.3 Out of scope 13
References 14
2 Future climatic change in the mountainous regions of Central Asia 19
2.1 Introduction 20
2.2 Study Area and Data 21
2.2.1 Study area and observed climate data 21
2.2.2 GCM simulation ensemble 22
2.3 BMA technique and its application on GCM simulation ensemble 24
2.3.1 Introduction of BMA technique 24
2.3.2 Application procedure 25
2.4 Results and Discussion 25
2.4.1 Performance of BMA technique 25
2.4.2 Future climate changes in MCA 29
2.4.3 Snowfall fraction 32
2.5 Conclusions 34

References....35
3 Hydrologic modeling in the Kaidu River Basin....39
3.1 Introduction....40
3.2 Hydrologic Model and Study Area....41
3.2.1 SWAT model....41
3.2.2 Study area and data collection....42
3.2.3 Model setup and initial parameter selection....44
3.3 Methodology....47
3.3.1 Sensitivity analysis....47
3.3.2 Model calibration and evaluation....49
3.4 Results and Discussion....50
3.4.1 Sensitivity analysis....50
3.4.2 Model calibration and evaluation....52
3.5 Conclusions....57
References....57
4 A comparison of bias correction methods in downscaling meteorological variables for hydrologic modelling in the Kaidu River Basin....61
4.1. Introduction....62
4.2 Study area and data....63
4.2.1 Study area and observed data....63
4.2.2 Simulated meteorological variables from the RCM....64
4.3 Methodology....64
4.3.1 Input sensitivity analysis....64
4.3.2 Bias correction methods....66
4.3.3 Performance evaluation....69
4.4 Results and discussion....71
4.4.1. Initial streamflow simulation driven with raw RCM simulations and sensitivity analysis....71
4.4.2 Evaluation of corrected precipitation and temperature....72
4.4.3 Evaluation of streamflow simulations....77
4.5 Conclusions....81
References....82
5 Impact of future climate change on hydrological processes in the Kaidu River Basin....87
5.1 Introduction....88
5.2 Study area and data....89
5.3 Methodology....89
5.3.1 Hydrologic model and uncertainty analysis method....89

5.3.2 Regional climate model....90
5.3.3 Bias correction methods....90
5.3.4 SCC data description and analysis procedures....90
5.4 Results and discussion....91
5.4.1 Validation of the hydrological model and the bias correction methods....91
5.4.2 RCM projected hydrometeorologic changes....93
5.4.3 Response of hydrological cycle to climate change....95
5.4.4 Sources of uncertainty and other considerations....99
5.5 Conclusions....100
References....100
6 General discussion....103
6.1 Summary and discussion on research questions....104
RQ1: How will the climate change in the 21st century for the mountainous regions of Central Asia?....105
RQ2: What are the major hydrologic processes and influential factors in hydrologic modeling in the Kaidu River Basin?....106
RQ3: How can we effectively downscale the climatic projections from climate models and apply them to the hydrological modeling?....107
RQ4: How will the hydrological processeses change in the 21st century in the Kaidu River Basin?....109
6.2 Critical reflection....110
6.3 Some recommendations for future work....111
6.3.1 Future work on climate change detection....111
6.3.2 Future work on hydrological modeling....111
6.3.3 Future work on impact evaluation and uncertainty analysis....111
References....112
7 General conclusion....115
Summary....117
Samenvatting (Dutch Summary)....121
摘要 (Chinese summary)....125
Curriculum Vitae (Bibliography)....129

List of Figures

Figure 1. 1 Dissertation outline 13
Figure 2.1 Topographic map of the mountainous region of Central Asia with the study area marked in red polygons: Tarim river basin, northern Tianshan basin, Ili river basin, Issyk_Kul basin, Syr Darya basin and Amu Darya basin. 21
Figure 2.2 Observation (a), mean of GCM simulation ensemble (b) and BMA mean of GCM simulation ensemble (c) for mean annual temperature, precipitation and snowfall during 1976~2005 28
Figure 2.3 Spatial biases between observation and BMA mean of GCM simulation ensemble with histograms for mean annual temperature (a), precipitation (b) and snowfall (c), and mean seasonal snowfall (d: Autumn; e: Winter; f: Spring) during 1976~2005. 28
Figure 2.4 Spatial distribution of temperature (a), precipitation (b), and snowfall (c) for their mean annual values during 2070~2099 (a1, b1, c1), their absolute changes compared to 1976-2005 (a2, b2, c2), annual change rates from 1976 to 2099 (a3, b3, c3), and their consistencies (a4, b4, c4) based on RCP8.5. Consistency is defined as the percentage of GCMs with change rate greater than 0.037 ℃/a (i.e. global warming rate under RCP8.5) for temperature, and positive change rates for precipitation and snowfall. 30
Figure 2.5 Changes of mean seasonal snowfalls during 2070-2099 compared to 1976-2005 under RCP8.5 (left: autumn; middle: winter; right: spring). 31
Figure 2.6 Future climatic change during 2070~2099 compared to 1976~2005 with RCP4.5 and RCP8.5, for six sub-regions and the Mountain region of Central Asia (MCA). Top: absolute temperature change (℃), relative precipitation change (%), and relative snowfall change (%). Bottom: variation of snowfall fraction. 31
Figure 2.7 Sensitivity distribution of relative snowfall change (δS) to absolute temperature change (ΔT); Spatial distribution of δS/δP for annual, autumn, winter and spring, respectively. 33
Figure 3.1 The location, topography and river system of the Kaidu River Basin 40
Figure 3.2 Hydrologic flow chart of SWAT. Boxes represent different hydrological processes, ellipses different water storages and arrows water flow directions (Adapted from Arnold et al. 1998) 42
Figure 3.3 The spatial distribution of soil (top) and landuse (bottom) in the Kaidu River Basin 44
Figure 3.4 Factor sensitivity based on the Morris method (diamond denotes extremely sensitive, triangle medially sensitive, and closed circle insensitive) 51
Figure 3.5 Observed and simulated outflow series at the Dashankou hydrological station

during the calibration period (a – daily streamflow) and the validation period (b and c - daily streamflow and d – monthly streamflow).....54
Figure 3.6 Topographical distribution of annual mean precipitation for simulations with lapse rates (a) and without lapse rates (b) 56
Figure 4.1 Flow chart of comparison procedure 64
Figure 4.2 Mean annual hydrographs of observed streamflow (obs) and simulated streamflow using observed meteorological data (default) during the period of 1986 ~ 2001 at the Dashankou Station. The simulated streamflow using raw RCM-simulated meteorological data after recalibration (raw_recali) is also plotted. The NS values are for the daily continuous data and not for the mean hydrograph. 72
Figure 4.3 Exceedance probabilities of the observed (obs), raw, and bias-corrected precipitation (top) and temperature (bottom) at the Bayanbulak Station. 75
Figure 4.4 Daily mean precipitation and temperature of observed (obs), raw RCM-simulated (raw), and bias-corrected values at Bayanbulak Station, which were smoothed with the 7-day moving average method. The precipitation and temperature during May-August is amplified to inspect the performance of each correction method. 75
Figure 4.5 Box plots of observed (obs) and simulated daily streamflows using observed (default), raw RCM-simulated (raw) and corrected meteorological data (setup of simulations 1-15 are listed in Table 4.3). The mean values are shown with diamonds...78
Figure 4. 6 Exceedance probability curves of observed (obs) and simulated streamflow driven by observed (default), and bias-corrected meteorological data (numbers from 4 to 15; see Table 4.3 for detailed setup of these simulations). 78
Figure 4.7 Monthly mean streamflow (top) and exceedance probability curves of annual 7-day peak flow (middle) and annual 7-day low flow (bottom) during 1986 ~ 2001 in the Kaidu River Basin (obs: observed streamflow; default: simulated with observed meteorological data; raw: simulated with RCM-simulated meteorological data; 1-15: simulated with corrected RCM meteorological data listed in Table 3). 80
Figure 5.1 Time series of daily observed streamflows (dots) and simulated streamflows forced by observed meteorological data (blue line) for calibration period (1986 – 1989) and validation period (1990 – 2005) with 95% prediction uncertainty bands (blue shaded area). 92
Figure 5.2 Summary of future climate inputs (P and T) and simulated hydrologic components (Q, R_s, R_{ss} and ET) under RCP4.5 and RCP8.5, compared to their values in the control period (1986~2005). All these hydrometeorologic factors are presented in terms of wet season, dry season and annual values.....94
Figure 5.3 Response surfaces of streamflow (Q), surface runoff (R_s), subsurface runoff (R_{ss}) and evapotranspiration (ET) to climate change. The simulations with RCM outputs for 2020 ~ 2039 under RCP4.5 and for 2080 ~ 2099 under RCP8.5 (their corresponding

meteorological changes are listed in Table 3) are indicated using blue and red stars with labels. 96

Figure 5.4 Exceedance probability curves of average annual streamflow (Q) in response to temperature change and precipitation change based on SCC with each plot either with fixed precipitation change (a ~ d) and fixed temperature change (e ~ h). Dotted blue line in each plot denotes exceedance probability curves of average annual streamflow for the simulation with RCM outputs given fixed δP and ΔT as summarized in Table 5.3....98

Figure 5.5 De Finetti diagram (ternary plot) of evapotranspiration (ET), surface runoff (R_s) and subsurface runoff (R_{ss}) for SCC (shown as dots) and RCM outputs (shown as stars, details of the projected changes in RCM outputs can refer to Table 5.3).....99

List of Tables

Table 2. 1 Information about the GCM models used in this study 23
Table 2. 2 Performances of BMA technique and GCM simulation ensemble for T, P and snowfall 27
Table 3.1 Proportions of the soil types (left) and the landuse types (right) in the watershed 43
Table 3.2 Selected factors and their initial values and ranges for sensitivity analysis, and their estimated values 46
Table 3.3 The main effect (S_i), quasi-total effect (S_{Di}) and the first-order interaction (S_{ij}, the triangular matrix on the right) of factors as percentage based on the SDP method. The values are given with only one decimal place. 52
Table 3.4 Model performances for the calibration and validation periods 55
Table 4.1 Sensitivity indices of the five meteorological variables based on the Sobol' method 66
Table 4.2 Bias correction methods for RCM-simulated precipitation and temperature. 66
Table 4.3 Performances of simulated streamflows driven by raw RCM-simulated (raw) and 15 combinations of bias-corrected precipitation and temperature data (denoted as numbers from 1 to 15) compared to the simulation driven by observed climate (default) during the period 1986 ~ 2001. For simulations 1-15, solar radiation is corrected with the LS method. 70
Table 4.4 Frequency-based statistics of daily observed (obs), raw RCM-simulated (raw) and bias-corrected precipitations at the Bayanbulak Station 73
Table 4.5 Frequency-based statistics (unit: ℃) of daily observed (obs), raw RCM-simulated (raw) and bias-corrected maximum temperatures at the Bayanbulak Station 74
Table 4.6 Time-series-based metrics of bias-corrected precipitation and temperature calculated on a monthly scale at the Bayanbulak Station 77
Table 5.1 Classification of magnitude for climatic and hydrological changes. δ and Δ represent relative change and absolute change. 91
Table 5.2 Statistics of bias-corrected RCM outputs and SWAT simulated streamflows forced by the observed climate variables and bias-corrected RCM outputs 92
Table 5.3 RCM projected precipitation change (δP), temperature change (ΔT) and streamflow change (δQ) for the 21st century under RCP4.5 and RCP8.5 compared to the control period (1986~2005) 93
Table 6.1 Overview of the main methodology and the results of each chapter 104

Preface

Since I was a kid, I had made my mind to pursue a PhD research. I followed my dream through primary school, middle school and university. And today, I am doing the final steps to obtain this degree. This road is filled with ups and downs, challenges and opportunities, stressful and wonderful moments. I have learned so much during this process, not only the subject of my PhD, but also concerning the world and people around me. This knowledge is valuable, and will help me a lot in future endeavors. Along the pursuing of my PhD, I have met so many interesting people, who have inspired me, supported me, guided me and provided me with much joy and happiness in life. It will be impossible to mention them all here, nevertheless, I would like to mention a handful of them who have contributed to my PhD study and this dissertation.

First of all, I would like to thank my supervisor, Prof. Philippe de Meayer! As a joint PhD, it really surprised me when Philippe agreed to accept me as a student in Ggent University. He gave me the opportunity to presume the doctorate degree in Ugent, supervised me along my study and dissertation and gave me the faith and support. Thank you for your wisdom, kindness, magnanimous, warm and tireless assistance.

Greatest thanks go to my co-promoter, Prof. Jing Yang! Since the first year of my PhD study, Jing has been there for me. He is the one, who guides me really into research and tells me how research works are done. When I need help, knowledge, or just some supports, I know I could rely on him. He is the one leading me into the PhD research, he is the one allowing me and supporting me to go abroad, he is the one tirelessly guiding me and improving all drafts of my papers, he is also the one inspiring me to bring great passion into my work and research. How many times I went into obstacles and was depressed, he shed light on my research and discussed new methods and thoughts. Thank you a lot!

Many thanks go to my co-promoter, Yaning Chen! Thank you for the generous supports and enlightening advices he provided me from time to time, which actually enhanced my work and illuminated on some wider aspects of research. He always encourages me, gives me faith and exorcises fears.

Another important professor, Alishir Kuban, should be mentioned in special. He created the opportunity for me to study in Ugent, and told me a lot things that really helpful in my future academic life. He is always so patient, helpful and generous in helping me with all those paper work.

I am also very grateful to department’s secretary, Helga Vermeulen for doing all the paper work for me. Warm thanks go to Therese Ongena and Karine Van Acker, for caring me, helping

me and being so kind to me. Special thanks goes to Sabine Cnudde, who kindlessly helped me edit and correct the language for several drafts of my papers and dissertation. I am in debt to Kristien Ooms and Michiel Van den Berghe for their kind help concerning course selecting and software learning. I am also very grateful that I have so many open minded and enthusiastic colleagues, who create a nice and exciting atmosphere to work in. It is not possible to name them all, but some of them deserve a special treatment because of their huge support during the past years. In particularly, I would like to thank Long, Berdien, Pepijn, Annelies, Bart, Alex, Pengdong, Koos, Britt, Soetkin, Rasha, Ann, Kavin for their kindness and care. I would like to give my eternal thanks to Miao and Jiao, with whom I spend most time and shared my sorrows and happiness.

I would like to express my gratitude to a lot of people at Xinjiang Institute of Ecology and Geography. Thanks for your accompany and help. I must express my thanks to Zhi, Shuhua and Haijun for their sparkling ideas and solutions. Best wishes to all the colleagues that have accompanied and helped me during me pursue of doctoral degree.

Special gratitude goes to my family - my parents, grandparents, sister, brother-in-law and my niece and nephew. You always brought me so much faith though I am at the other side of the world. Thank you for caring me and giving me the most immense love. Finally, my eternal thanks go to my boyfriend Yuhui for your amazing love, support and patience.

Thank you!

Gonghuan

23 Feb, 2016

1 Introduction

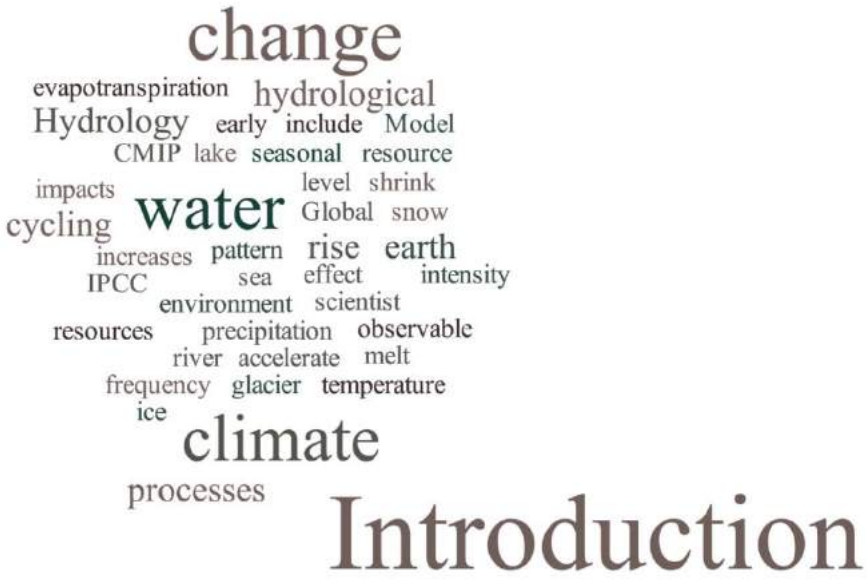

Over the last decades, climate change impact study has become the focus for governments and scientists. This dissertation studies climate change impact on the hydrological processes in the Kaidu River Basin.

This chapter introduces the concept of normally used models, methods and the research progresses. As an important part of introduction, this chapter gives the research questions and outline of this dissertation.

1.1 Context

Global climate change has already exerted observable effects on the environment. It has already begun to transform life on earth. Around the globe, temperature is climbing and the sea level is rising, glaciers are shrinking, ice on rivers and lakes is breaking up earlier and trees are flowering sooner, hydrological processes are changing.

The social, economic and ecological problems caused by climate change have been highly concerned by the scientific community, the public and government. The United Nations Intergovernmental Panel on Climate Change (IPCC) Fifth Assessment Report (AR5) uses the Coupled Model Intercomparison Project Phase 5 (CMIP5) to forecast future climate change. They stated that over all land and ocean surfaces, average temperature have warmed roughly 1.53 ℉ (0.85 ℃) from 1880 to 2012 and the temperature will continually rise with the global average surface temperature rising 0.3 ~ 4.8 ℃ at the end of the 21st century. The impact of climate change on the earth system will continue. In the 21st century, extreme heat waves will increase further, extremely cold events will reduce, the intensity and frequency of heavy precipitation in mid-latitude land areas and humid tropical regions may augment. Climate change could exert pressures on water system (Christierson et al., 2012), agriculture (Rosenzweig et al., 2014), forestry (Hanewinkel et al., 2013), ecological balance (Bellard et al., 2012), human health (Martens, 2014) and other aspects.

Changes in the hydrological cycling due to climate change have become one of the hottest topics and issues which has been widely concerned by scholars and scientists (Milly, 2007; Vorosmarty et al., 2000). Particularly, the World Meteorological Organization (WMO), the United Nations Educational Scientific and Cultural Organization (UNESCO), the United Nations Environment Programme (UNEP), the United Nations Development Programme (UNDP) and the International Association of Hydrological Sciences (IAHS) etc., have implemented a series of international cooperation projects or research projects working on climate change and water resources. These programmes include the IPCC, the World Climate Research Programme (WCRP), the International Geosphere-Biosphere Programme (IGBP), the International Hydrological Programme (IHP) and Global Water System Project (GWSP) and so on. These organizations intend to investigate the climate change induced environmental problems concerning to water cycling and water resources at different scales (e.g., global, regional and watershed scale). By analyzing the hydrologic mechanism and water resources under the context of climate change, they systematically evaluate the driving forces of the changes and their contributions. These works contribute greatly to the water resources planning and management, disaster prevention and mitigation for policy-makers to ensure the sustainable development

economically, socially and ecologically.

The impacts of climate change on water resources include changes in intensity and frequency of precipitation, accelerated snow melting and increased evapotranspiration (ET) caused by raised temperature. Climate change leads to changes in hydrological processes and affects the hydrological components, e.g. the IPCC (2013) stated that global glaciers and spring snow cover in the north hemisphere have already decreased 15%-85% and 7%-15% in area, which could definitely lead to the re-distribution of water resources spatially and temporarily. Climate change does not only result in changes in hydrological processes and water recharge to rivers but also in water demand. For instance, as global warming, the crop water requirement has also increased. In short, the impact of climate change on water resources is profound and has great significance, therefore how to effectively interpret future changes in hydrologic regime has become a hot issue.

Arid regions with a fragile ecological system and a weak stability are sensitive to climate change. Water means life for human and the ecosystem here. Hydrological processes in arid zones are sensitive to climate change. Central Asia is an arid, politically sensitive and water-scarce region, whose water resources are strongly influenced by climate change. The mountainous regions, providing water for the oasis, are suffering from precipitation and temperature change and snow/glacier retreat. The Kaidu River Basin, one of the most important rivers on the southern slope of the Tianshan Mountains, is considered as the typical watershed to study the climate change impact on hydrological processes.

1.2 Climate model

The climate system is a complex system to grasp with a series of equations that explain the interactions between atmosphere, ocean and land. With the development of computer techniques, the scientists were able to model the global climate and simulate the interactions of important drivers of climate, including atmosphere, oceans, land surface and ice to understand current climate and to forecast future climate change.

The climate model could be divided into two categories according to their spatial resolution and range: the General Circulation Models (GCM) and the Regional Climate Model (RCM).

1.2.1 GCM models

The physical basis of GCM is to establish the equations to explain the climate system. GCM research began in 1955 and to the 1970s, theoretical and numerical techniques have basically developed (Edwards, 2000). For the past 20 years, the world's meteorologists have made a lot of progress in dynamic framework including the application of the semi-Lagrangian method, incorporation of reference atmosphere, construction of energy balance and improvement of the

land surface model (Dai et al., 2003) and also the computing technique. After continuous development, GCMs have been seen as the main tool in studying complex interactions between atmosphere, oceans and land *(Edwards, 2010).*

GCM is normally used in big regions to predict climate change. For example, IPCC5 uses the GCM simulation ensemble in CMIP5 to give the climate change basis in the future. However, the GCMs with a low spatial resolution, which normally vary between *100~300 km (http://cmip-pcmdi.llnl.gov/cmip5/) cannot capture the regional circulation. For example, the GCMs fail to capture the complex terrain, surface situation and some physical processes for the mountainous areas. This d*eficit could be fatal in the application of GCMs to model the region-scale or basin-scale climate. In the mountainous regions, the GCM could have great bias since the meteorological data is scarce and the atmospheric circulation is greatly uncertain in complex mountainous regions. The previous studies indicated several GCMs simulated fake precipitation for Mid-west China (Gao et al., 2013).

1.2.2 RCM models

To combat the low resolution of GCMs, RCM has been developed due to its high spatial resolution and better picture of the topography. RCMs incorporate more physical processes and could better simulate the climate characteristics for a special terrain with complex geomorphology.

Currently, the RCMs have achieved great development. Several regional-scale programmes have been established in order to meet the increasing demand for finer spatio-temporal resolution climate datasets. For example, the Ensembles-Based Predictions of Climate Changes and Their Impacts (ENSEMBLES) project (http://ensembles-eu.metoffice.com/index.html), Prediction of regional scenarios and uncertainties for defining European climate change risks and effects (PRUDENCE) project (http: // www. dmi.dk/fou/klima/prudence/index.html), Modeling Impacts of Climate Extremes (MICE, http: // www.cru.uea.ac.uk/cru/projects/mice/), Statistical and Regional dynamic Downscaling of Extremes for European regions (STARDEX, http: //www.cru uea.ac.uk/cru/projects/stardex/), the Coordinated Regional Climate Downscaling Experiment (CORDEX) (Giorgi et al., 2009) and the North American Regional Climate Change Assessment Programme (NARCCAP) (Mearns et al., 2013) are some typical projects working on the regional climate change impact and uncertainty quantification. With the development of RCMs, scientists are using RCMs such as RegCM, PRECIS and the regional environmental integrated simulation system (RIEMS) driven by the reanalysis or GCM to investigate the future climate change as well as to evaluate the impact of climate change. Further, the global change SysTem for Analysis, Research and Training (START, http://start.org/) together with a modeling framework Regional Integrated Environmental Modeling System (RIEMS), was developed (Fu et al., 2005). However,

the RCM also have considerable biases for some region, which can be attributed to the incomplete description of topography, forcing technique and parameterizing of land surface together with scarce observation data (Salzmann & Mearns, 2012). Therefore, when evaluating climate change or its impact on water resources, it should always be used with caution.

RCMs are also deemed to be a dynamical downscaling of GCMs, which will be introduced in Section 1.4.1.

1.3 Hydrological models

In order to better understand the hydrological processes of natural law and to serve hydrological practices and management, hydrological models have emerged and have been applied in practice widely. The hydrological model is a simplification of complex hydrological phenomena and is an important tool to study the hydrological processes. Hydrological models generally cover several submodels, such as soil-moisture migration models, overland flow, precipitation model (e.g. quantification of precipitation, the calculation of surface precipitation, et al.), evapotranspiration models, groundwater models (the deterministic model is mainly based on the mathematical model like Darcy's law and continuity equation calculated using the finite difference method and finite element method) (Z. Xu, 2009).

The hydrological models can be divided into three categories according to their structures. The first category is the black-box model, which uses the statistical relation to explain the hydrological processes, therefore the physical meaning is missing. This kind of models includes Markov chains, wavelet cycle analysis, regression based on least squares, fuzzy mathematics and artificial neural networks. The second category is the conceptual hydrological model, which uses a generalized equation to represent the hydrological processes. It has a physical basis to some extent and is also based on empirical statistics. The typical conceptual models include the water balance model, Xin'anjiang model, Sacramento model, Tank model, HBV.

The third category is distributed hydrological models, which generally have a strict physical foundation and parameters are distributed. The establishment and application of distributed hydrological models requires accurate design and estimation of model parameters. Distributed hydrological models could be used for simulation and forecast in no-data watersheds. Distributed watershed models are increasingly being employed to support decisions regarding alternative management strategies in the areas of land use change, climate change, water allocation and pollution control (J. Yang et al., 2008). Compared to other kinds of hydrological models, distributed hydrological models represent the spatial variability and also preserve the nonlinear characteristics of hydrological processes within watersheds. Several advantages of distributed hydrological models could be summarized: 1) it is more accurate and effective in describing the mechanism of hydrological processes; 2) it is easy to combine with the geographic information

and Remote Sensing data; 3) hydrological models can be coupled with climate models to evaluate the climate change induced hydrologic response change; 4) it is easy to simulate the response of hydrological processes to changes of an underlying surface (land use/cover change) ; 5) since most of the distributed models are based on grids or sub-basins, the spatial variation of the hydrolgical variables could be analyzed clearly and it is capable of expressing the spatial surface heterogeneity. The widely used distributed models include the Variable Infiltration Capacity (VIC) model, MIKE -SHE model and Soil and Water Assessment Tool (SWAT), etc.

The SWAT model is a distributed, basin-scale, open-source hydrological model developed by the USDA Research Center (USDA-ARS) (Arnold et al., 1998). Hydrological modules incorporated in SWAT include the surface runoff, infiltration, underground runoff, return flow, evapotranspiration, snow melting. The SWAT model is widely used in many hydrological problems concerning the hydrologic processes and mass change, such as evaluation of water resources, runoff forecasts (including the flow, hydrodynamic, soil water, snow melting and water resource management, etc.), water quality assessment (land use and land management effect on water quality, agriculture, development of best management practices in agriculture, etc.) and climate change impact studies.

The SWAT model has been widely used around the world for different landscape and climate conditions. SWAT is an open source model, thus scientists were able to alter the code so as to make the model suitable to their unique basins. The SWAT model has been successfully used in humid areas, arid and hemi-arid regions and also in snow cover areas, forest dominated regions and grassland dominated regions. For the central Asia, the SWAT model also shows some applications. Shi et al. (Shi et al., 2011) simulated daily streamflow and SWAT outperformed the Xin'anjiang model in flood forecasting. Recently, Luo et al. (2013) improved the glacier melting module to better simulate the hydrological processes for glacier dominated regions.

In summary, the SWAT model has been widely used for various landscapes and morphological units effectively. However, it is mostly applied to watersheds with a good vegetation cover and enough measured data. The use of SWAT in arid and semi-arid regions with scarce data (meteorological, hydrological, hydraulic data) is relatively challenging. Since the SWAT model is an open source model and has a physical basis expressing the hydrological process, it is selected to model the hydrological processes in the Kaidu River Basin.

1.4 Impact of climate change on hydrological processes

Normally, there are two ways to predict future changes of hydrological processes and water resources in the context of climate change. The first one is based on the statistical relations between climatic and hydrological variables using a regression analysis, wavelet cycle analysis,

neural network model et al. (Xu et al., 2008). This kind of methods does not have a physical basis and is often used in short term forecasts. The other one couples future climate change information and the hydrological model to predict the future hydrologic regime. It could also be divided in two categories based on how to generate future climate: the hypothetical changes in precipitation and temperature and the GCM or RCM predicted climate change. The hypothetical climate change scenarios generally set a range of temperature and precipitation changes, such as assuming that the future temperature will increase 0, 1, 2, 3, 4, 5 ℃ and precipitation will change ±5%, ±10%, ±20%. These scenarios are set to explore the responses and sensitivities of the hydrological system to climate change but it fails to effectively predict hydrological extremes and seasonal changes. The GCM or RCM climate change scenarios incorporate the CO_2 emission scenarios, economic growth and are based on physical processes. However, the GCM/RCM simulated climate normally has considerable biases, especially in precipitation (e.g., wet day probability, precipitation extremes) and sometimes, it is not suitable for watershed-scale modeling, due to its low spatial resolution. The following chapters will discuss in detail the problems in downscaling climate models, bias correction and uncertainties associated with the hydrological predictions.

1.4.1 Downscaling

Predicting the future responses of hydrological processes to climate change based on one-way coupling of the climate model and hydrological model is challenging due to the low spatial resolution of GCM (horizontal resolution of most GCMs used in CMIP5 is 100 km ~ 300 km), while high resolution of the hydrological model (e.g. the large and medium-scale hydrological model SWAT covers tens of thousands of km^2, covering only a few grids). And it is unreasonable to force the hydrological model with the outputs of the low resolution climate models directly. Therefore, to fill this gap, different types of downscaling methods have been developed.

Downscaling techniques mainly include two categories: dynamic downscaling and statistical downscaling. Dynamic downscaling, namely the use of a high-resolution regional climate model (RCM) nested in GCM to project the details of future climate change for different topographical conditions. Dynamic downscaling has a physical basis to imitate climate extremes and is proved to have significant improvement compared to its corresponding GCMs (Christensen & Lettenmaier, 2007). However, its drawback is also obvious, e.g. it requires a lot of computing and is time-consuming. Main idea of statistical downscaling is to subgrid the coarse output from the low resolution GCM statistically. Statistical downscaling uses long term observational data to establish the relationship between large-scale climate variables (mainly atmospheric circulation factors) and regional scale meteorological variables, and it then applies this relationship in future GCM outputs to forecast future regional, fine resolution climate. Some advantage of statistical downscaling can

be summarized: it can provide detailed climate information and has removed the biases in GCMs, it does not consider the boundary conditions and requires a relatively small amount of calculation, which can be applied easily. Its drawback is it needs enough observations to build the statistical model and the instinct relationships among the meteorological variables are missing.

Statistical downscaling has been used to simulate the regional climate and to predict future changes (Fowler et al., 2007). Normally, statistical downscaling of temperature is better than that of precipitation because precipitation is more influenced by the local climate and topography and as a result resulted in a lower rainfall prediction accuracy (Wilby & Wigley, 2000). For a more detailed review, please refer to (Wilby et al., 2004; Wilby et al., 1998).

1.4.2 Impact of climate change on hydrological processes

Climate changes lead to changes in hydrological processes. Scientists generally believe that higher temperature accelerates the hydrologic cycle, leading to more precipitation and evaporation and that it consequently resulted in severe droughts and heavy rains in some areas (Mango, 2010). In recent decades, many studies have been carried out focusing on the effect of climate change on hydrological processes.

Concerning evaporation, assuming that other meteorological conditions stay stable, a rising temperature will lead to an increased potential evaporation according to the Penman-Monteith method (Monteith, 1965) but it is difficult to calculate the actual evaporation since it is also heavily affected by other factors, e.g. available water. For the runoff, it is the main variable in the evaluation of the impact of climate change on water resources, droughts and floods. Bultot et al. (Bultot et al., 1988) suggested that global warming and increased winter rainfall significantly augmented the runoff, which also increases the frequency of winter flooding. (Chiew & McMahon, 1994) investigated the climate change impact on hydrological processes of 28 representative catchments in Australia and concluded that changes in precipitation could amplify the changes in runoff, particularly in the arid basins. In wet and temperate regions, the runoff percentage change exceeds about 2 times of precipitation amount, while in arid areas it could be more than 5 times. (Kwadijk & Rotmans, 1995) suggested that the Rhine River might shift from a mixed snowmelt-rainfall to a rainfall dominated regime. Regarding soil moisture, it affects the actual evaporation and runoff generation. In the climate change context, soil moisture change has also gained attention (Seneviratne et al., 2010).

1.4.3 Uncertainties in the projection of future hydrological processes

In the prediction of the climate change impact on hydrological processes and water resources,

the sources of uncertainties are multiple, such as atmospheric circulation patterns, greenhouse gas emission scenarios, downscaling methods, hydrological modeling, which includes uncertainties that originated from model input, model parameter and structure. (H. Xu et al., 2011) assessed the runoff uncertainty of the Xiangxi and Huangfuchuan river while using seven GCM models from CMIP3. Yang et al. (2008) compared the advantages and disadvantages of five widely used uncertainty methods. Recently, many studies focused on the quantification of uncertainty sources in hydrological modeling and prediction. Buytaert et al. (2010) indicated that GCMs account for the biggest part of uncertainty (50.8%), based on the exceedance curves when he managed to discuss the impact of forecast uncertainty on decision making. Paton et al. (2013) studied uncertainty sources from GCMs, emissions scenarios, downscaling methods, hydrological model, water supply, water demand and concluded that the water demand demonstrates the greatest uncertainty, while the emission scenario shows the least uncertainty. Chen et al. (2011) evaluated uncertainty sources in the coupled model of GCM and the hydrological model, including uncertainties from GCMs, downscaling methods and the hydrological models. And they pointed out that uncertainty in GCMs forms an important source of uncertainty, while parameter uncertainty in the hydrological model is minimal and the quantity of uncertainties is closely related to the objective function. Bosshard et al. (2013) applied a variance decomposition method to assess the uncertainties in GCMs, downscaling methods, hydrological models and their interactions.

As the Bayesian theory is getting mature, scientists are trying to apply the Bayesian method in analyzing uncertainties in hydrological modeling. Steinschneider et al. (2012) quantitatively investigated the uncertainties in runoff prediction using Bayesian methods. Gain et al. (2011) proposed a weighted averaging method to deal with the uncertainties in the GCM simulation ensemble predicted a future extreme low and extreme high runoff. Yang et al. (2007) improved the Bayesian uncertainty analysis by replacing the normal distribution of innovations by a Student *t* distribution. Bayesian model averaging technique has also been used to incorporate competing information of climate forecast and hydrological modeling in recent years (Duan et al., 2007; Fraley et al., 2010; Sloughter et al., 2007).

1.4.4 Water resources related decision-making

Climate change leads to changes in hydrologic regime and has a tremendous effect on human life. Ficklin et al. (2013) used the GCM simulation ensemble to predict the future climatic and hydrologic change in the Colorado River and they concluded that the spring runoff would decrease 36%, ranging between -100% to + 68%, summer runoff reduces 46% ranging from -100% to +22%. With a constant warming, which greatly increases the evapotranspiration (about 23%), the

Colorado River Basin is transferring from a semi-humid to an arid watershed. Jung & Chang (2011) predicted hydrological changes in Oregon's Willamette River and results showed that spring and summer runoff reduce, autumn and winter runoff increase and snow water equivalent reduces substantially. Setegn et al. (2011) predicted the impact of future climate change on the hydrological processes of Lake Tana, the results show that four of the nine GCMs used projected a significant decline in the annual streamflow in 2080–2100 but the direction of water balance changes are not determined due to great uncertainty.

Hydrological extremes normally have a much bigger effect on human society compared to the mean climatic change. Beauchamp et al. (2013) evaluated changes of the probable maximum precipitation and the probable maximum flood in the context of future climate change. They found that extreme precipitation intensity could increase 0.5–6% by the 2071–2100 horizon for Manic-5 River Basin in Canada, while the flood extremes show no significant increase or decrease. Taye et al. (2011) predicted the impacts of climate change on hydrological extremes for the Nile River Basin based on 17 GCM models under 2 emission scenarios for several small watersheds and results indicated that the average and extreme runoff of the Nyando River located at sub-humid climatic zones has a significant increase, while the runoff of the Lake Tana Basin in the tropical plateau monsoon climate shows no significant change for neither average state and extreme state.

In addition, not only for the hydrologic cycle, scientists have also investigated changes of available water, water supply and demand in the future. Koutroulis et al. (2013) modeled water availability using GCM as well as RCM under B1 emission scenarios and pointed out that, a reduced amount of water availability could meet the basic demand assuming that the future water demand is maintained at the current level, which means that the future water conservancy will improve significantly. Chenoweth et al. (2011) evaluated the climate change impact on water resources for the Mediterranean and the Middle East region and results show that half of the water needs to be desalinated or brought in under the form of virtual water for the mid-21st century, assuming that the water footprint is growing at the same speed as the population growth.

In conclusion, the prediction of future hydrological processes and water resources can provide a reference for policymakers so as to develop a more rational water management program and to create a scientific basis for climate change scenarios in the development of "no regrets" and "best" management practices.

1.5 Rationale and synopsis

1.5.1 Research objectives and questions

Over the past few decades, global climate change has already exerted influence on the

hydrological processes. The central Asia region is one of the most arid regions in the world and is a politically complicated region. The special feature of this region can be summarized as follows: the water mainly comes from the mountainous region while the plain (i.e. oasis) cannot generate water due to the small amount of precipitation while large potential evaporation. Therefore, understanding the future climate change and the associated changes in hydrologic processes are important for policy-making concerning hydrological project planning, agricultural structure adjustment and even industrial distribution strategy.

From this general research objective, 4 specific research questions (RQ) were designed to specifically account for the hydrological changes in this area and their related uncertainties.

- **RQ1: How will the climate change in the 21st century for the mountainous regions of Central Asia?**

  Climate changes in the mountainous regions are essential for the change in hydrologic regime in mountainous regions of Central Asia. How will temperature, precipitation and snowfall temporally and spatially change in the 21st century? We used the GCM simulation ensembles to predict climate change in this region. Since different GCMs normally give different climate predictions, it is important to take all these GCM simulations into account when providing future climate projection. To achieve this goal, this dissertation applied the Bayesian model averaging method in order to combine the predictions of these GCMs effectively.

- **RQ2: What are the major hydrologic processes and influential factors in hydrologic modeling in the Kaidu River Basin?**

  The hydrological processes in the mountainous regions of Central Asia are unclear, partly due to the scarce data. In this research question, we aim to establish a distributed hydrological model SWAT to simulate the hydrological processes in the Kaidu River Basin. To better understand important hydrological processes and influential factors, a combined sensitivity analysis method was proposed to screen out the unimportant processes and study different contributions.

- **RQ3: How can we effectively downscale the climatic projections from climate models and apply them to the hydrological modeling?**

  The climate model normally has a very low spatial resolution while the hydrological models normally need a high spatial resolution, which accounts for the mismatch of the climate model and the hydrological model. Given the scarce observation data, it is a challenge to downscale the outputs of climate models to a finer resolution. In this research, we compared the performance of 5 widely used precipitation bias correction methods and 3 temperature bias correction methods for downscaling climate models. The downscaling and

comparing strategy and some results can be applied to other areas and models.

- **RQ4: How will the hydrological processes change in the 21st century in the Kaidu River Basin?**

  The future changes of hydrological processes greatly depend on climate changes. After downscaling the future climate simulation from RegCM, we used two strategies to account for future climate to analyze the response of hydrological processes to climate change and predict future changes in the hydrologic processes.

RQ1 investigates the climate change context of mountainous regions of Central Asia. RQ2 provides the basis for the hydrological analysis and is essential in understanding the local hydrologic mechanism. RQ3 studies how to effectively downscale the outputs of climate model and apply them to hydrological models. RQ4 actually depends on RQ1, RQ2 and RQ3, and is somewhat a practical problem solving research and could provide a scientific basis for decision making.

1.5.2 Outline of the dissertation

The above mentioned research questions are discussed and analyzed in the following part of the dissertation. With the formulation of the above research questions, all chapters are connected in a framework which aims to solve the final problem. Figure 1.1 illustrates the structure of this dissertation and the link between them. Note that the chapter design is corresponding to the research questions and that each chapter aims to solve one research question. Chapters 2 through 5 correspond to papers which are published or prepared for publication in international peer-reviewed journals.

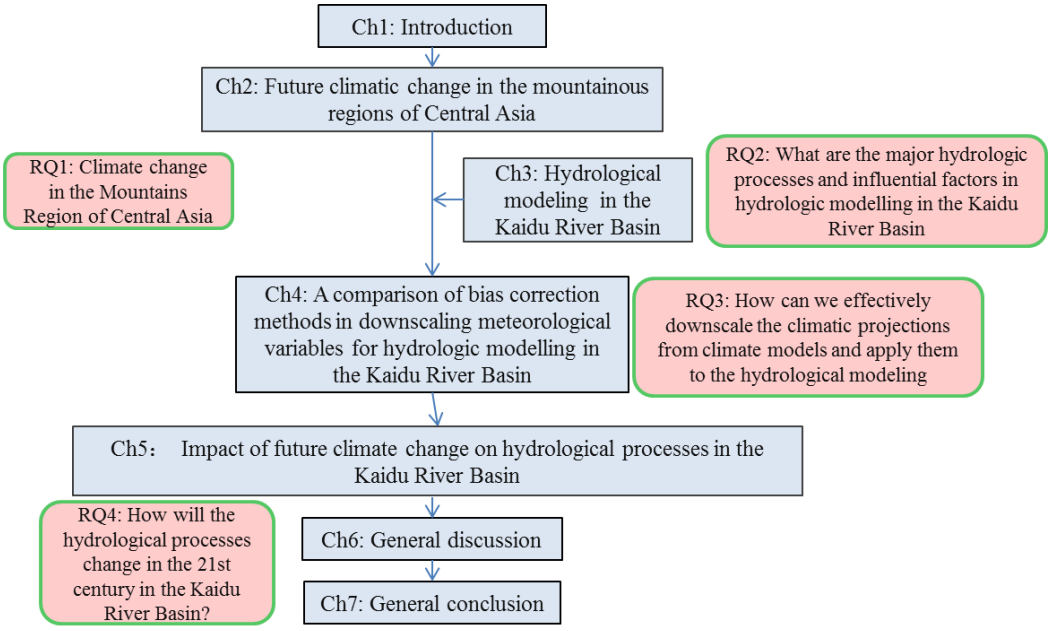

Figure 1. 1 Dissertation outline

Chapter 2: *Future climatic change in the mountainous regions of Central Asia*

This chapter (Yang et al., submitted paper) investigated the climate change in the mountainous regions of Central Asia, one of the most sensitive regions in the world. In this chapter, a 21-GCM simulation ensemble in CMIP5 was used to project climate changes in the 21st century.

Chapter 3: *Hydrologic modelling in the Kaidu River Basin*

This chapter – published in the *Environmental Earth Sciences* (Fang et al., 2015) - describes the hydrological model established in the Kaidu River Basin. It also explains how the combined sensitivity analysis was implemented in identifying important hydrological processes and in quantifying the impact of meteorological input on streamflow modeling.

Chapter 4: A *comparison of bias correction methods in downscaling meteorological variables for hydrologic modeling in the Kaidu River Basin*

This chapter – published in the *Hydrology and Earth System Sciences* (Fang et al., 2015) compared the widely used bias correction methods in downscaling RegCM outputs. The comparison scheme includes the comparison of both climatic variables and simulated hydrological variables, using a well-calibrated hydrological model. The statistics include both frequency based statistics and also time series based statistics.

Chapter 5: *Impact of future climate change on hydrological processes in the Kaidu River Basin*

This chapter – published in the *Advances of Meteorology* (Fang et al., 2015) - investigated the climatic change impact on the hydrological processes in the Kaidu River Basin using simple climate change (SCC) and Regional Climate Models. The goal is to assess the hydrological sensitivity to climate change and the impact of climate change on the hydrological processes in the Kaidu River Basin.

Chapter 6 and Chapter 7 summarize and discuss the results of the previous chapter and also shed some light on future research. Chapter 6 discusses the results from the previous chapters and discusses the advances of the peer reviewed works from other parts of the world. Chapter 7 summarizes the main conclusions of this dissertation and gives some prospect on the evaluation of climate change hydrological processes and water resources.

1.5.3 Out of scope

Impact assessment of climate change on hydrological processes faces many uncertainties, including uncertainties from GCMs, climate downscaling, hydrological models, and etc. In this

study, we only evaluated the climate change impact on the Kaidu River Basin, instead of the entire mountainous regions of Central Asia.

Glacier area is 1.6% of the watershed and glacier melt accounting for 14.1% of runoff (Chen et al., 2009). The glacier melting and accumulation processes in Kaidu River Basin were not accounted for in this study although its contribution to flow is 14.1%, which may cause potential error in the assessment of climate change impact studies. This may be the next aim of our work.

In addition, the Kaidu River Basin is kind of unreachable due to the complex topography and there are no roads up there. This results in the fact that the coverage of metrological stations and hydrologic stations is very low compared to the catchment size. This will definitely add uncertainty to the hydrological modeling.

References

Arnold, J. G., Srinivasan, R., Muttiah, R. S., & Williams, J. (1998). Large area hydrologic modeling and assessment part I: Model development1. *JAWRA Journal of the American Water Resources Association, 34*(1), 73-89.

Beauchamp, J., Leconte, R., Trudel, M., & Brissette, F. (2013). Estimation of the summer-fall PMP and PMF of a northern watershed under a changed climate. *Water Resources Research, 49*(6), 3852-3862. doi:10.1002/wrcr.20336

Bellard, C., Bertelsmeier, C., Leadley, P., Thuiller, W., & Courchamp, F. (2012). Impacts of climate change on the future of biodiversity. *Ecology letters, 15*(4), 365-377.

Bosshard, T., Carambia, M., Goergen, K., Kotlarski, S., Krahe, P., Zappa, M., & Schär, C. (2013). Quantifying uncertainty sources in an ensemble of hydrological climate-impact projections. *Water Resources Research, 49*(3), 1523-1536. doi:10.1029/2011WR011533

Bultot, F., Coppens, A., Dupriez, G., Gellens, D., & Meulenberghs, F. (1988). Repercussions of a CO 2 doubling on the water cycle and on the water balance—A case study for Belgium. *Journal of Hydrology, 99*(3), 319-347.

Buytaert, W., Vuille, M., Dewulf, A., Urrutia, R., Karmalkar, A., & Celleri, R. (2010). Uncertainties in climate change projections and regional downscaling in the tropical Andes: implications for water resources management. *Hydrology and Earth System Sciences, 14*(7), 1247-1258. doi:10.5194/hess-14-1247-2010

Chen, J., Brissette, F. P., & Leconte, R. (2011). Uncertainty of downscaling method in quantifying the impact of climate change on hydrology. *Journal of Hydrology, 401*(3), 190-202.

Chen, Y., Xu, C., Hao, X., Li, W., Chen, Y., Zhu, C., & Ye, Z. (2009). Fifty-year climate change and its effect on annual runoff in the Tarim River Basin, China. *Quaternary International, 208*(1–2), 53-61. doi:http://dx.doi.org/10.1016/j.quaint.2008.11.011

Chenoweth, J., Hadjinicolaou, P., Bruggeman, A., Lelieveld, J., Levin, Z., Lange, M. A., Hadjikakou, M. (2011). Impact of climate change on the water resources of the eastern Mediterranean and Middle East region: Modeled 21st century changes and implications. *Water Resources Research, 47*(6), W06506. doi:10.1029/2010WR010269

Chiew, F., & McMahon, T. (1994). Application of the daily rainfall-runoff model MODHYDROLOG to 28 Australian catchments. *Journal of Hydrology, 153*(1-4), 383-416. doi:10.1016/0022-1694(94)90200-3

Christensen, N. S., & Lettenmaier, D. P. (2007). A multimodel ensemble approach to assessment of climate change impacts on the hydrology and water resources of the Colorado River Basin. *Hydrology and Earth System Sciences Discussions, 11*(4), 1417-1434.

Christierson, B., Vidal, J.-P., & Wade, S. D. (2012). Using UKCP09 probabilistic climate information for UK water resource planning. *Journal of Hydrology, 424*, 48-67.

Dai, Y., Zeng, X., Dickinson, R. E., Baker, I., Bonan, G. B., Bosilovich, M. G., Niu, G. (2003). The common land model. *Bulletin of the American Meteorological Society, 84*(8), 1013-1023.

Duan, Q., Ajami, N. K., Gao, X., & Sorooshian, S. (2007). Multi-model ensemble hydrologic prediction using Bayesian model averaging. *Advances in Water Resources, 30*(5), 1371-1386.

Edwards, P. N. (2000). A brief history of atmospheric general circulation modeling. *International Geophysics Series, 70*, 67-90.

Edwards, P. N. (2010). *A vast machine: Computer models, climate data, and the politics of global warming*: Mit Press.

Ficklin, D. L., Stewart, I. T., & Maurer, E. P. (2013). Climate Change Impacts on Streamflow and Subbasin-Scale Hydrology in the Upper Colorado River Basin. *PloS one, 8*(8), e71297.

Fowler, H., Blenkinsop, S., & Tebaldi, C. (2007). Linking climate change modelling to impacts studies: recent advances in downscaling techniques for hydrological modelling. *International Journal of Climatology, 27*(12), 1547-1578.

Fraley, C., Raftery, A. E., & Gneiting, T. (2010). Calibrating multimodel forecast ensembles with exchangeable and missing members using Bayesian model averaging. *Monthly Weather Review, 138*(1), 190-202.

Fu, C., Wang, S., Xiong, Z., Gutowski, W. J., Lee, D.-K., McGregor, J. L., Suh, M.-S. (2005). Regional climate model intercomparison project for Asia. *Bulletin of the American Meteorological Society, 86*(2), 257-266.

Gain, A. K., Immerzeel, W. W., Weiland, F. C. S., & Bierkens, M. F. P. (2011). Impact of climate change on the stream flow of the lower Brahmaputra: trends in high and low flows based on discharge-weighted ensemble modelling. *Hydrology and Earth System Sciences, 15*(5), 1537-1545. doi:10.5194/hess-15-1537-2011

Gao, X., Wang, M., & Giorgi, F. (2013). Climate change over China in the 21st century as simu-lated by BCC_CSM1. 1-RegCM4. 0. *Atmos. Oceanic Sci. Lett, 6*, 381-386.

Giorgi, F., Jones, C., & Asrar, G. R. (2009). Addressing climate information needs at the regional level: the CORDEX framework. *World Meteorological Organization (WMO) Bulletin, 58*(3), 175.

Hanewinkel, M., Cullmann, D. A., Schelhaas, M.-J., Nabuurs, G.-J., & Zimmermann, N. E. (2013). Climate change may cause severe loss in the economic value of European forest land. *Nature Climate Change, 3*(3), 203-207.

IPCC. (2013). The Physical Science Basis. Working Group I Contribution to the Fifth Assessment Report of the Intergovernmental Panel on Climate Change. *Cambridge, United Kingdom and New York, USA*.

Jung, I.-W., & Chang, H. (2011). Assessment of future runoff trends under multiple climate change scenarios in the Willamette River Basin, Oregon, USA. *Hydrological Processes, 25*(2), 258-277. doi:10.1002/hyp.7842

Koutroulis, A. G., Tsanis, I. K., Daliakopoulos, I. N., & Jacob, D. (2013). Impact of climate change on water resources status: A case study for Crete Island, Greece. *Journal of Hydrology, 479*, 146-158. doi:10.1016/j.jhydrol.2012.11.055

Kwadijk, J., & Rotmans, J. (1995). The impact of climate change on the river rhine: A scenario study. *Climatic Change, 30*(4), 397-425. doi:10.1007/BF01093854

Luo, Y., Arnold, J., Liu, S., Wang, X., & Chen, X. (2013). Inclusion of glacier processes for distributed hydrological modeling at basin scale with application to a watershed in Tianshan Mountains, northwest China. *Journal of Hydrology, 477*(0), 72-85.

Mango, L. M. (2010). *Modeling the effect of land use and climate change scenarios on the water flux of the upper mara river flow, Kenya.*

Martens, P. (2014). *Health and climate change: modelling the impacts of global warming and ozone depletion*: Routledge.

Mearns, L., Sain, S., Leung, L., Bukovsky, M., McGinnis, S., Biner, S., Takle, E. (2013). Climate change projections of the North American regional climate change assessment program (NARCCAP). *Climatic Change, 120*(4), 965-975.

Milly, P. (2007). *Global warming and water availability: the" big picture".* Paper presented at the 21st Conference on Hydrology.

Monteith, J. L. (1965). *Evaporation and the environment. In: The State and Movement of Water I Living Organisms. XIXth Symposium Society for Experimental Biology*. Swansea: Cambridge University Press.

Paton, F. L., Maier, H. R., & Dandy, G. C. (2013). Relative magnitudes of sources of uncertainty in assessing climate change impacts on water supply security for the southern Adelaide water supply system. *Water Resources Research, 49*(3), 1643-1667. doi:10.1002/wrcr.20153

Rosenzweig, C., Elliott, J., Deryng, D., Ruane, A. C., Müller, C., Arneth, A.,Khabarov, N. (2014). Assessing agricultural risks of climate change in the 21st century in a global gridded crop model intercomparison. *Proceedings of the National Academy of Sciences, 111*(9), 3268-3273.

Salzmann, N., & Mearns, L. O. (2012). Assessing the Performance of Multiple Regional Climate Model Simulations for Seasonal Mountain Snow in the Upper Colorado River Basin. *Journal of Hydrometeorology, 13*(2), 539-556. doi:10.1175/2011jhm1371.1

Seneviratne, S. I., Corti, T., Davin, E. L., Hirschi, M., Jaeger, E. B., Lehner, I., Teuling, A. J. (2010). Investigating soil moisture–climate interactions in a changing climate: A review. *Earth-Science Reviews, 99*(3–4), 125-161. doi:http://dx.doi.org/10.1016/j.earscirev.2010.02.004

Setegn, S. G., Rayner, D., Melesse, A. M., Dargahi, B., & Srinivasan, R. (2011). Impact of climate change on the hydroclimatology of Lake Tana Basin, Ethiopia. *Water Resources Research, 47*(4), W04511. doi:10.1029/2010WR009248

Shi, P., Chen, C., Srinivasan, R., Zhang, X., Cai, T., Fang, X., Li, Q. (2011). Evaluating the SWAT Model for Hydrological Modeling in the Xixian Watershed and a Comparison with the XAJ Model. *Water resources management, 25*(10), 2595-2612.

Sloughter, J. M. L., Raftery, A. E., Gneiting, T., & Fraley, C. (2007). Probabilistic quantitative precipitation forecasting using Bayesian model averaging. *Monthly Weather Review, 135*(9), 3209-3220.

Steinschneider, S., Polebitski, A., Brown, C., & Letcher, B. H. (2012). Toward a statistical framework to quantify the uncertainties of hydrologic response under climate change. *Water Resources Research, 48*(11), W11525. doi:10.1029/2011WR011318

Taye, M. T., Ntegeka, V., Ogiramoi, N. P., & Willems, P. (2011). Assessment of climate change impact on hydrological extremes in two source regions of the Nile River Basin. *Hydrology and Earth System Sciences, 15*(1), 209-222. doi:10.5194/hess-15-209-2011

Vorosmarty, C. J., Fekete, B. M., Meybeck, M., & Lammers, R. B. (2000). Geomorphometric attributes of the global system of rivers at 30-minute spatial resolution. *Journal of Hydrology, 237*(1-2), 17-39. doi:10.1016/s0022-1694(00)00282-1

Wilby, R. L., Charles, S., Zorita, E., Timbal, B., Whetton, P., & Mearns, L. (2004). Guidelines for use of climate scenarios developed from statistical downscaling methods.

Wilby, R. L., & Wigley, T. (2000). Precipitation predictors for downscaling: observed and general circulation model relationships. *International Journal of Climatology, 20*(6), 641-661.

Wilby, R. L., Wigley, T., Conway, D., Jones, P., Hewitson, B., Main, J., & Wilks, D. (1998). Statistical downscaling of general circulation model output: a comparison of methods. *Water Resources Research, 34*(11), 2995-3008.

Xu, H., Taylor, R. G., & Xu, Y. (2011). Quantifying uncertainty in the impacts of climate change on river discharge in sub-catchments of the Yangtze and Yellow River Basins, China. *Hydrololy and Earth System Science, 15*(1), 333-344. doi:10.5194/hess-15-333-2011

Xu, J., Chen, Y., Ji, M., & Lu, F. (2008). Climate change and its effects on runoff of Kaidu River, Xinjiang, China: a multiple time-scale analysis. *Chinese Geographical Science, 18*(4), 331-339.

Xu, Z. (2009). *Hydrological model*. Beijing: Science press.

Yang, J., Reichert, P., Abbaspour, K., Xia, J., & Yang, H. (2008). Comparing uncertainty analysis techniques for a SWAT application to the Chaohe Basin in China. *Journal of Hydrology, 358*(1), 1-23.

Yang, J., Reichert, P., & Abbaspour, K. C. (2007). Bayesian uncertainty analysis in distributed hydrologic modeling: A case study in the Thur River basin (Switzerland). *Water resources research, 43*(10), W10401.

2 Future climatic change in the mountainous regions of Central Asia

Modified from:

Yang J., Fang G., Chen Y., De Maeyer P. (2016). Climate change in the mountainous region of Central Asia based on GCM simulation ensemble with Bayesian Model Averaging. To be submitted

Climate change in mountainous regions will have significant impacts on hydrological processes and ecological system, especially in the arid Central Asia. In this paper, future temperature, precipitation and snowfall in the 21st century in the Mountainous region of the Central Asia (MCA) were studied based on 21-GCMs (General Circulation Model) simulation ensemble from the Coupled Model Intercomparison Project Phase 5 (CMIP5) for two Representative Concentration Pathway scenarios (RCP4.5 and RCP8.5), by using the Bayesian Model Averaging (BMA) technique. Results show: 1) BMA significantly outperformed the simple ensemble analysis, and BMA mean matches all three observed climate variables (i.e., temperature, precipitation, & snowfall); 2) At the end of 21st century, generally, mean annual temperature will rise considerably by 5.0 ℃, mean annual precipitation will increase by 5.9% from 186 mm to 197 mm, and mean annual snowfall will dramatically decrease by 26.4% from 72 mm to 53 mm under RCP8.5 compared to those in the control period (1976-2005); 3) Precipitation will increase in the North Tianshan while decrease in the Amu Darya region, and snowfall show a significant decreasing in the west. Mean annual snowfall fraction (S/P) will also decrease from 0.58 in 1976~2005 to 0.43 in 2070~2099 (RCP8.5); 4) Snowfall show high sensitivity to temperature in autumn and spring while low sensitivity in winter, with highest sensitivity at the boundary of MCA. In general, climate change in the MCA is featured with increasing temperature and precipitation but decreasing snowfall, which poses a potential risk of flood and may cause loss of solid water storage in the MCA and seasonal shifts of runoff.

Keywords: Climate change; Central Asia; GCM; ensemble; Bayesian Model Averaging

2.1 Introduction

IPCC (2013) states "Warming of the climate system is unequivocal" and how the climate system changes is important to human activity as it will change the temporal-spatial distribution of temperature and precipitation. In the past two decades, climate change has received worldwide attention (e.g., IPCC series reports in www.ipcc.org), ranging from physical science basis and scenario modelling, to impact assessment, countermeasures and mitigation. In the context of climate change, the mountainous regions are particularly sensitive with increases in temperature coupled with changes in precipitation regimes that are often larger than the global average (Dedieu et al., 2014; Piazza et al., 2014).), which could pose water management problems as in some mountain regions snow and glacier are important water resources to downstream. For example, Kure et al.(2013) shows that melted water from snow, glacier and permafrost supplies about 80% of the total river runoff in Central Asia. Snowfall is very sensitive to climate change in the high-mountain Asia (Kapnick et al., 2014). Therefore, understanding snowfall change as well as precipitation and temperature change is important for hydrological and climatological purposes in mountainous regions, especially for the arid mountainous regions, e.g., the Mountainous region in Central Asia (MCA), where snow and glacial are the main water sources to human activity (Chen, 2014).

Previous studies show the MCA has experienced notable climate change in the past few decades. The average rising rates in air temperature and precipitation were about 0.1 ℃/10a and 12 mm/10a for the Tianshan Mountains from 1940 to 1991 (Aizen et al., 1997). Li et al. (2013) also shows that mean temperature and precipitation increased 0.86 ℃ and 47.3 mm in the mountainous areas of the northwest China over the period 1960-2010. As precipitation state (liquid or solid) is a main factor determining the change in river runoff (Aizen et al., 1997), it is important to investigate changes in snowfall. Guo & Li (2014) investigated the ratio of snowfall to precipitation (S/P) in the Tianshan Mountains using the historical climate data and indicated that average S/P experienced a downward trend during 1961~2010. However, most studies mainly focus on the climate change in the past several decades, and few researches (e.g., IPCC, 2013; Shi et al., 2007) investigate the future climatic change in the 21st century for the MCA. The projected temperature in IPCC5 in Central Asia is likely to increase by 2 to 4 ℃ by 2081–2100 with respect to 1986–2005 for the RCP4.5 scenario while precipitation for the wet season (April to September) is expected to change by -20% ~ -30% whereas precipitation for the dry season (October to March) increases 0~ 40%. Shi et al. (2007) simulated that the future climate for doubled CO2 concentration based on a nested approach with the regional climate model-RegCM2 and obtained that annual temperature will increase by 2.0 ℃ and annual

precipitation by 19% for the arid northwest China.

Since analyses from one climate model might be biased, in this study, we try to study future precipitation (rainfall and snowfall) and temperature change over the MCA using a simulation ensemble of 21 General Circulation Models (GCMs) from the Coupled Model Intercomparison Project Phase 5 (CMIP5) with Bayesian model averaging (BMA). In addition, the snowfall changes in both annual and seasonal patterns were analyzed. The chapter is structured as follows: Section 2.2 introduces the study area, the observed climate dataset APHRODITE, and CMIP5 climate simulations from 21 GCMs; Section 2.3 describes the BMA technique and the analysis procedure; and results and discussion are given in Section 2.4 followed by conclusions in Section 2.5.

2.2 Study Area and Data

2.2.1 Study area and observed climate data

Central Asia, far from the ocean, is situated in the innermost region of the Eurasia continent. Freshwater supply strongly depends on the occurrence and amount of precipitation and snow/glacier melt in the mountainous regions (Dietz et al., 2014; Ososkova et al., 2000). In this paper, the study area MCA is referred to as the mountainous region in Central Asia with elevation higher than 1,300 m, including the entire Tianshan Mountains and the northern slope of the Kunlun Mountains whose water flows into the Tarim basin (Figure 2.1).

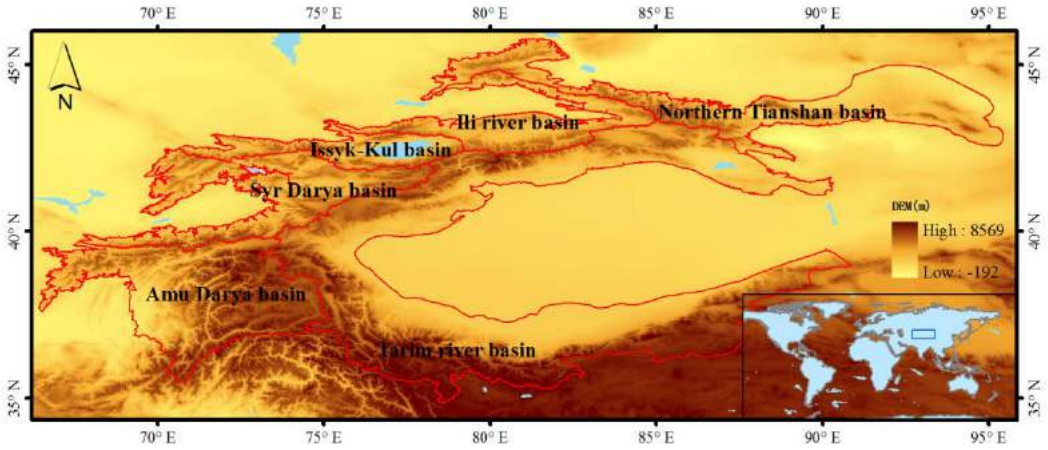

Figure 2.1 Topographic map of the mountainous region of Central Asia with the study area marked in red polygons: Tarim river basin, northern Tianshan basin, Ili river basin, Issyk_Kul basin, Syr Darya basin and Amu Darya basin.

MCA is characterized as the continental climate, with a hot and dry summer and cold winter. Based on climate dataset APHRODITE (Asian Precipitation - Highly-Resolved Observational Data Integration Towards Evaluation of Water Resources; Yasutomi et al., 2011;

Yatagai et al., 2012), mean annual temperature ranges from -9.8 to 15.5 ℃, with daily temperature variation from – 35.9 to 43.1 ℃ and mean annual precipitation ranges from 70 to 1000 mm with a large portion as snowfall and precipitation has a clear spatial pattern with heavy precipitation occurs in the northwestern region. Six hydrological regions were identified using watershed discretization in ArcGIS: the Tarim river basin, Northern Tianshan region, Ili river basin, Issyk-Kul basin, Syr Darya basin and Amu Darya basin (Figure 1). These hydrological regions provide freshwater for Central Asia including the densely populated, arid lowlands in Kyrgyzstan, Kazakhstan, Uzbekistan, Tajikistan, Turkmenistan, and Xinjiang in China. The northern slope of the Kunlun Mountains mainly provides water for the Tarim river basin in Xinjiang. These rivers are sensitive to climate change, since climate change not only influences the rainfall-runoff process but also the snow/glacier melt.

The daily gridded climate dataset APHRODITE was used as the observation data for validation since it provides snowfall data except for precipitation and temperature. The dataset is made primarily based on station observations and a quality control and interpolation system is used to interpolate into 0.50 × 0.50 degree grid for the Asian region. The dataset is widely used in studies such as the diagnosis of climate changes, evaluation of Asian water resources, forecast improvements, and verification of numerical model simulation and satellite precipitation estimates (http://www.chikyu.ac.jp/precip/scope/).

2.2.2 GCM simulation ensemble

Climate simulations from 1976 to 2099 are based on 21 state-of-the-art GCMs from CMIP5 (Coupled Model Intercomparison Project Phase 5; IPCC, 2013) for two emission scenarios of the Representative Concentration Pathways - RCP4.5 (lower emission scenario) and RCP8.5 (higher emission scenario) (Kawase et al., 2011; Van Vuuren et al., 2011), which form GCM simulation ensemble to be used for climate change assessment. Information about these 21 GCMs is listed in Table 2.1. These models including Earth System Models (inclusion of the biogeochemical cycles) are from 20 institutes or universities. Spatial resolutions of the GCMs range from 0.75 °to 3.75 °. Of all GCM simulated climate variables, we only considered 3 variables, i.e., air temperature, precipitation and snowfall.

Table 2.1 Information about the GCM models used in this study

No.	Model	Institution	Atmosphere resolution
1	BCC-CSM1.1-m	Beijing Climate Center, China Meteorological Administration	1.12 °× 1.12 °
2	CanESM2	Canadian Centre for Climate Modelling and Analysis	2.79 °× 2.82 °
3	CMCC-CM	Centro Euro-Mediterraneo per I Cambiamenti Climatici	0.75 °× 0.75 °
4	CNRM-CM5	Centre National de Recherches Meteorologiques / Centre Europeen de Recherche et Formation Avancees en Calcul Scientifique	1.4 °× 1.4 °
5	ACCESS1.3	CSIRO (Commonwealth Scientific and Industrial Research Organisation, Australia), and BOM (Bureau of Meteorology, Australia)	1.25 °× 1.87 °
6	CSIRO-Mk3.6.0	CSIRO (Commonwealth Scientific and Industrial Research Organisation) in collaboration with the Queensland Climate Change Centre of Excellence	1.87 °× 1.87 °
7	BNU-ESM	College of Global Change and Earth System Science, Beijing Normal University	2.77 °× 2.81 °
8	INM-CM4	Institute for Numerical Mathematics	2.0 °× 2.0 °
9	IPSL-CM5B-LR	Institute Pierre-Simon Laplace	1.9 °× 3.75 °
10	FGOALS-g2	LASG, Institute of Atmospheric Physics, Chinese Academy of Sciences; and CESS, Tsinghua University	2.79 °× 2.81 °
11	MIROC5	Atmosphere and Ocean Research Institute (The University of Tokyo), National Institute for Environmental Studies, and Japan Agency for Marine-Earth Science and Technology	1.4 °× 1.4 °
12	MIROC-ESM	Atmosphere and Ocean Research Institute (The University of Tokyo), National Institute for Environmental Studies, and Japan Agency for Marine-Earth Science and Technology	2.79 °× 2.81 °
13	HadGEM2-ES	Met Office Hadley Centre	1.875 °× 2.5 °
14	MPI-ESM-LR	Max Planck Institute for Meteorology (MPI-M)	1.87 °× 1.87 °
15	MRI-ESM1	Meteorological Research Institute	1.125 °× 1.125 °
16	GISS-E2-R	NASA Goddard Institute for Space Studies	2 °× 2.5 °
17	CCSM4	National Center for Atmospheric Research	1.25 °× 1.87 °
18	NorESM1-M	Norwegian Climate Centre	1.9 °× 2.5 °
19	GFDL-CM3	Geophysical Fluid Dynamics Laboratory	2.0 °× 2.5 °
20	GFDL-ESM2G	Geophysical Fluid Dynamics Laboratory	2 °× 2.5 °
21	CESM1(BGC)	National Science Foundation, Department of Energy, National Center for Atmospheric Research	0.94 °× 1.25 °

2.3 BMA technique and its application on GCM simulation ensemble

2.3.1 Introduction of BMA technique

BMA technique (Hoeting et al., 1999) is a statistical method to infer a probabilistic projection that produces more skillful and reliable outputs than the original ensemble from several competing models (Duan et al., 2007; Raftery et al., 2005). Over the past decades, it has be widely used in weather forecast (e.g. Fraley et al., 2010; Sloughter et al., 2007), and hydrologic modeling (e.g., Duan et al., 2007).

Based on BMA, for a forecast variable *y* with training data $\mathrm{D} = [y_{obs,1}, y_{obs,2}, \cdots\ y_{obs,T}]$ and K forecast models (M_1, M_2,… M_k), the probability density function (PDF) of *y* , $\mathrm{p(y)}$, is given by:

$$\mathrm{p(y)} = \sum_{k=1}^{K} p_k(y|M_k)w_k \qquad \text{(Equation 2-1)}$$

where $p_k(y|M_k)$ is the forecast PDF of *y* based on model M_k. w_k is the likelihood of M_k being correct given the training data D, $w_k = p(M_k|D)$, with $\sum_{k=1}^{K} w_k$=1. BMA predictions are the weighted averages of the individual model predictions. The conditional distribution $p_k(y|M_k)$ normally can be represented as a normal distribution, $\mathrm{N}(a_{0k} + a_{1k}y_k, \sigma_k^2)$ or gamma distribution $\Gamma(\frac{(b_{0k}+b_{1k}y_k^p)^2}{(c_{0k}+c_{1k}y_k^p)^2}, \frac{(c_{0k}+c_{1k}y_k^p)^2}{b_{0k}+b_{1k}y_k^p})$, where a_{0k}, a_{1k} , b_{0k}, b_{1k} , c_{0k}, and c_{1k} regression coefficients, *p* is the power index, σ_k is standard deviation, and y_k is the prediction of model M_k.

To apply BMA, one needs to firstly choose $p_k(y|M_k)$ (e.g. Normal distribution or Gamma distribution), and then determines related coefficients (i.e., a_{0k}, a_{1k} , and σ_k for normal distribution, or b_{0k}, b_{1k} , c_{0k}, c_{1k} and *p* for gamma distribution). In this study, we assumed normal distributions for temperature, and gamma distributions for precipitation and snow as in Sloughter (2007), and coefficient estimation was based on expectation-maximization algorithm as described in Raftery et al (2005).

More details of the BMA method and expectation-maximization algorithm could refer to (Duan et al., 2007; Raftery et al., 2005; Sloughter et al., 2007).

2.3.2 Application procedure

First, to overcome different spatial resolutions of GCM simulations (or outputs), GCM simulation ensemble were firstly rescaled to 0.5 °×0.5 °to match APHRODITE resolution with the bilinear approach. BMA was then applied grid-wise with training data APHRODITE and GCM simulation ensemble from 1976 to 2005 to obtain a constructed statistical model on each grid, for monthly temperature, monthly precipitation, and monthly snowfall, respectively. Finally, these constructed grid-wise models were used to generate corresponding future climate variable predictions from 2006 to 2099.

To assess the performances of constructed BMA statistic models, three indices were used: mean absolute error (MAE), mean continuous ranked probability score (CRPS), and the Percentage of observations Included in 95% Confidence Interval (PI95CI). The smaller the MAE is, the smaller biases would be in the prediction; the large PI95CI is, the better prediction is. For a time series, CRPS at time t is defined as:

$$\mathrm{CRPSt} = \int_{-\infty}^{+\infty} (F_t(y) - H(y - y_t))^2 dy \qquad \text{(Equation 2-2)}$$

where $F_t(y)$is the predicted cumulative function (CDF) at time *t*, H is the Heaviside function (returning zero for negative and unity for non-negative), and y_t is observation at time *t*. CRPS is the mean of CRPSt at each time step. These indices are widely used in weather forecast as a measure of the closeness of the predicted and observed cumulative distributions and sharpness of the predicted probability density function (Hersbach, 2000). The smaller the CRPS the narrower would be for the prediction uncertainty and better prediction is achieved.

As a comparison, these three indices were also calculated for GCM simulation ensemble.

2.4 Results and Discussion

In this section, the general performances of BMA technique were firstly demonstrated for three climate variables with observations and compared to GCM simulation ensemble for period of 1976~2005. Then BMA technique was performed to obtain future climate for period of 2006~2099 for both RCP4.5 and RCP8.5, respectively, and results were analyzed.

2.4.1 Performance of BMA technique

Table 2.2 shows a comparison of performances between GCM simulation ensemble and BMA technique for temperature, precipitation, and snowfall. For all these three climate variables, BMA technique outperformed GCM simulation ensemble with significantly reduced MAE and CRPS values, and significantly increased PI95CI. For temperature, MAE and CRPS

were reduced from 8.23 ℃ and 8.74 to 2.24 ℃ and 1.47, while PI95CI increased from 46% to 94%; for precipitation, MAE and CRPS were reduced from 16.06 mm and 21.87 to 5.88 mm and 4.27, while PI95CI increased from 46% (61%) to 94% (89%); for snowfall, MAE and CRPS were reduced from 15.92 mm and 20.26 to 5.91 mm and 4.01, respectively, while PI95CI increased from 63% to 91%.

Table 2.2 Performances of BMA technique and GCM simulation ensemble for T, P and snowfall

Variable	Method	MAE (mm/month or ℃/month)	CRPS (-)	Percentage of observations included in 95% confidence interval (%)
Temperature	Ensemble	8.23	8.74	46
	BMA	2.24	1.47	94
Precipitation	Ensemble	16.06	21.87	61
	BMA	5.88	4.27	89
Snowfall	Ensemble	15.92	20.26	63
	BMA	5.91	4.01	93

Figure 2.2 and Figure 2.3 further shows the spatial comparison of observed mean annual climate variables with their GCM simulation ensemble means and BMA means. For mean annual temperature, observation is generally high in the low elevation areas while low in the high elevation areas with a spatial mean of 2.2 ℃ ranging from -9.8 ℃ to 15.5 ℃ in MCA. Compared to observation, ensemble mean has an obvious over-prediction in high elevation areas in northern MCA, and extreme over-prediction in western MCA; BMA mean has a good spatial match of observation, and its histogram in Figure 2.3 shows the majority of biases concentrate in 0 ~ 0.5 ℃. For mean annual precipitation, observation is high in the west and low in the east and south with spatial mean of 237 mm ranging from 32.4 mm to 803 mm in MCA. Obviously, the ensemble mean over predicts the south part, while BMA mean matches the observation quite well spatially. The histogram in Figure 2.3 shows the majority of biases concentrate in 0 ~ 100 mm. For mean annual snowfall, its spatial pattern of observation is similar to precipitation, and ensemble mean underestimated the west MCA and overestimated the south MCA while BMA mean gave a fairy good spatial match and its spatial bias concentrate around 0 ~ 30 mm (Figure 2.3) given the average observation being 98 mm, ranging from 2.9 mm to 555.6 mm.

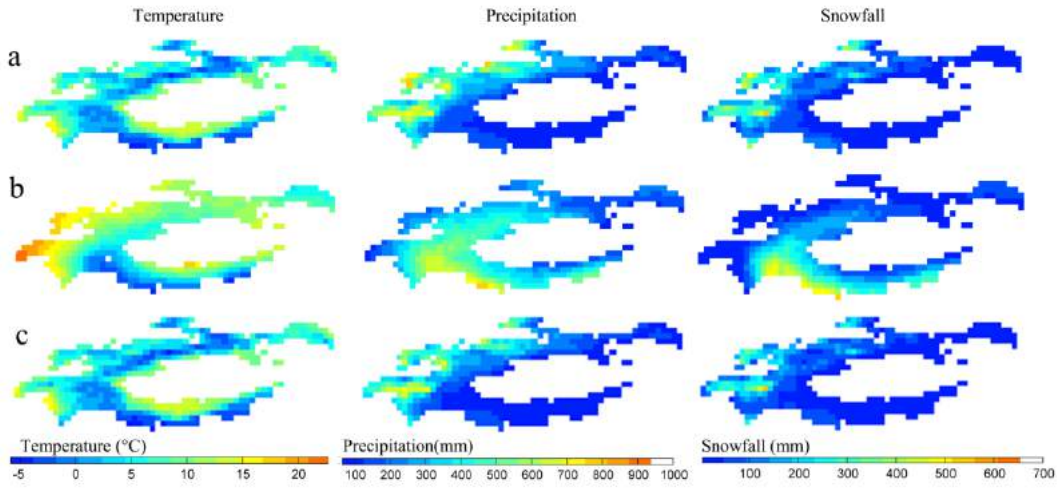

Figure 2.2 Observation (a), mean of GCM simulation ensemble (b) and BMA mean of GCM simulation ensemble (c) for mean annual temperature, precipitation and snowfall during 1976~2005.

Figure 2.3 also shows seasonal spatial pattern of snowfall biases of the BMA means. Compared to observation, snowfall biases are small and the majority is smaller than 10 mm in autumn and winter, and 25 mm in spring. The large estimation errors occur only on several grids on the north and west.

All above indicate that compared to GCM simulation ensemble, BMA had a great improvement to estimate all these three variables and BMA mean is good approximation to the observations. BMA mean was then used to assess future climate change for the period of 2006~2099.

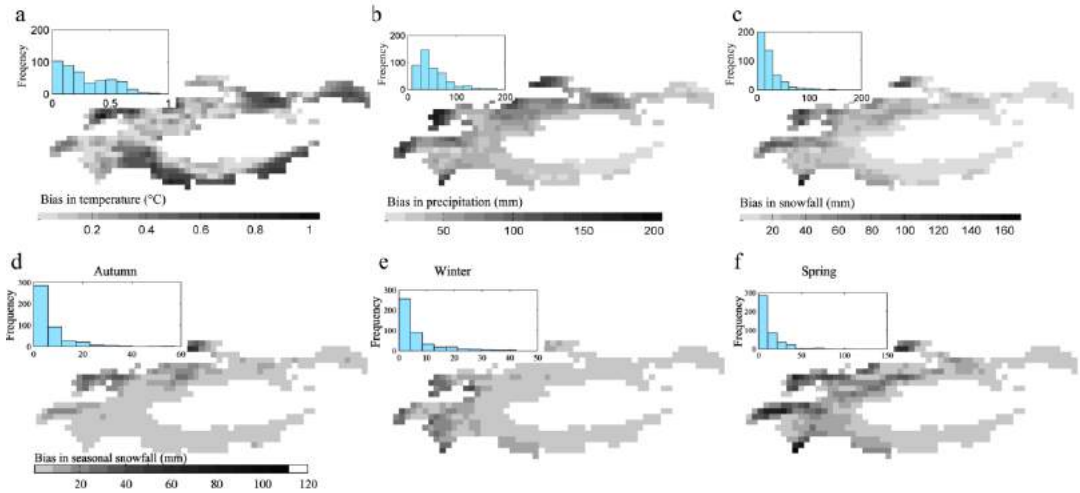

Figure 2.3 Spatial biases between observation and BMA mean of GCM simulation ensemble with histograms for mean annual temperature (a), precipitation (b) and snowfall (c), and mean seasonal snowfall (d: Autumn; e: Winter; f: Spring) during 1976~2005.

2.4.2 Future climate changes in MCA

Figure 2.4 shows simulated mean annual temperature, precipitation, and snowfall for 2070~2099, their absolute changes for 2070~2099 compared to 1976~2005, their annual change rates in 1976~2099, and GCM consistencies based on GCM simulation ensembles under RCP8.5 over the 21st century. GCM consistency is defined as percentage of GCM models predicting annual increasing rate large than the average global warming rate under RCP8.5 (i.e. 0.037 ℃/a) for temperature, or positive annual increase rate for precipitation and snowfall.

At the end of 21st century, the spatial patterns of temperature, precipitation and snowfall are close to those in the control period. For temperature, high values are distributed in the low elevation areas while low values in the high elevation areas; for precipitation and snowfall, values remain high in the west and low in the east and south in the end of the 21st century with less spatial heterogeneity for snowfall.

Generally there is an increase in temperature for the entire region and the mean temperature will increase 5.0 ℃ for 2070~2099 (the end of 21st century) with spatial increases ranging from 3.0 ℃ to 8.7 ℃ (plot a2 in Figure 2.4) and highest increase is in the southwest. The average annual change rate (Plot a3) is 0.054 ℃/a ranging from 0.03 ℃/a to 0.08 ℃/a. Spatially, the increase rate is highest in the south west (the Amu Darya basin). Plot a4 shows spatial distribution of model consistencies. Almost 100% models gave annual changing rates larger than the global average, indicating temperature change in MCA is higher than global average. This agrees with some other studies, for example, global temperature increasing rate was 0.0175~0.0197 ℃/a while 0.0343 ℃/a for the northwestern China during 1951~2012 (Li et al. 2012; IPCC 2013).

Mean annual precipitation will increase from 186 mm in the control period to 197 mm for 2070~2099 with relative increase being 5.9% and the increment is higher in the north than the south and west regions (b2 in Figure 2.4). Annual precipitation change rate (b3) will be 0.11 mm/a with a slight increase in the central Tianshan Mountains (about 0.4 mm/a) and a slight decrease in the northern Kunlun Mountains (about -0.2 mm/a). Plot b4 shows spatial distribution of model consistency. Clearly, over 70% of the GCM models give an increased precipitation in the east while only 40% of the GCMs for the western MCA (b4).

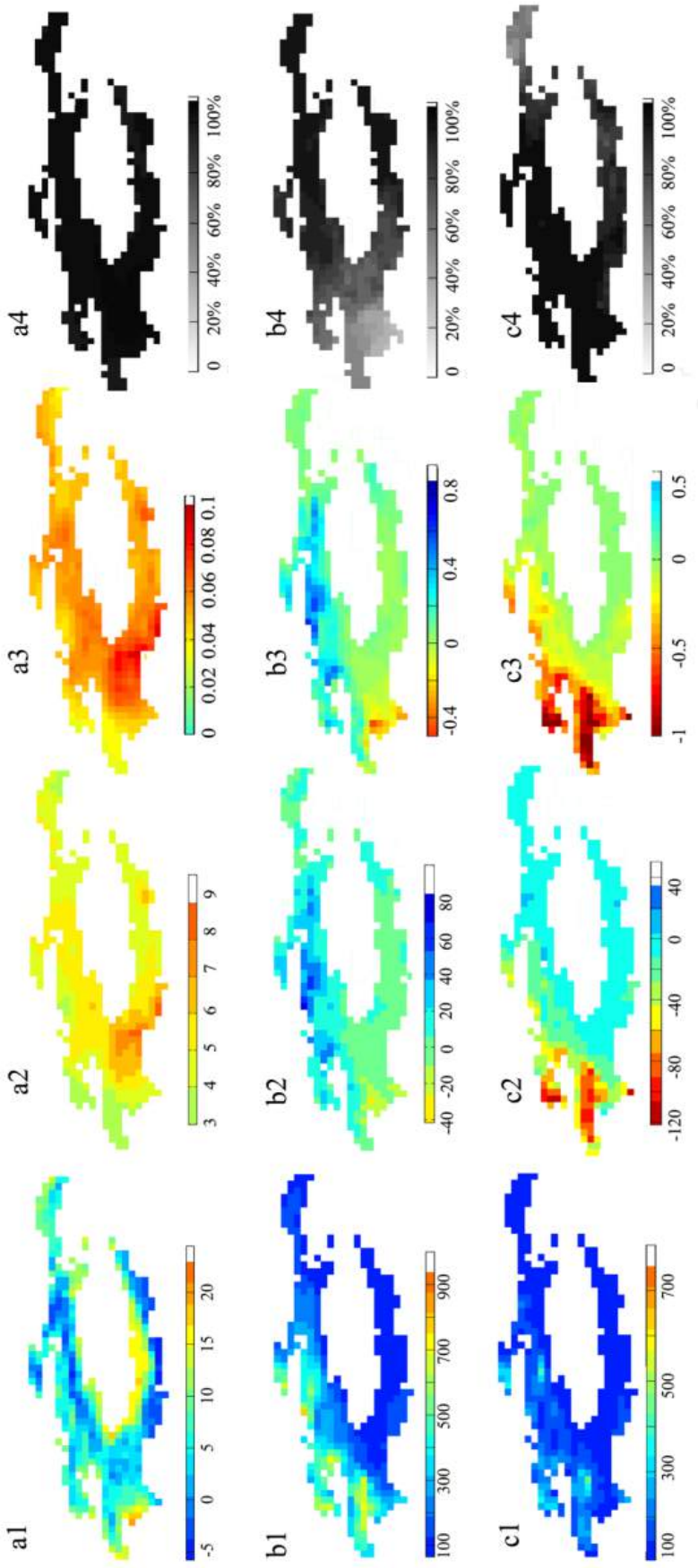

Figure 2.4 Spatial distribution of temperature (a), precipitation (b), and snowfall (c) for their mean annual values during 2070~2099 (a1, b1, c1), their absolute changes compared to 1976-2005 (a2, b2, c2), annual change rates from 1976 to 2099 (a3, b3, c3), and their consistencies (a4, b4, c4) based on RCP8.5. Consistency is defined as the percentage of GCMs with change rate greater than 0.037 ℃/a (i.e. global warming rate under RCP8.5) for temperature, and positive change rates for precipitation and snowfall.

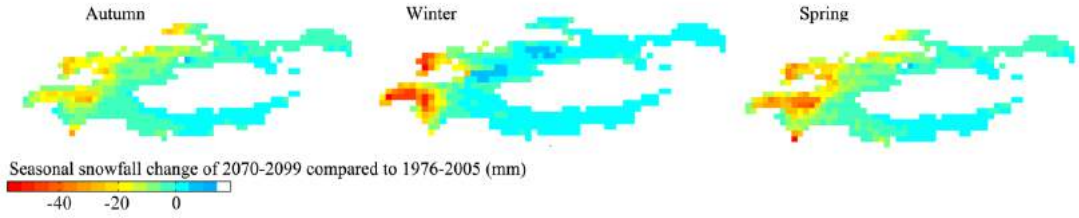

Figure 2.5 Changes of mean seasonal snowfalls during 2070-2099 compared to 1976-2005 under RCP8.5 (left: autumn; middle: winter; right: spring).

Mean annual snowfall will generally experience a decrease from 72 mm in the control period to 53 mm in 2070~2099 (relative decrease is 26.4%) with average changes ranging from -120 mm in the west to 40 mm in the high mountain area in the east (c2 in Figure 2.4). The annual change rate is -0.20 mm/a. Substantial decrease will be expected in the western MCA though the total precipitation remains above normal. The results serve as a support for (Winkelmann et al., 2012) that concluded that annual snowfall was projected to decrease across much of the Northern Hemisphere in the 21st century. Most models demonstrated a decreasing trend (consistency close to 100%) in most area except the northeast part. Seasonally, snowfall shows considerable decrease in the western region in autumn, winter and spring (Figure 2.5). Slightly increase only occurred on several grids in the central Tianshan in winter.

Similar results were obtained for RCP4.5 except its magnitude is lower than those for RCP8.5. Hence its results are not shown here.

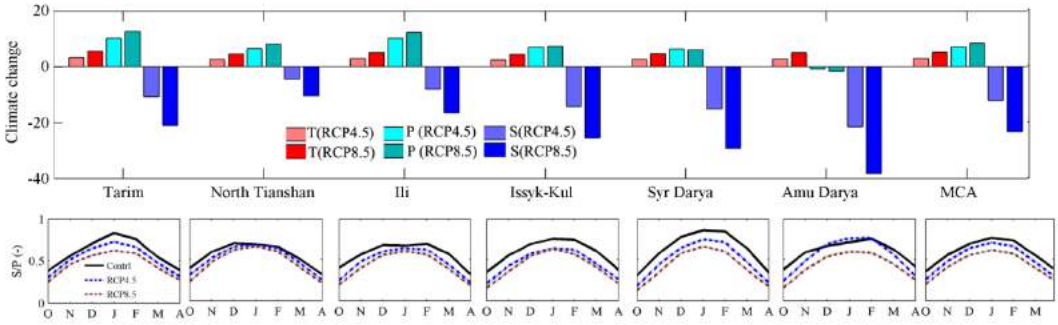

Figure 2.6 Future climatic change during 2070~2099 compared to 1976~2005 with RCP4.5 and RCP8.5, for six sub-regions and the Mountain region of Central Asia (MCA). Top: absolute temperature change (℃), relative precipitation change (%), and relative snowfall change (%). Bottom: variation of snowfall fraction.

Figure 2.6 shows basin-averaged changes of mean annual temperature, precipitation and snowfall in 2070~2099 under RCP4.5 and RCP8.5 with respect to those in 1976~2005. Generally, all basins will experience an increase in temperature, an increase in precipitation

except in Amu Darya, and a decrease in snowfall. Temperature change will be around 2.5 ℃ ~ 3.3 ℃ for RCP4.5 and 4.3 ℃ ~ 5.5 ℃ for RCP8.5 with larger increments in the Tarim River basin (3.3 and 5.5 ℃), the Ili river basin (2.9 and 5.0 ℃) and the Amu Darya basin (2.8 and 5.0 ℃). The increase in precipitation (except Amu Darya) is similar to China with 8.6%-13.4% increase under RCP4.5 and 6.3%-8.0% increase under RCP8.5 using a RegCM model (Gao et al., 2013). Decrease in snowfall is largest in Amu Darya, followed by Syr Darya, Issyk-Kul, Tarim river basin and then Ili river basin and north Tianshan. These decreases mainly result from a warmer climate and are enlarged by decreasing precipitation for Amu Darya which should be paid attention to for water management. As temperature rise of 2.2 ℃ ~ 3.1 ℃ will reduce the current glacier extent by 36 ~ 45% (Hagg et al., 2013), strong warming and slightly increased precipitation will pose a great risk of reduced glacier and snow storage and therefore decrease water availability at the long term.

2.4.3 Snowfall fraction

Snowfall fraction (ratio of snowfall to precipitation, S/P) was used to study the precipitation shift from snowfall to rain. Shift from snow to rain could be quite important because such change could influence the timing of spring runoff, cause water shortage in summer and sometimes result in larger flows (Feng & Hu, 2007; Bocchiola, 2014). "S/P"s in most areas will decrease significantly in 2070 ~ 2099 under RCP4.5 and RCP8.5 compared to the control period (Figure 2.6), except that in winter for Amu Darya under RCP4.5. Average "S/P"s decrease from 0.58 (ranging from 0.55 to 0.62 for each subregion) in the control period to 0.50 (0.46 ~0.54) under RCP4.5 and 0.43 (0.41 ~ 0.46) under RCP8.5. This result is consistent with studies of Berghuijs et al. (2014) and Guo & Li (2014), which concluded that S/P has been decreasing for the last few decades over the Karakoram and Tianshan Mountains in recent decades. Decrease in S/P and S_{days}/P_{days} (snowfall days over precipitation days) were also detected in the contiguous United States and Switzerland (Feng & Hu, 2007; Serquet et al., 2011). Therefore, it is very likely that the snowfall fraction will decrease with the increasing temperature.

Seasonally, S/P decreases largely in the transient seasons (October, November, March, April) and slightly in the coldest season (January and February) in the north Tianshan regions, Ili basin and Amu Darya. In the western region (Issyk-Kul and Syr Darya), S/P decreases almost evenly in each month, and in the Tarim Basin, S/P decreases the most significantly in coldest months.

Figure 2.7 shows sensitivity of snowfall to temperature and precipitation for annual, autumn, winter and spring. Annual map shows in most area temperature will have a negative impact on snowfall (97% of grids) and most influential area is the west. Sensitivity values range

from -30.2 %/ ℃ to 4.0 %/ ℃, with its 90% quantiles being (-12.6 %/ ℃ , -1.5 %/ ℃). Seasonally, the negative impact is significant in most areas in autumn and spring, while in winter besides negative impact area there are also positive impact influenced area, mainly in the high elevation area. The sensitivity values mainly concentrate in -25.9 ~ -2.4%/ ℃ and -25.9 ~ -1.5 %/ ℃ (90% quantiles) in autumn and spring, with high sensitivity occurs at the boundary of MCA (over -30%/°C), which supports to some extent the conclusion "snowfall trends are more sensitive to climate change below an elevation of 4000 m asl" (Mir et al., 2015). In winter, response of snowfall to temperature is not noticeable for most area of MCA (-8.6 ~ 3.8%/ ℃), but for the high mountains of eastern part, temperature has a positive impact on snowfall with sensitivity being 5%/ ℃. This is consistent with studies in the high Alps of 10%/ ℃ (Hezel et al., 2012) and the cold Antarctic of 5%/ ℃ (Monaghan et al., 2008). The negative impact could happen "as warmer conditions would increase the amount of precipitation that falls as rain relative to snow" (Davis et al., 1999), while the positive impact could happen "since saturation vapor pressure increases exponentially as a function of temperature, thereby allowing for the possibility of a more moist atmosphere" (Davis et al., 1999) as far as temperature is still lower than snowfall point. In autumn and spring, temperature changes to and from snowfall temperature and hence have more negative impact than positive impact. The results indicate that temperature is an important factor influencing precipitation form, as suggested by (Krasting et al., 2013).

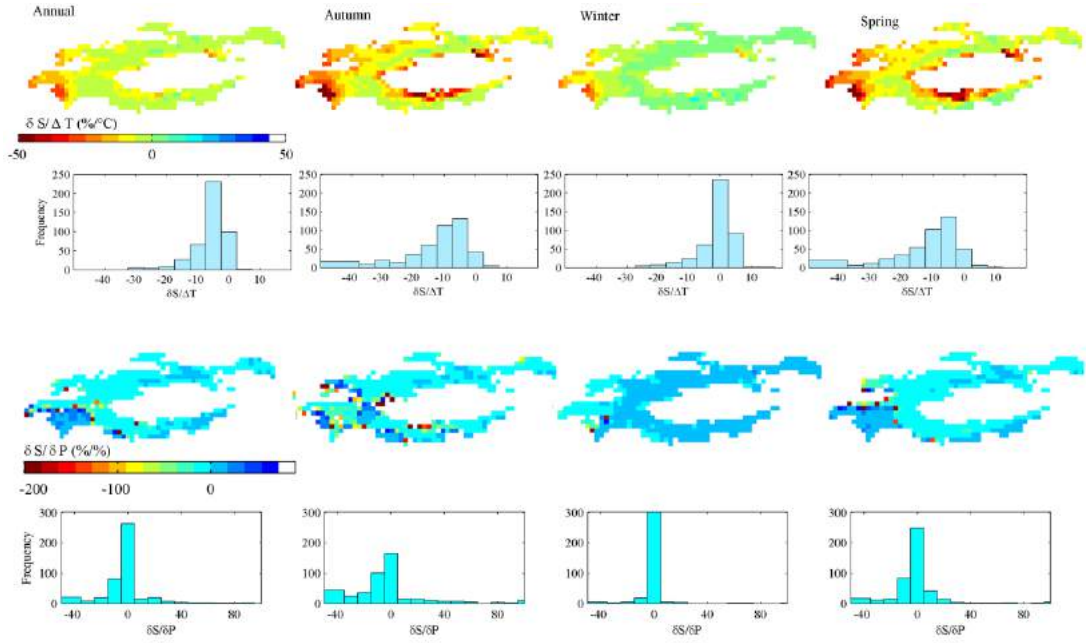

Figure 2.7 Sensitivity distribution of relative snowfall change (δS) to absolute temperature change (ΔT); Spatial distribution of δS/δP for annual, autumn, winter and spring, respectively.

The relationship of annual snowfall change to annual precipitation change is calculated. It is only significant in west and southwest areas and there are more negatives than positives,

which indicates most snowfall fraction in these areas will decrease as precipitation increases. Seasonal sensitivity maps show similar results with the annual map, indicating that temperature plays an important role as discussed above.

2.5 Conclusions

This chapter evaluated air temperature, precipitation and snowfall change in the MCA using BMA technique based on an simulation ensemble of 21 GCMs from CMIP5. The following conclusions can be drawn:

1. BMA technique high outperformed GCM simulation ensemble and can be used to incorporate GCM simulation ensemble and observations for future climate change assessment.
2. Generally, the study area will expect a big increasing mean temperature at an annual rate of 0.054 ℃/a, a slightly increasing mean precipitation at an annual rate of 0.11 mm/a, and a dramatically decreasing snowfall at an annual rate of 0.20 mm/a under RCP8.5 during 1976~2099.
3. For basin averages, temperature increment is 5.0 ℃ (ranging from 4.3 ℃ to 5.5 ℃); precipitation has an increase for all basins except Amu Darya; snowfall decreases the most in Amu Darya, followed by Syr Darya, Issyk-Kul and Tarim, and it decreases the least in North Tianshan and Ili.
4. Snowfall fraction (S/P) decreases substantially from 0.58 in the control period (1976-2005) to 0.43 for the end of 21st century (2070-2099) under RCP8.5. Snowfall show great sensitivity to temperature in autumn and spring of -25.9 ~ -1.5%/ ℃, while low sensitivity in winter (about -8.6 ~ 3.8%/ ℃). Positive impact of temperature to snowfall only occur in the high mountains in winter.

Given the importance of climate change in the hydrological system, this analysis could be used to improve the understanding of future water resources distribution and hence for water resources management and planning.

Acknowledgment

We acknowledge the World Climate Research Programme's Working Group on Coupled Modelling, which is responsible for CMIP, and we thank the climate modeling groups for their efforts in producing their model outputs. For CMIP the U.S. Department of Energy's Program for Climate Model Diagnosis and Intercomparison provides coordinating support and led development of software infrastructure in partnership with the Global Organization for Earth System Science Portals.

References

Aizen, V. B., Aizen, E. M., Melack, J. M., & Dozier, J. (1997). Climatic and hydrologic changes in the Tien Shan, central Asia. *Journal of Climate, 10*(6), 1393-1404.

Berghuijs, W., Woods, R., & Hrachowitz, M. (2014). A precipitation shift from snow towards rain leads to a decrease in streamflow. *Nature Climate Change, 4*(7), 583-586.

Bocchiola, D. (2014). Long term (1921–2011) hydrological regime of Alpine catchments in Northern Italy. *Advances in Water Resources, 70*, 51-64.

Chen, Y. (2014). *Water resources research in Northwest China*: Springer Science & Business Media.

Davis, R. E., Lowit, M. B., Knappenberger, P. C., & Legates, D. R. (1999). A climatology of snowfall‐temperature relationships in Canada. *Journal of Geophysical Research: Atmospheres, 104*(D10), 11985-11994.

Dedieu, J., Lessard-Fontaine, A., Ravazzani, G., Cremonese, E., Shalpykova, G., & Beniston, M. (2014). Shifting mountain snow patterns in a changing climate from remote sensing retrieval. *Science of the Total Environment, 493*, 1267-1279.

Dietz, A. J., Conrad, C., Kuenzer, C., Gesell, G., & Dech, S. (2014). Identifying Changing Snow Cover Characteristics in Central Asia between 1986 and 2014 from Remote Sensing Data. *Remote Sensing, 6*(12), 12752-12775.

Duan, Q., Ajami, N. K., Gao, X., & Sorooshian, S. (2007). Multi-model ensemble hydrologic prediction using Bayesian model averaging. *Advances in Water Resources, 30*(5), 1371-1386.

Feng, S., & Hu, Q. (2007). Changes in winter snowfall/precipitation ratio in the contiguous United States. *Journal of Geophysical Research: Atmospheres (1984–2012), 112*(D15).

Fraley, C., Raftery, A. E., & Gneiting, T. (2010). Calibrating multimodel forecast ensembles with exchangeable and missing members using Bayesian model averaging. *Monthly Weather Review, 138*(1), 190-202.

Gao, X., Wang, M., & Giorgi, F. (2013). Climate change over China in the 21st century as simu-lated by BCC_CSM1. 1-RegCM4. 0. *Atmos. Oceanic Sci. Lett, 6*, 381-386.

Guo, L., & Li, L. (2014). Variation of the proportion of precipitation occurring as snow in the Tian Shan Mountains, China. *International Journal of Climatology*.

Hagg, W., Hoelzle, M., Wagner, S., Mayr, E., & Klose, Z. (2013). Glacier and runoff changes in the Rukhk catchment, upper Amu-Darya basin until 2050. *Global and Planetary Change, 110, Part A*, 62-73.

Hersbach, H. (2000). Decomposition of the continuous ranked probability score for ensemble prediction systems. *Weather and Forecasting, 15*(5), 559-570.

Hezel, P. J., Zhang, X., Bitz, C. M., Kelly, B. P., & Massonnet, F. (2012). Projected decline in spring snow depth on Arctic sea ice caused by progressively later autumn open ocean freeze-up this century. *Geophysical Research Letters, 39*(17). doi:10.1029/2012GL052794

Hoeting, J. A., Madigan, D., Raftery, A. E., & Volinsky, C. T. (1999). Bayesian model averaging: a tutorial. *Statistical science*, 382-401.

IPCC. (2013). *Climate Change 2013: The Physical Science Basis. Contribution of Working Group I to the Fifth Assessment Report of the Intergovernmental Panel on Climate Change* (T. F. Stocker, D. Qin, G.-K. Plattner, M. Tignor, S. K. Allen, J. Boschung, A. Nauels, Y. Xia, V. Bex, & P. M. Midgley Eds.). Cambridge, United Kingdom and New York, NY, USA: Cambridge University Press.

Kapnick, S. B., Delworth, T. L., Ashfaq, M., Malyshev, S., & Milly, P. (2014). Snowfall less sensitive

to warming in Karakoram than in Himalayas due to a unique seasonal cycle. *Nature Geoscience, 7*(11), 834-840.

Kawase, H., Nagashima, T., Sudo, K., & Nozawa, T. (2011). Future changes in tropospheric ozone under Representative Concentration Pathways (RCPs). *Geophysical Research Letters, 38*(5).

Krasting, J. P., Broccoli, A. J., Dixon, K. W., & Lanzante, J. R. (2013). Future changes in northern hemisphere snowfall. *Journal of Climate, 26*(20), 7813-7828.

Kure, S., Jang, S., Ohara, N., Kavvas, M. L., & Chen, Z. Q. (2013). Hydrologic impact of regional climate change for the snow-fed and glacier-fed river basins in the Republic of Tajikistan: statistical downscaling of global climate model projections. *Hydrological Processes, 27*(26), 4071-4090. doi:10.1002/hyp.9536

Li, B., Chen, Y., Chen, Z., Li, W., & Zhang, B. (2013). Variations of temperature and precipitation of snowmelt period and its effect on runoff in the mountainous areas of Northwest China. *Journal of Geographical Sciences, 23*(1), 17-30.

Li, B., Chen, Y., & Shi, X. (2012). Why does the temperature rise faster in the arid region of northwest China? *Journal of Geophysical Research, 117*(D16115).

Mir, R. A., Jain, S. K., Saraf, A. K., & Goswami, A. (2015). Decline in snowfall in response to temperature in Satluj basin, western Himalaya. *Journal of Earth System Science, 124*(2), 365-382.

Monaghan, A. J., Bromwich, D. H., & Schneider, D. P. (2008). Twentieth century Antarctic air temperature and snowfall simulations by IPCC climate models. *Geophysical Research Letters, 35*(7).

Ososkova, T., Gorelkin, N., & Chub, V. (2000). Water resources of central Asia and adaptation measures for climate change. *Environmental Monitoring and Assessment, 61*(1), 161-166.

Piazza, M., Boé, J., Terray, L., Pagé, C., Sanchez-Gomez, E., & Déqué, M. (2014). Projected 21st century snowfall changes over the French Alps and related uncertainties. *Climatic change, 122*(4), 583-594.

Raftery, A. E., Gneiting, T., Balabdaoui, F., & Polakowski, M. (2005). Using Bayesian model averaging to calibrate forecast ensembles. *Monthly Weather Review, 133*(5), 1155-1174.

Serquet, G., Marty, C., Dulex, J. P., & Rebetez, M. (2011). Seasonal trends and temperature dependence of the snowfall/precipitation‐day ratio in Switzerland. *Geophysical Research Letters, 38*(7).

Shi, Y., Shen, Y., Kang, E., Li, D., Ding, Y., Zhang, G., & Hu, R. (2007). Recent and future climate change in northwest China. *Climatic change, 80*(3-4), 379-393.

Sloughter, J. M. L., Raftery, A. E., Gneiting, T., & Fraley, C. (2007). Probabilistic quantitative precipitation forecasting using Bayesian model averaging. *Monthly Weather Review, 135*(9), 3209-3220.

Van Vuuren, D. P., Edmonds, J., Kainuma, M., Riahi, K., Thomson, A., Hibbard, K., Lamarque, J.-F. (2011). The representative concentration pathways: an overview. *Climatic Change, 109*, 5-31.

Winkelmann, R., Levermann, A., Martin, M. A., & Frieler, K. (2012). Increased future ice discharge from Antarctica owing to higher snowfall. *Nature, 492*(7428), 239-242.

Yasutomi, N., Hamada, A., & Yatagai, A. (2011). Development of a long-term daily gridded temperature dataset and its application to rain/snow discrimination of daily precipitation. *Global Environ. Res, 15*(2), 165-172.

Yatagai, A., Kamiguchi, K., Arakawa, O., Hamada, A., Yasutomi, N., & Kitoh, A. (2012).

APHRODITE: Constructing a Long-Term Daily Gridded Precipitation Dataset for Asia Based on a Dense Network of Rain Gauges. *Bulletin of the American Meteorological Society, 93*(9), 1401-1415.

3 Hydrologic modeling in the Kaidu River Basin

Modified from:

Fang, G., Yang, J., Chen, Y., Xu, C., & De Maeyer, P. (2015). Contribution of meteorological input in calibrating a distributed hydrologic model in a watershed in the Tianshan Mountains, China. Environmental Earth Sciences, 74(3), 2413-2424. doi:10.1007/s12665-015-4244-7.

Water resources are essential to the ecosystem and social economy worldwide, especially in the desert and oasis of the Tarim River Basin, whose water originates largely from the Tianshan Mountains characterized by complicated hydrologic processes and scarce meteorological observations. In this chapter, distributed hydrologic model of SWAT (Soil and Water Assessment Tool) was applied to the Kaidu River Basin, a watershed in the Tianshan Mountains and one of the headwaters of the Tarim River. To quantify the contribution of meteorological input to model output, a sensitivity analysis approach (SDP method, State-Dependent Parameter method) was applied before and after the model was calibrated. The sensitivity analysis shows meteorological input contributes up to 64 % of model uncertainty due to scarcity of observed meteorological data especially in the alpine region, and the groundwater flow is the most important hydrologic process in this watershed. Model calibration is robust with Nash–Sutcliffe coefficients ("NS"s) and "R^2"s over 0.80 for both the calibration period and the validation period where the length of the validation period is five times longer than the calibration period. The significance is obvious when compared to the simulation without considering the effect of spatial variation in meteorological input (NS = 0.80 and NS = 0.47 for "with lapse rates" and "without lapse rates", respectively). Accurate meteorological input is of great importance to the distributed hydrological model, especially in the mountainous regions.

Keywords: meteorological input; hydrologic modeling; hydrologic process; sensitivity analysis; model calibration

3.1 Introduction

The Tarim River (Figure 3.1), the longest inland river in China, is suffering from the ecological degradation, which is caused by over-consumption of water and its special hydrological conditions (Chen et al., 2011; Liu et al., 2011). It mainly originates from the Tianshan Mountains, runs through the oasis and finally disappears in the desert. With critical ecological problems such as the drying of river channel, weak water reproducible ability, deterioration of groundwater quality, degradation of natural vegetation and desertification in recent decades, water is even crucial in the Tarim River Basin (Li et al., 2014; Wu, 2012). As one of its headwaters, the Kaidu River, provides 78 % water demand of the artificial oasis around the Bosten Lake with a population of 1.15 million (Chen et al., 2013). Therefore, the Kaidu River is crucial to the eco-environmental and economic development of the lower reaches of the Tarim River.

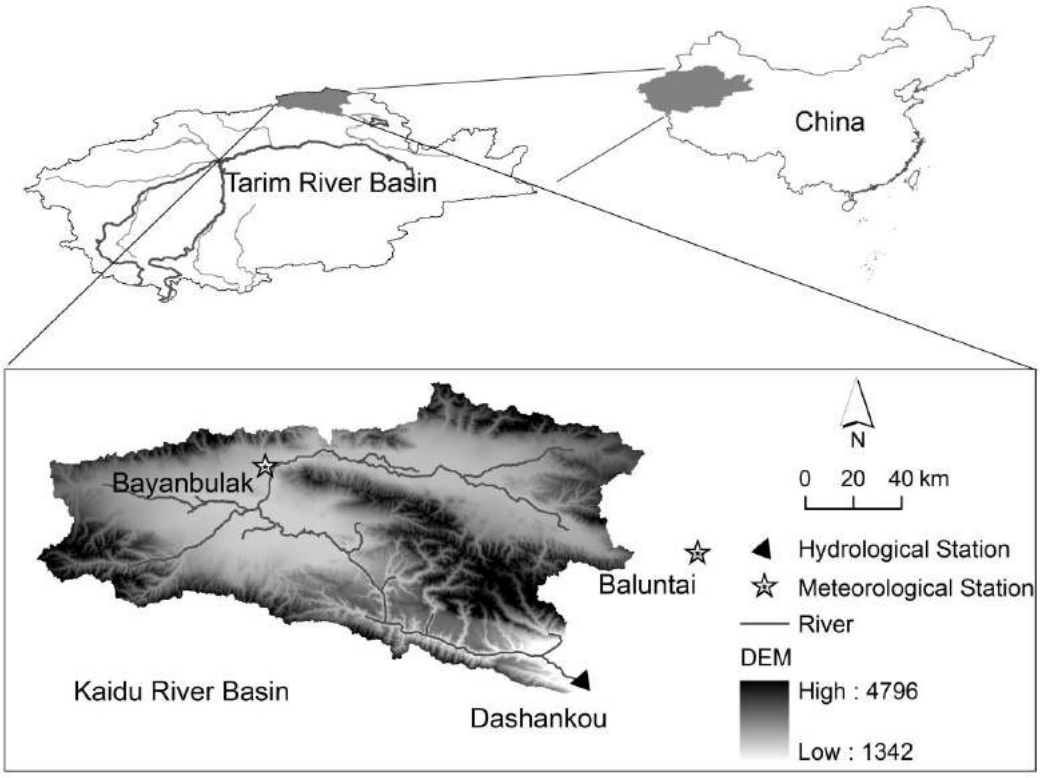

Figure 3.1 The location, topography and river system of the Kaidu River Basin

In spite of the importance of this watershed, there are few studies focusing on hydrological process due to the complicated topographic features and data scarcity (e.g., few meteorological data) in the alpine area and almost no study on the impact of meteorological input. Most studies

either focus on flow forecast (e.g., de la Paix et al., 2012; Kalra et al., 2012), conducting a short-period of flow simulation (e.g., Dou et al., 2011; Huang et al., 2010), or simulations with lumped models (e.g., Yang et al., 1987). As these studies are limited in understanding the watershed hydrology, distributed hydrologic modeling with a long-term simulation is appealing. Furthermore, as there is a data scarcity in meteorological input, which is very crucial to hydrologic modeling (Bobba et al., 1999; Gourley & Vieux, 2005), it is necessary to study the impact of meteorological input. More generally, though it has been proven that meteorological input influences the hydrologic model a lot (e.g., Tavakoli & De Smedt, 2013), to our best knowledge, few papers deal with how much this influence is and how much it affects model calibration. This is the major goal of this paper.

To achieve this goal, distributed hydrologic model of SWAT (Arnold et al., 1998), was applied to this watershed. To handle a large number of distributed parameters and understand the impact of meteorological input, a sensitivity analysis approach which combines the Morris method (Morris, 1991) and the SDP method (Ratto et al., 2007) was conducted to understand dominant hydrologic processes and quantify the effect of meteorological inputs on model calibration. The remaining of this chapter is constructed as follows: Section 3.2 introduces the hydrologic model and study area; Section 3.3 describes the sensitivity analysis and calibration approaches; and then Section 3.4 gives results and discussions, followed by conclusions in Section 3.5.

3.2 Hydrologic Model and Study Area

3.2.1 SWAT model

SWAT (Soil and Water Assessment Tool; Arnold et al., 1998), developed at the Agriculture Research Service of the United States Department of Agriculture, has been used for comprehensive modeling of the impacts of management practices and climate change on the hydrologic cycle and water resources at a watershed scale (e.g., Arnold et al., 2000; Arnold & Fohrer, 2005; Setegn et al., 2010). It is a distributed and time continuous watershed hydrologic model that runs on a daily step. To represent the spatial variability, a watershed is firstly divided into subbasins and each subbasin is then divided into hydrologic response units based on soil and landuse data. In SWAT, the simulation is based on water balance theory and runoff is predicted separately for each subbasin, which is illustrated in Figure 3.2, and route to obtain total runoff for the basin.

The climatic input (driving force) consists of daily precipitation, maximum/minimum temperature, solar radiation, wind speed and relative humidity. To account for orographic effects on precipitation and temperature, elevation bands were used. Within each elevation band, the precipitation and temperature are estimated based on their lapse rates and elevation. For more

details, refer to SWAT manuals (http://www.brc.tamus.edu/).

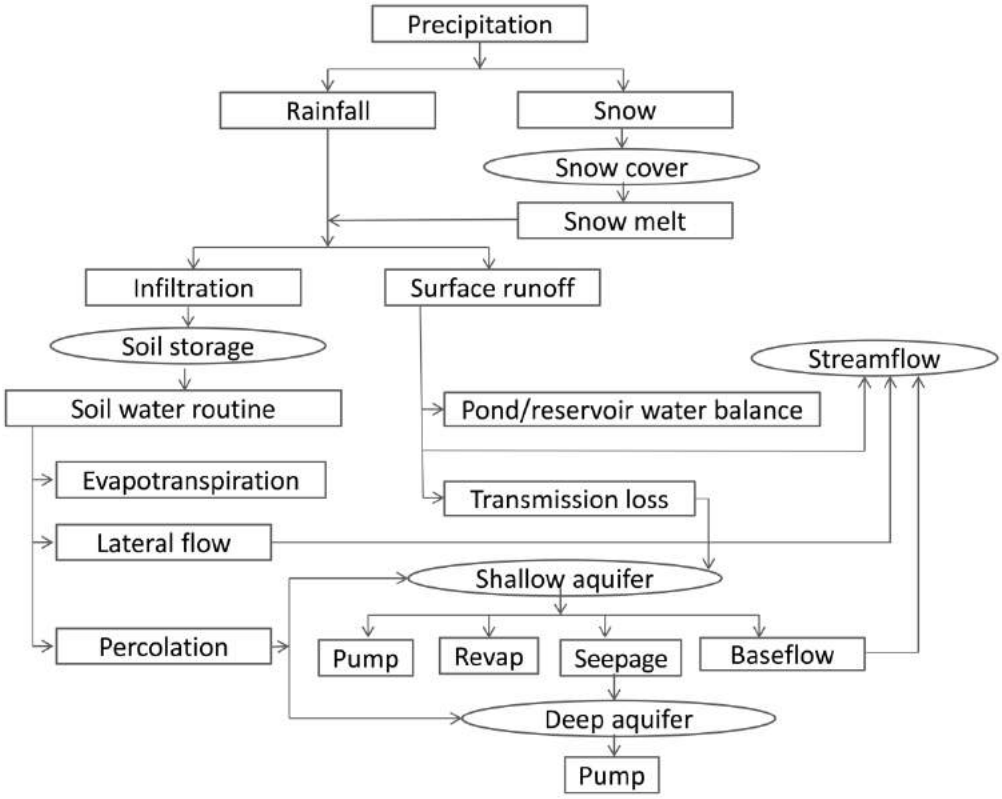

Figure 3.2 Hydrologic flow chart of SWAT. Boxes represent different hydrological processes, ellipses different water storages and arrows water flow directions (Adapted from Arnold et al. 1998)

3.2.2 Study area and data collection

The Kaidu River Basin, with a drainage area of 18,634 km^2 above the Dashankou hydrological station, is located on the south slope of the Tianshan Mountains, Northwest China. The basin extends from 82°58′ to 86°05′E, and from 42°14′ to 43°21′N. The altitude ranges from 1,340 m to 4,796 m above sea level (asl) with an average elevation of 2,995 m and an average slope of 23 %. This watershed has a complex topography including grassland, marsh, and surrounding mountainous alpine areas (Dou et al., 2011).

This watershed is characterized as temperate continental climate with alpine climate characteristic. The average annual temperature at the Bayanbulak meteorological station is -4.16 ℃ and annual precipitation is 287 mm, and generally precipitation falls as rain from May to September each year and as snow from October to April of the next year. The average daily flow at the Dashankou hydrological station is around 110 m^3/s(equivalent to 185 mm runoff), ranging from 15 m^3/s to 973 m^3/s. Watershed hydrology is driven by snowmelt in spring and rainfall/snowmelt in summer. Data used in this study include:

Meteorological data and hydrologic data: daily meteorological data of two stations are from China Meteorological Data Sharing Service System (http://cdc.cma.gov.cn/) from 1960 to 2010. One station is the Bayanbulak Station (2,458 m asl), which lies in the valley of mountainous regions in the watershed, and the other is the Baluntai Station (1,740 m asl), which is near the study region. Discharge data at the Dashankou hydrologic station are from Xinjiang Tarim River Basin Management Bureau. Available data include daily discharge from 1980 to 2002 and monthly discharge from 2003 to 2010.

Digital Elevation Model (DEM): 90 m DEM is from the Shuttle Radar Topography Mission (NASA, http://www2.jpl.nasa.gov/srtm/). DEM forms the basis for determining the drainage area, flow direction, basin boundary, etc.

Soil data: soil map, with a scale of 1:1000,000 is from Xinjiang Institute of Ecology and Geography, Chinese Academy of Sciences. The spatial distribution of soil is shown in Figure 3.3 (top) and the corresponding proportions are listed in Table 3.1 (left). Soil texture, soil depth and other information of each soil type were from Agricultural bureau and soil survey office of Xinjiang (1996).

Landuse data: landuse map with a scale of 1:100,000 is from the Environmental and Ecological Science Data Center for West China. Spatial distribution of landuse type is shown in Figure 3.3 (bottom) and relevant proportions are listed in Table 3.1 (right).

Table 3.1 Proportions of the soil types (left) and the landuse types (right) in the watershed

Soil type	Proportion (%)	Landuse type	Proportion (%)
Alpine meadow soil	38.0	Pasture	61.3
Subalpine steppe soil	21.4	Water and Ice	20.9
Alpine frost desert soil	16.0	Unexploited land	11.0
Brown desert soil	12.4	Wetland	6.1
Meadow steppe soil	7.0	Forest	0.5
Chestnut soil	2.6	Rural Settlements	0.1
Meadow-boggy soil	1.9	Cultivated Land	0.1
Fluvo-aquic soils	0.4		
Gray cinnamonic soil	0.1		

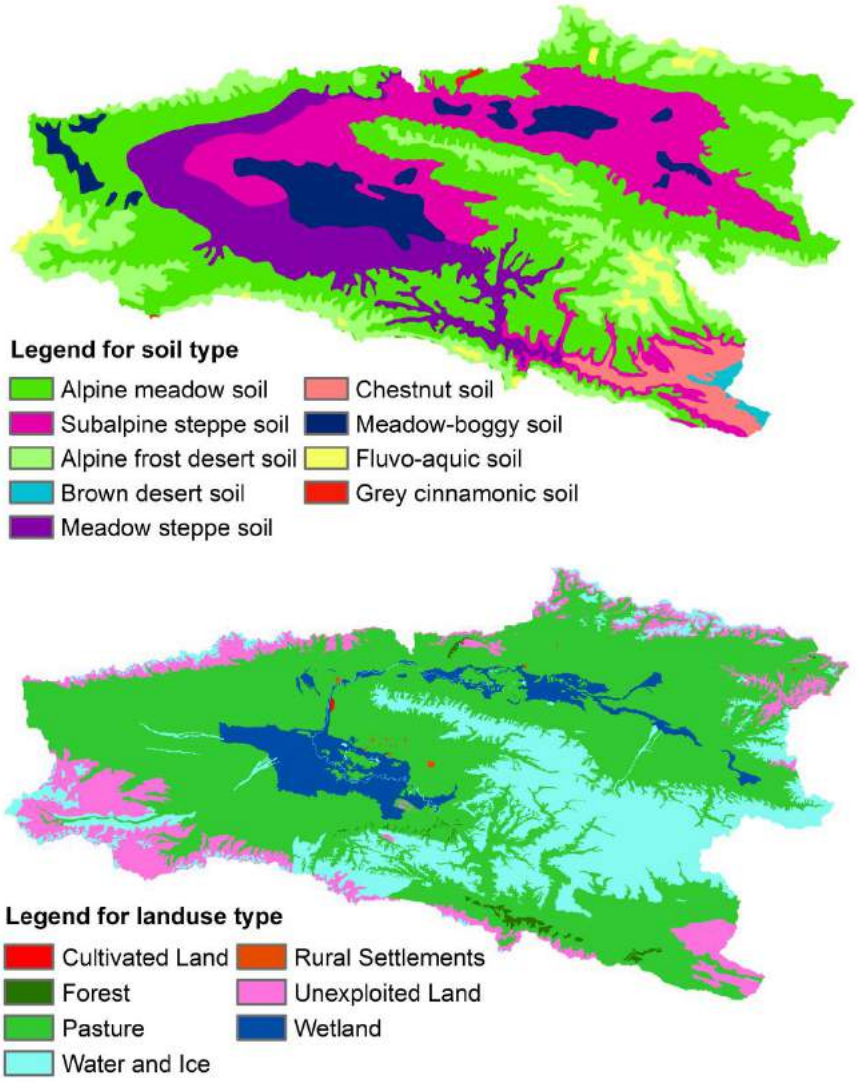

Figure 3.3 The spatial distribution of soil (top) and landuse (bottom) in the Kaidu River Basin

3.2.3 Model setup and initial parameter selection

After pre-processing these data in ArcSWAT (swat.tamu.edu/software/arcswat/), the SWAT model (version 2009) was set up with the following options: 1) Elevation band and lapse rate were used to represent the topographic effects on precipitation and temperature in the mountainous region; 2) Penman-Monteith method (Monteith, 1965) was utilized to calculate potential evapotranspiration; 3) The degree-day approach, which is generally deemed as an effective method to handle snow pack and snowmelt in data scarce mountains (Li & Williams, 2008), was used to model snowmelt; 4) Variable storage routing method (Williams, 1969) was used for river routing.

Model parameters related to flow simulation were initially selected based on literature

review and SWAT user manual (J. Arnold et al., 2011). When calibrating distributed model parameters, a factor which denotes a way to change a group of parameters was used to avoid confusion with model parameters (e.g., factor *r__CN2* is to relatively change all distributed parameters *CN2*, and *v__Tlaps* is to replace all parameters *Tlaps*), as proposed in (J. Yang et al., 2007). Table 3.2 lists these factors along with their meanings of their underlying parameters and ranges, among which *v__Tlaps* and *v__Plaps*, the values of the lapse rates of temperature and precipitation, are two factors to measure the topographical variation of meteorological input. This work studied the contribution of meteorological input through these two factors. To investigate the impact of spatial variation of meteorological input, another simulation was set up without these two lapse rates (i.e., excluding *v__Tlaps* and *v__Plaps*), and refer this to "without lapse rates" and the previous to "with lapse rates", respectively.

A warm-up period is normally used to eliminate the influence of initial state variables (e.g., soil moisture, groundwater storage, etc.) on simulation, and the longer the warm-up period, the less effect initial state variables will have on the simulation (J. Yang et al., 2012). In this study, a seven-year period (1979 ~ 1985) was used for model warm-up after some tests. To calibrate the model, the split sample procedure was used: daily data from 1986 to 1989 were used for model calibration, and daily data from 1990 to 2002 (first validation period) and monthly data from 2003 to 2010 (second validation period) were used to test the model performance. Both calibration and validation contain dry and wet years, and longer validation period was used to show the robustness of the calibrated model.

Table 3.2 Selected factors and their initial values and ranges for sensitivity analysis, and their estimated values

No.	Factor [a]	Range [b]	Underlying SWAT parameter	Initial value	Estimated value
1	*v__Tlaps*	[-10, 0]	*Tlaps:* Temperature lapse rate (℃ km^{-1})	0	-9.23
2	*v__Alpha_bf*	[0, 1]	*Alpha_bf:* Baseflow alpha factor	0.048	0.94
3	*v__Plaps*	[100, 200]	*Plaps:* Precipitation lapse rate (mm km^{-1})	0	165.00
4	*v__Gwqmn*	[0, 1000]	*Gwqmn:* Threshold water level in shallow aquifer for baseflow (mm)	0	72.00
5	*r__Sol_k*	[-0.5, 2]	*Sol_kl*: Saturated hydraulic conductivity (mm h^{-1})	0	0.87
6	*v__Gw_delay*	[0, 500]	*Gw_delay*: Groundwater delay time (day)	31	340.60
7	*v__Esco*	[0, 1]	*Esco*: Soil evaporation compensation factor (-)	0.95	0.36
8	*r__Slsubbsn*	[-0.3, 0.3]	*Slsubbsn*: Average slope length (m)	0	0.15
9	*v__Ch_k2*	[0, 500]	*Ch_k2*: Effective hydraulic conductivity in main channel alluvium (mm h^{-1})	0	253.10
10	*r__Sol_awc*	[-0.5, 0.5]	*Sol_awc*: Available water capacity of the soil layer (-)	0	-0.21
11	*r__CN2*	[-0.15, 0.15]	*CN2*: SCS runoff curve number for moisture condition	0	0.04
12	*v__Smfmx*	[-0, 10]	*Smfmx*: Snowmelt factor on June 21 (mm $℃^{-1}$ d^{-1})	4.5	7.71
13	*r__Sol_z*	[-0.5, 0.5]	*Sol_z*: Depth from soil surface to bottom of layer (mm)	0	-
14	*v__Gw_revap*	[-0.02, 0.2]	*Gw_revap*: Groundwater "revap" coefficient	1.0	-
15	*v__Surlag*	[0, 24]	*Surlag*: Surface runoff lag time (day)	4	-
16	*v__Revapmn*	[0, 500]	*Revapmn*: Threshold depth of water in shallow aquifer for revap (mm)	1.0	-
17	*r__Slope*	[-0.1, 0.1]	*Slope*: Average slope steepness (-)	0	-
18	*v__Ch_k1*	[0, 300]	*Ch_k1*: Effective hydraulic conductivity in tributary channel alluvium (mm h^{-1}).	0	-
19	*v__Smfmn*	[0, 10]	*Smfmn*: Snowmelt factor on Dec. 21 (mm $℃^{-1}$ d^{-1})	4.5	-
20	*v__Epco*	[0, 1]	*Epco*: Plant uptake compensation factor	1.0	-
21	*v__Ch_n2*	[0, 0.3]	*Ch_n2*: Manning's "n" for main channel (-)	0.18	-
22	*r__OV_N*	[-0.5, 0.5]	*OV_N*: Manning's "n" for overland flow (-)	0.15	-
23	*r__Sol_alb*	[-0.2, 0.2]	*Sol_alb*: Moist soil albedo (-)	0	-
24	*v__Sftmp*	[-1, 1]	*Sftmp*: Snowfall temperature (℃)	1.0	-
25	*v__Smtmp*	[-1, 1]	*Smtmp*: Snow melt base temperature(℃)	0.5	-

[a] Here, '*v__*' or '*r__*' means a replacement or a relative change to the initial parameter values.

[b] The ranges for the factors are based on literature data (e.g., the range of *v__Plaps* is from (Zhou, 1999) and SWAT user's manual (Arnold et al. 2011).

3.3 Methodology

3.3.1 Sensitivity analysis

Sensitivity analyses are valuable tools for identifying important model parameters (in this case is "factors"). In this study, a sensitivity analysis approach combining the Morris method (Morris, 1991) and the SDP method (Ratto et al., 2007) was applied to screen out unimportant factors and identify the most important ones. Its applications range from simple conceptual model (e.g., HYMOD in Yang 2011) to physical and distributed models (e.g. TOPMODEL in Ratto et al. 2007; Wetspa in Yang et al. 2012; MOBIDIC in Yang et al., 2014), and it has been proven to be effective and efficient. Firstly the Morris method was used to screen out insensitive hydrological factors and thus to reduce the number of factors for next sensitivity analysis. In the second step, the SDP was implemented to quantitatively compute the main effect and first-order interactions between these reduced factors.

Morris method

The Morris method is a qualitative method to measure factor sensitivity and factor interaction or nonlinearity. For a *n*-dimensional random variable $\mathrm{X} = (x_1, \cdots, x_i, \cdots, x_n)$ at its j^{th} sample $(x_{1j}, \cdots, x_{ij}, \cdots, x_{nj})$, the local sensitivity measure (elementary effect) d_{ij} for x_i at j^{th} sample is computed based on OAT (One-At-a-Time) as follows:

$$d_{ij} = \frac{f(x_{1j}, \cdots, x_{ij}+\Delta, \cdots, x_{nj}) - f(x_{1j}, \cdots, x_{ij}, \cdots, x_{nj})}{\Delta}, \; i = 1,2,\ldots n; \; j = 1,2,\ldots,m \qquad \text{(Equation 3-1)}$$

where *f(.)* is the model output (or relevant objective function), X are model factors with x_i normalized to [0,1] to eliminate the scale effect, and $\Delta = \frac{p}{2(p-1)}$ is the predefined increment and normally *p* takes the value within the range of [4,10] (Saltelli et al., 1999) and in this study *p* was set to 10 meaning Δ = 5/9. Local sensitivity measures of each input factor are estimated by randomly sampling in the factor space, by which a finite distribution of the local sensitivity measures obtained. For example, for basic sample size *m*, one can obtain a group of elementary effects d_{ij} (i = 1, ..., m) for factor x_i. From these values, two statistics are obtained: one is the mean of absolute values of the elementary effects (μ^*), which measures the factor sensitivity (e.g., for x_i, $\mu_i^* = \sum_{j=1}^{m} |d_{ij}|/m$), and the other is the standard deviation of the elementary effects (σ), which measures the degree of factor interaction or nonlinearity (e.g., for x_i,

$\sigma_i = \sqrt{\sum_{j=1}^{m}\left(d_{ij} - \frac{\sum_{j=1}^{m} d_{ij}}{m}\right)^2 /(m-1)}$). The higher μ^* is, the more important the factor is to model output, and the higher (σ), the more interactions are with other factors or more nonlinear to the model output. Totally, the Morris method needs *m*(n+1)* model runs to estimate these two sensitivity indices for each factor, and normally *m = 50* is sufficient (J. Yang et al., 2012).

State-Dependent Parameter method (SDP)

For independent input factors, SDP method is based on the idea of the decomposition of variance of model output *Y* to factors *X*:

$$V = \sum_i V_i + \sum_i \sum_{j>i} V_{ij} + \cdots + V_{1,2,\cdots,n} \quad \text{(Equation 3-2)}$$

Where

$$V_i = V(E(Y|X_i))$$

$$V_{ij} = V\left(E(Y|X_i, X_j)\right) - V_i - V_j$$

and so on. Herein, *V*(.) and E(.) denote variance and expectation operators, *V* is the total variance, and V_i and V_{ij} are total variance and partial variances of the i^{th} factor. Normalize these variances with *V*, the following sensitivity indices can be obtained:

$$S_i = \frac{V_i}{V}, 1 \le i \le n \quad \text{(Equation 3-3)}$$

$$S_{ij} = \frac{V_{ij}}{V}, 1 \le i < j \le n \quad \text{(Equation 3-4)}$$

$$S_{Ti} = S_i + \sum_j S_{ij} + \sum_j \sum_k S_{ijk} + \cdots + S_{1,2,\ldots,n}, 1 \le i \le n \quad \text{(Equation 3-5)}$$

where S_i is the main effect, which represents the average achieved reduction of output variance when factor X_i is fixed, S_{ij} is the second order interaction between X_i and X_j, and S_{Ti} is the total effect representing the average output variance when X_i stays unfixed. In practice, S_i is used to measure the average variance in the output that can be reduced when X_i is fixed and S_{Ti} is used to measure the average variance in the output remains when X_i stays unfixed (Tarantola et al., 2002).

The SDP method is based on recursive filtering and smoothing estimation and can estimate these main effects (S_i) and first-order interactions (S_{ij}) based on its approximation to second-order ANOVA regression model. And "quasi-total effect", $S_{Di} = S_i + \sum_j S_{ij}$, is used to approximate S_{Ti} when R^2 of second-order ANOVA is high enough (e.g., larger than 0.80).

3.3.2 Model calibration and evaluation

To calibrate the distributed hydrological model, SCE-UA method (Duan et al., 1992)was used. This algorithm has been proven to be consistent, effective, and efficient in locating the globally optimal model parameters of a hydrologic model (Gupta et al., 1999).

The objective function for calibration is Nash-Sutcliffe coefficient (*NS*) (Nash & Sutcliffe, 1970):

$$NS = 1 - \frac{\sum_{i=1}^{n}\left(Y_i^{obs} - Y_i^{sim}\right)^2}{\sum_{i=1}^{n}\left(Y_i^{obs} - Y^{mean}\right)^2} \quad \text{(Equation 3-6)}$$

Where Y_i^{obs} and Y_i^{sim} are the i^{th} observed and simulated flows, Y^{mean} is the mean of observed data, and n is the number of observations. *NS* donates how well the simulation matches the observation. *NS* ranges between -∞ and 1.0, with *NS* = 1 meaning a perfect fit. The higher this value, the more reliable the model is.

To evaluate model performance, in addition to *NS*, percent bias (*PBIAS*) and coefficient of determination (R^2) were also used. *PBIAS* is computed as:

$$PBIAS = \frac{\sum_{i=1}^{n}\left(Y_i^{sim} - Y_i^{obs}\right)}{\sum_{i=1}^{n}\left(Y_i^{obs}\right)} \quad \text{(Equation 3-7)}$$

PBIAS measures the average deviation of the simulated data from their observed counterparts. Positive values indicate an overestimation of the observation, while negative values indicate an underestimation. The smaller of $|PBIAS|$, the smaller deviation of the simulation. Generally, $|\text{PBIAS}|$ < 10 % shows good modeling. R^2 describes the degree of collinearity between simulated and measured data. Normally NS > 0.50, $|\text{PBIAS}|$ < 25 % and R^2 > 0.6 are taken as the criteria of satisfactory modeling of the river discharge, and model performance can be evaluated as excellent if *NS* > 0.75 and $|PBIAS|$ < 10 % (Moriasi et al., 2007).

In this study, the simulation “with lapse rates” and simulation “without lapse rates” were analyzed separately following the same procedure. Firstly, the Morris method was applied to initially selected factors (Table 3.2) to screen out the unimportant factors, and then the sensitivities of the sensitive ones were quantified by the SDP method. Secondly, the calibration was applied to the important factors, followed by another sensitivity analysis with the SDP method. The contribution of the meteorological input was analyzed based on the sensitivity and calibration results, and the comparison between the simulation “with lapse rates” and simulation “without lapse rates”.

3.4 Results and Discussion

In this section, we mainly presented and discussed the result of the simulation "with lapse rates", and the result of simulation "without lapse rates" was only for the comparison purpose. Hereafter, results and discussion are based on the simulation "with lapse rates" unless otherwise specified.

3.4.1 Sensitivity analysis

With m = 50, the Morris method took 1300 model runs. Figure 3.4 shows the sensitivity result for each factor based on the Morris method, where μ^* represents its sensitivity and σ its interaction with other factors or nonlinearity of the factor. These twenty-five factors were grouped into three classes visually based on their "μ^*"s: extremely sensitive, medially sensitive and insensitive. *v__Tlaps*, *v__Alpha_bf* and *v__Plaps* are the extremely sensitive factors with strong nonlinearity in the meanwhile. *v__Tlaps* and *v__Plaps* influence the temperature and precipitation input in each elevation band, and have intense impact on water yield and water balance. *v__Alpha_bf*, representing the baseflow recession constant, describes the response of groundwater to recharge change and is an important factor that influences groundwater flow. The medium sensitivity class includes 7 factors: *v__Gwqmn* and *v__Gw_delay* are factors related to groundwater flow and groundwater–stream water interactions; *v__Ch_k2*, *r__Sol_k* and *r__Sol_awc* dominate the infiltration of surface water into groundwater; *v__Esco*, with its underlying parameter *Esco* being the compensation factor of soil evaporation, controls the actual evapotranspiration; r__*Slsubbsn* is factor indicating the changes of average slope length. Factors at the bottom left of Figure 3.4 including *r__CN2* and *v__Smfmx* are insensitive. Note that *r__CN2* is not sensitive in this study while it was extremely sensitive in many previous studies (e.g., Saha et al., 2014; Van Griensven et al., 2006). This might be attributed to the hydrological characteristics of the Kaidu River Basin: it has a large area of wetland (1,137 km^2) and flatland (37 % of the study area with a slope under 8.7 %). The high proportion of wetland and flatland resulted in the low sensitivity of *r__CN2* as identified by (Schmalz & Fohrer, 2009). All snowmelt related factors, e.g., *v__Smfmx*, *v__Sftmp*, *v__Smtmp*, are not sensitive, which indicates snow process is not so important in the Kaidu River Basin. This is corroborated with an analysis of average monthly precipitation allocation: the precipitation from October to March (winter season) only consists of 9 % and 4 % of the yearly precipitation at Bayanbulak and Balutai, respectively.

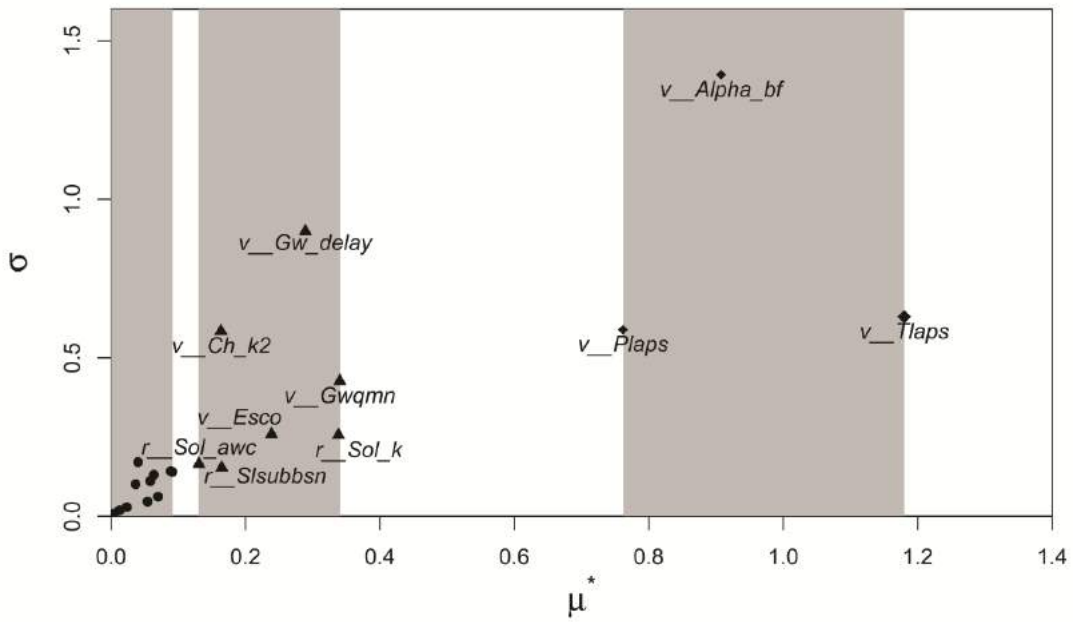

Figure 3.4 Factor sensitivity based on the Morris method (diamond denotes extremely sensitive, triangle medially sensitive, and closed circle insensitive)

After excluding insensitive factors identified by the Morris method, the SDP method was applied to estimate the main effect (S_i) and first-order interaction (S_{ij}) of the sensitive factors. To ensure that all potential sensitive factors are quantified, another two factors, i.e., *r__CN2* and *v__Smfmx*, the most sensitive ones in the insensitive group, were also included. Therefore, 12 factors were analyzed using SDP method. It took 600 model runs and the R^2 of the second order ANOVA model is 93.0 %, which means it explains over 90 % of the model uncertainty (i.e., variation of *NS*). The result is shown in Table 3.3. The most sensitive factor is *v__Tlaps*, followed by *v__Plaps* and *v__Alpha_bf*. Other factors are not so sensitive for both S_i and S_{Di}. *v__Tlaps* and *v__Plaps* control the driving force (i.e., precipitation and temperature), and the main effect of these two factors is 64.0 % (i.e. sum of main effects of *v__Tlaps* and *v__Plaps*, and their first order interaction), contributing to over half of the model uncertainty. *v__Alpha_bf* influences the groundwater flow and its main effect is 13 %. This suggests that fixing of these three factors (e.g. through calibration) leads to over 77 % reduction of model uncertainty. This result is the same as that based on the Morris method. It is worth noting that the low sensitivity indices of other factors do not mean that they are not sensitive but that their contribution to the model output is not as significant as these three factors.

Table 3.3 The main effect (S_i), quasi-total effect (S_{Di}) and the first-order interaction (S_{ij}, the triangular matrix on the right) of factors as percentage based on the SDP method. The values are given with only one decimal place.

Factor	S_i	S_{Di}	S_{ij}											
			v__Tlaps	*v__Alpha_bf*	*v__Plaps*	*v__Gwqmn*	*r__Sol_k*	*v__Gw_delay*	*v__Esco*	*r__Slubbon*	*v__Ch_k2*	*r__Sol_awc*	*r__CN2*	*v__Smfmx*
v__Tlaps	37.8	41.5												
v__Alpha_bf	13.0	13.3	0.2											
v__Plaps	24.6	27.5	1.6	0.0										
v__Gwqmn	1.6	2.0	0.3	0.0	0.0									
r__Sol_k	7.3	9.0	1.1	0.0	0.3	0.1								
v__Gw_delay	0.3	1.2	0.2	0.0	0.7	0.0	0.0							
v__Esco	0.9	1.2	0.2	0.0	0.0	0.0	0.1	0.0						
r__Slubbon	0.9	1.3	0.1	0.0	0.2	0.0	0.1	0.0	0.0					
v__Ch_k2	0.0	0.1	0.0	0.1	0.0	0.0	0.0	0.0	0.0	0.0				
r__Sol_awc	0.3	0.3	0.0	0.0	0.0	0.0	0.0	0.0	0.0	0.0	0.0			
r__CN2	0.0	0.0	0.0	0.0	0.0	0.0	0.0	0.0	0.0	0.0	0.0	0.0		
v__Smfmx	0.9	1.0	0.0	0.0	0.1	0.0	0.0	0.0	0.0	0.0	0.0	0.0	0.0	
R^2	87.6	93.0												

3.4.2 Model calibration and evaluation

Calibration was then carried out on these twelve factors using SCE-UA method. With daily *NS* = 0.80 during the calibration period, the optimal values are given in Table 3.2. The calibrated *v__Plaps* is 165 mm km^{-1}, which is very close to other studies in this region (e.g., 162 mm km^{-1}

in Lin (1985); 156.4 mm km^{-1} in Zhao et al. (2011)). *v__Tlaps* is -9.23 ℃ km^{-1}, within the range of the study of Chen (2012) (i.e., from -11.8 ℃ km^{-1} to -7.3 ℃ km^{-1}) based on temperature data from several stations in the south slope of Tianshan Mountains. This temperature lapse rate, which is close to the dry adiabatic lapse rate (-9.8 ℃ km^{-1}), is related to the characteristics of our study region, i.e., a mountainous watershed located in the arid area with low pressure, low humidity and high wind speed (Blandford et al., 2008). The mean pressure and relative humidity are 0.828 × 10^5 Pa and 42 % at Baluntai Station, and 0.758 × 10^5 Pa and 69 % at Bayanbulak Station. Besides, there are over 12 % of days with wind speed higher than 5 m s^{-1} (strong wind) and 38 % of days higher than 3 m s^{-1} (moderate to strong wind) at Bayanbulak Station.

As discussed above, the hydrologic response is dominated by the meteorological input. By fixing two factors *v__Tlaps* and *v__Plaps* to their optimal values, another SDP application was performed to the remaining ten factors to study the important hydrologic processes without the influence of meteorological input. As it turns out, the most sensitive factors are *v__Alpha_bf* (S_i = 0.57) and *v__Gw_delay* (S_i = 0.29), less sensitive factors are *r__Sol_k* (S_i = 0.02) and *v__Smfmx* (S_i = 0.02) and other factors are only sensitive through the interaction with these factors. Factors related to groundwater process (i.e. *v__Alpha_bf*, *v__Gw_delay*) account for more than 80 % of the model uncertainty (sum of main effects of these two factors and first order interactions between them). Although by the Morris method, *v__Smfmx* is an insensitive factor, it is a relatively sensitive one by the SDP method when fixing *v__Tlaps* and *v__Plaps*. It is indicative that the dominant hydrological process is the groundwater flow, and then the snowmelt flow and evapotranspiration. To verify the importance of groundwater, a baseflow separation was done to the observed discharge using the digital filter technique (J. Arnold et al., 1995), which shows that groundwater contributes to 72 % ~ 86 % of the total flow (or runoff). The high percentage of groundwater might be due to the large flat valley area between steep mountains, i.e., large area of wetland and flatland as is indicated in Section 3.4.1.

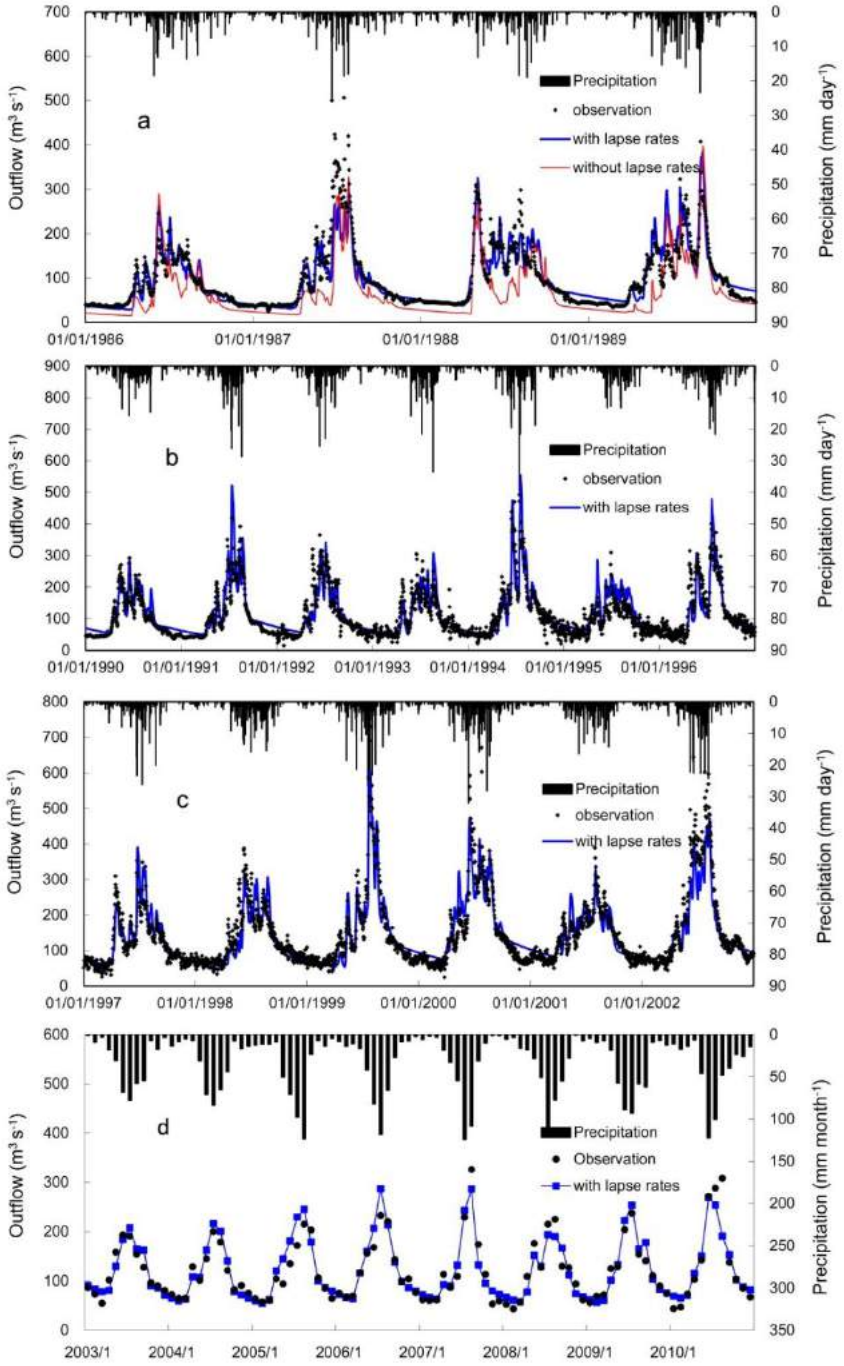

Figure 3.5 Observed and simulated outflow series at the Dashankou hydrological station during the calibration period (a – daily streamflow) and the validation period (b and c - daily streamflow and d – monthly streamflow)

Table 3.4 and Figure 3.5 show agreement between the simulated and observed flow series. As indicated by the statistics in Table 3.4, the model performs well for both the calibration period (1986 ~ 1989) and validation periods (first validation period 1990 ~ 2002 and second validation period 2003 ~ 2010), in spite of the length of the validation period is five times longer than the calibration period. The "*NS*"s, "*PBIAS*"s, "R^2"s are 0.80, 0.01 %, 0.80 for the

calibration period, 0.81, 2.94 %, 0.81 for the first validation period, and 0.86, 1.31 %, 0.87 for the second validation period. These "*NS*"s, "*PBIAS*"s, and "R^2"s are within the excellent range proposed by Moriasi et al. (2007).

Table 3.4 Model performances for the calibration and validation periods

Statistics	*NS*	*PBIAS*	R^2
"With lapse rates"			
Calibration period 1986~1989 (daily data)	0.80	0.01 %	0.80
First validation period 1990~2002 (daily data)	0.81	2.94 %	0.81
Second validation period 2003~2010 (monthly data)	0.86	1.31 %	0.87
"Without lapse rates"			
Calibration period 1986~1989 (daily data)	0.47	-30.22 %	0.66
First validation period 1990~2002 (daily data)	0.49	-32.22 %	0.71
Second validation period 2003~2010 (monthly data)	0.35	-36.51 %	0.80

The statistics above are corroborated by Figure 3.5. In Figure 3.5, the simulated flow matches the observation very well except for some peaks in summer seasons in 1987, 1999 and 2002. This might be due to the glacier melt in summer which is not accounted for in this model. Generally, the model can simulate the flow response to the rainfall and snowmelt. Notice there is a fluctuation in the baseflow since 1992 when the Dashankou hydropower station (4 km above the Dashankou hydrological wtation) started to operate. However, this hydropower station does not seem to have too much effect on the daily outflow.

To demonstrate the effect of the meteorological input, the results of the simulation "without lapse rates" were also shown in Table 3.4 and Figure 3.6a. Compared to simulation "with lapse rates", simulation "without lapse rates" was unable to capture most of the discharges in the Kaidu River Basin, with *NS* equals to 0.47 for the calibration period, 0.49 for the first validation period and 0.35 for the second validation period. Snowmelts in spring (e.g., in 1986, 1987 and 1989) were underestimated, peaks in summer (e.g., in 1988) were not captured, and baseflow was extremely underestimated. For "without lapse rates", the underestimation of the baseflow is mainly related to over-simplification of spatial distribution of precipitation and temperature. As a result, this leads to less average annual precipitation (252 mm) and higher average temperature (5.1 ℃) than these of "with lapse rate" whose average annual precipitation is 378 mm and average temperature is -1.9 ℃. When driving the hydrologic model, it will cause less precipitation input and higher evapotranspiration, and this leads to less groundwater recharge,

and eventually less groundwater discharge. Figure 3.6 shows how different the spatial variation of annual average precipitation using precipitation lapse rate from the one without precipitation lapse rate. This shows the importance of spatial variation of meteorological input in calibrating a distributed hydrological model and confirms the conclusion that high quality of distributed rainfall data contributes to good hydrological model performance (Lee et al., 2013; Tavakoli & De Smedt, 2013).

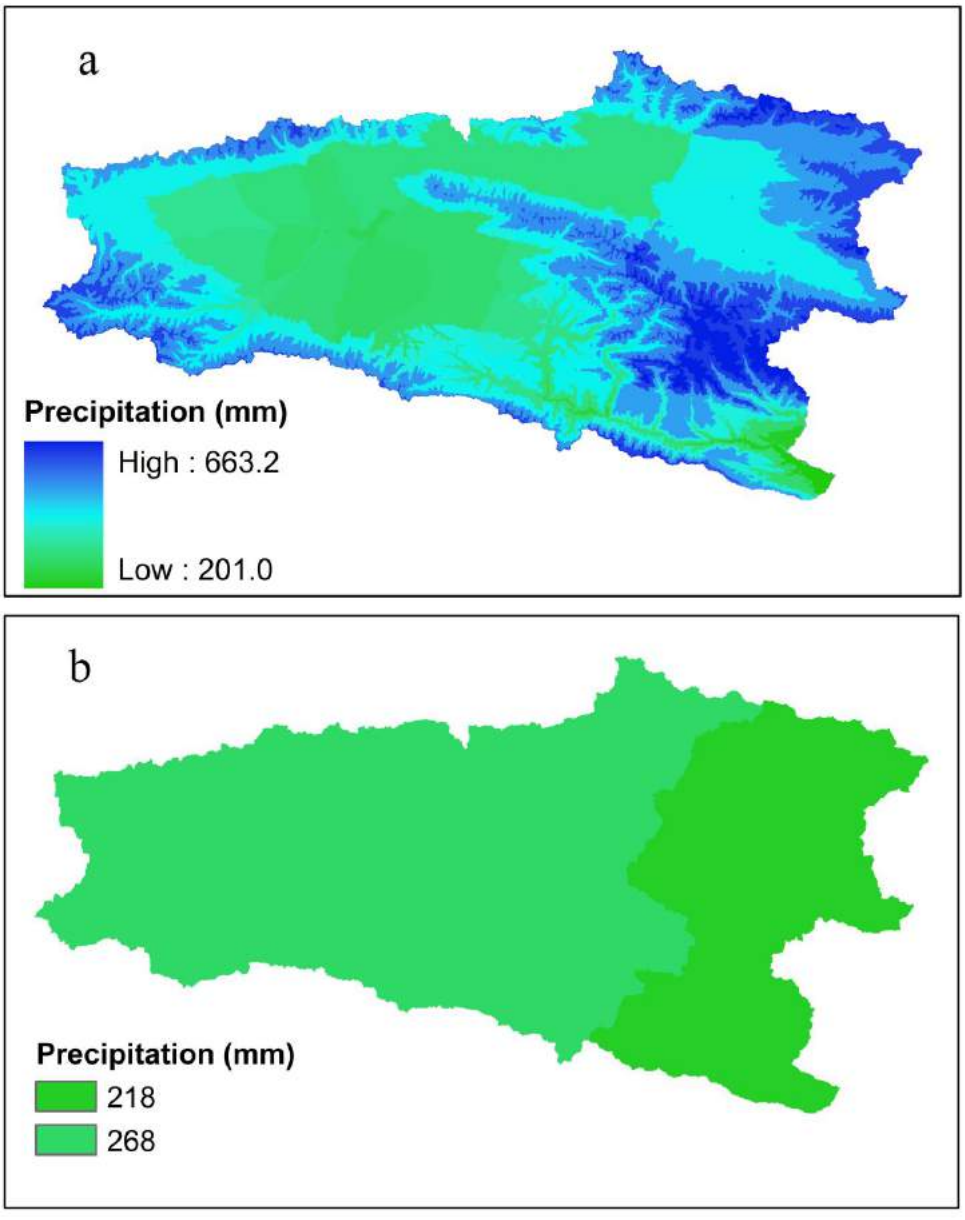

Figure 3.6 Topographical distribution of annual mean precipitation for simulations with lapse rates (a) and without lapse rates (b)

3.5 Conclusions

This paper implemented a combined sensitivity analysis approach to the application of SWAT in the Kaidu River Basin to investigate the contribution of meteorological input in calibrating distributed hydrologic model. The following conclusions can be drawn:

1) Our model is an effective tool to simulate the hydrologic processes. Simulated daily flow series are in agreement with the observed ones, with "NS"s and "R^2"s over 0.80 and $|PBIAS| < 3\%$ for both calibration period and validation period. This calibration is robust and tested by the validation period whose length is five times longer than the calibration period.

2) Sensitivity analysis shows *v__Tlaps* and *v__Plaps* are the two most important factors with main effects of 64.0 %. This indicates the model uncertainty largely results from the meteorological inputs due to the scarcity of observed meteorological data, especially in the alpine regions.

3) Groundwater flow is the most important hydrologic process in this watershed. Fixing *v__Tlaps* and *v__Plaps* to their optimal values, factors related to groundwater process account for over 80 % of the model uncertainty, which is consistent with the result of baseflow separation using digital filter technique.

4) Compared to the simulation "without lapse rates", the simulation "with lapse rates" shows significant improvement on daily flows, especially in baseflow simulation (groundwater discharge), which suggests high spatial resolution meteorological data (e.g., satellite data) should be used for hydrologic modeling in this region.

References

Agricultural bureau and soil survey office of Xinjiang (1996) Xinjiang soil. Science Press, Beijing

Chen X (2012) Hydrological model of inland river basin in arid land. China Environmental Science Press, Beijing

Arnold, J., Allen, P., Muttiah, R., & Bernhardt, G. (1995). Automated base flow separation and recession analysis technicues. *Ground water, 33*(6), 1010-1018.

Arnold, J., Kiniry, J., Srinivasan, R., Williams, J., Haney, E., & Neitsch, S. (2011). *Soil and Water Assessment Tool input/output file documentation, version 2009*. Retrieved from

Arnold, J., Muttiah, R., Srinivasan, R., & Allen, P. (2000). Regional estimation of base flow and groundwater recharge in the Upper Mississippi river basin. *Journal of Hydrology, 227*(1), 21-40.

Arnold, J. G., & Fohrer, N. (2005). SWAT2000: current capabilities and research opportunities in applied watershed modelling. *Hydrological Processes, 19*(3), 563-572. doi:10.1002/hyp.5611

Arnold, J. G., Srinivasan, R., Muttiah, R. S., & Williams, J. R. (1998). Large area hydrologic modeling and assessment - Part 1: Model development. *Journal of the American Water Resources Association, 34*(1), 73-89. doi:10.1111/j.1752-1688.1998.tb05961.x

Blandford, T. R., Humes, K. S., Harshburger, B. J., Moore, B. C., Walden, V. P., & Ye, H. (2008).

Seasonal and synoptic variations in near-surface air temperature lapse rates in a mountainous basin. *Journal of Applied Meteorology and Climatology, 47*(1), 249-261.

Bobba, A. G., Jeffries, D. S., & Singh, V. P. (1999). Sensitivity of hydrological variables in the Northeast Pond River Watershed, Newfoundland, Canada, due to atmospheric change. *Water resources management, 13*(3), 171-188.

Chen, Y., Du, Q., & Chen, Y. (2013). *Sustainable water use in the Bosten Lake Basin*. Beijing: Science press.

Chen, Z., Chen, Y., Li, W., & Chen, Y. (2011). Changes of runoff consumption and its human influence intensity in the mainstream of Tarim river. *Acta Geographica Sinica, 66*(1), 89-98.

de la Paix, M. J., Lanhai, L., Jiwen, G., de Dieu, H. J., & Theoneste, N. (2012). Analysis of snowmelt model for flood forecast for water in arid zone: case of Tarim River in Northwest China. *Environmental Earth Sciences, 66*(5), 1423-1429.

Dou, Y., Chen, X., Bao, A., & Li, L. (2011). The simulation of snowmelt runoff in the ungauged Kaidu River Basin of TianShan Mountains, China. *Environmental Earth Sciences, 62*(5), 1039-1045.

Duan, Q., Sorooshian, S., & Gupta, V. (1992). Effective and efficient global optimization for conceptual rainfall-runoff models. *Water Resources Research, 28*(4), 1015-1031.

Gourley, J. J., & Vieux, B. E. (2005). A method for evaluating the accuracy of quantitative precipitation estimates from a hydrologic modeling perspective. *Journal of Hydrometeorology, 6*(2), 115-133.

Gupta, H. V., Sorooshian, S., & Yapo, P. O. (1999). Status of automatic calibration for hydrologic models: Comparison with multilevel expert calibration. *Journal of Hydrologic Engineering, 4*(2), 135-143.

Huang, Y., Chen, X., Bao, A., & Ma, Y. (2010). Distributed Hydrological Modeling in Kaidu Basin: MIKE-SHE Model Calibration and Uncertainty Estimation. *Journal of Glaciology and Geocryology, 32*(3), 567-572.

Kalra, A., Li, L., Li, X., & Ahmad, S. (2012). Improving Streamflow Forecast Lead Time Using Oceanic-Atmospheric Oscillations for Kaidu River Basin, Xinjiang, China. *Journal of Hydrologic Engineering*.

Lee, G., Yu, W., & Jung, K. (2013). Catchment-scale soil erosion and sediment yield simulation using a spatially distributed erosion model. *Environmental Earth Sciences, 70*(1), 33-47. doi:10.1007/s12665-012-2101-5

Li, Q., Zhou, J. L., Zhou, Y. Z., Bai, C. Y., Tao, H. F., Jia, R. L., Yang, G. Y. (2014). Variation of groundwater hydrochemical characteristics in the plain area of the Tarim Basin, Xinjiang Region, China. *Environmental Earth Sciences, 72*(11), 4249-4263. doi:10.1007/s12665-014-3320-8

Li, X., & Williams, M. W. (2008). Snowmelt runoff modelling in an arid mountain watershed, Tarim Basin, China. *Hydrological Processes, 22*(19), 3931-3940.

Lin, R. (1985). Characteristics on the vertical distribution of precipitation and runoff in the south slope of the Tianshan Mountain. *Hydrology*(2), 28-33.

Liu, T., Willems, P., Pan, X. L., Bao, A. M., Chen, X., Veroustraete, F., & Dong, Q. H. (2011). Climate change impact on water resource extremes in a headwater region of the Tarim basin in China. *Hydrology and Earth System Sciences, 15*(11), 3511-3527. doi:10.5194/hess-15-3511-2011

Monteith, J. L. (1965). *Evaporation and the environment. In: The State and Movement of Water I Living Organisms. XIXth Symposium Society for Experimental Biology*. Swansea: Cambridge University Press.

Moriasi, D. N., Arnold, J. G., Van Liew, M. W., Bingner, R. L., Harmel, R. D., & Veith, T. L. (2007). Model evaluation guidelines for systematic quantification of accuracy in watershed simulations. *Transactions of the ASABE, 50*(3), 885-900.

Morris, M. D. (1991). Factorial sampling plans for preliminary computational experiments. *Technometrics, 33*(2), 161-174.

Nash, J. E., & Sutcliffe, J. (1970). River flow forecasting through conceptual models part I—A discussion of principles. *Journal of hydrology, 10*(3), 282-290.

Ratto, M., Pagano, A., & Young, P. (2007). State dependent parameter metamodelling and sensitivity analysis. *Computer Physics Communications, 177*(11), 863-876. doi:10.1016/j.cpc.2007.07.011

Saha, P., Zeleke, K., & Hafeez, M. (2014). Streamflow modeling in a fluctuant climate using SWAT: Yass River catchment in south eastern Australia. *Environmental Earth Sciences, 71*(12), 5241-5254. doi:10.1007/s12665-013-2926-6

Saltelli, A., Tarantola, S., & Chan, K.-S. (1999). A quantitative model-independent method for global sensitivity analysis of model output. *Technometrics, 41*(1), 39-56.

Schmalz, B., & Fohrer, N. (2009). Comparing model sensitivities of different landscapes using the ecohydrological SWAT model. *Advances in Geosciences, 21*, 91-98.

Setegn, S. G., Srinivasan, R., Melesse, A. M., & Dargahi, B. (2010). SWAT model application and prediction uncertainty analysis in the Lake Tana Basin, Ethiopia. *Hydrological Processes, 24*(3), 357-367.

Tarantola, S., Giglioli, N., Jesinghaus, J., & Saltelli, A. (2002). Can global sensitivity analysis steer the implementation of models for environmental assessments and decision-making? *Stochastic Environmental Research and Risk Assessment, 16*(1), 63-76.

Tavakoli, M., & De Smedt, F. (2013). Validation of soil moisture simulation with a distributed hydrologic model (WetSpa). *Environmental Earth Sciences, 69*(3), 739-747. doi:10.1007/s12665-012-1957-8

Van Griensven, A., Meixner, T., Grunwald, S., Bishop, T., Diluzio, M., & Srinivasan, R. (2006). A global sensitivity analysis tool for the parameters of multi-variable catchment models. *Journal of Hydrology, 324*(1), 10-23.

Williams, J. (1969). Flood routing with variable travel time or variable storage coefficients. *Trans. ASAE, 12*(1), 100-103.

Wu, J. (2012). Evaluation of the water resource reproducible ability on Tarim River Basin in south of Xinjiang, northwest China. *Environmental Earth Sciences, 66*(7), 1731-1737. doi:10.1007/s12665-011-1396-y

Yang, J. (2011). Convergence and uncertainty analyses in Monte-Carlo based sensitivity analysis. *Environmental Modelling & Software, 26*(4), 444-457. doi:10.1016/j.envsoft.2010.10.007

Yang, J., Castelli, F., & Chen, Y. (2014). Multiobjective sensitivity analysis and optimization of distributed hydrologic model MOBIDIC. *Hydrol. Earth Syst. Sci., 18*(10), 4101-4112. doi:10.5194/hess-18-4101-2014

Yang, J., Liu, Y., Yang, W., & Chen, Y. (2012). Multi-objective sensitivity analysis of a fully distributed hydrologic model WetSpa. *Water resources management, 26*(1), 109-128.

Yang, J., Reichert, P., Abbaspour, K. C., & Yang, H. (2007). Hydrological modelling of the Chaohe Basin in China: Statistical model formulation and Bayesian inference. *Journal of Hydrology, 340*(3), 167-182.

Yang, X., Jiang, H., & Huang, C. (1987). An applied study on the snowmelt type of Xinanjiang Watershed Model at the Kaidu River Baisn. *Journal of August 1st Agri.Collage*(4), 82-90.

Zhao, C., Shi, F., Sheng, Y., Li, J., Zhao, Z., Han, M., & Yilibula, Y. (2011). Regional differentiation characteristics of precipitation changing with altitude in Xinjiang region in recent 50 years. *Journal of Glaciology and Geocryology, 6*, 1203-1213.

Zhou, Y. (1999). *Xinjiang river hydrology and water resources*. Urumqi: Xinjiang science and Technology Press.

4 A comparison of bias correction methods in downscaling meteorological variables for hydrologic modelling in the Kaidu River Basin

Modified from:

Fang, G. H., Yang, J., Chen, Y. N., & Zammit, C. (2015). Comparing bias correction methods in downscaling meteorological variables for a hydrologic impact study in an arid area in China. Hydrology and Earth System Sciences, 19(6), 2547-2559. doi:10.5194/hess-19-2547-2015

Water resources are essential to the ecosystem and social economy in the desert and oasis of the arid Tarim River basin, northwestern China, and expected to be vulnerable to climate change. It has been demonstrated that regional climate models (RCM) provide more reliable results for regional impact study of climate change (e.g., on water resources) than general circulation models (GCM). However, due to their considerable bias it is still necessary to apply bias correction before they are used for water resources research. In this paper, after a sensitivity analysis on input meteorological variables based on the Sobol' method, we compared five precipitation correction methods and three temperature correction methods in downscaling RCM simulations applied over the Kaidu River Basin, one of the headwaters of the Tarim River basin. Precipitation correction methods applied include linear scaling (LS), local intensity scaling (LOCI), power transformation (PT), distribution mapping (DM) and quantile mapping (QM), while temperature correction methods are LS, variance scaling (VARI) and DM. The corrected precipitation and temperature were compared to the observed meteorological data, prior to being used as meteorological inputs of a distributed hydrologic model to study their impacts on streamflow. The results show 1) Streamflow is sensitive to precipitation, temperature and solar radiation but not to relative humidity and wind speed; 2) Raw RCM simulations are heavily biased from observed meteorological data, and its use for streamflow simulations results in large biases from observed streamflow, and all bias correction methods effectively improved these simulations; 3) For precipitation, PT and QM methods performed equally best in correcting the frequency-based indices (e.g., standard deviation, percentile values) while the LOCI method performed best in terms of the time-series-based indices (e.g., Nash-Sutcliffe coefficient, R^2); 4) For temperature, all correction methods performed equally

well in correcting raw temperature; and 5) For simulated streamflow, precipitation correction methods have more significant influence than temperature correction methods and the performances of streamflow simulations are consistent with those of corrected precipitation; i.e., the PT and QM methods performed equally best in correcting flow duration curve and peak flow while LOCI method performed best in terms of the time-series-based indices. The case study is for an arid area in China based on a specific RCM and hydrologic model, but the methodology and some results can be applied to other areas and models.

4.1. Introduction

In recent decades, the ecological situation of the Tarim River basin in China has seriously degraded, especially in the lower reaches of the Tarim River due to water scarcity. In the meantime, climate change is significant in this region with an increase in temperature at a rate of 0.33 ~ 0.39 ℃ decade^{-1} and a slight increase in precipitation (Li et al., 2012) over the past 5 decades. Under the context of regional climate change, water resources in this region are expected to be more unstable and ecosystems are likely to suffer from severe water stress because the hydrologic system of the arid region is particularly vulnerable to climate change (Arnell, 1992; Shen & Chen, 2010; Wang et al., 2013). The impact of climate change on the hydrologic system has already been observed and it is expected that the hydrological system will continue to change in the future (Chen et al., 2010; T. Liu et al., 2011; Z. Liu et al., 2010). Therefore, projecting reliable climate change and its impact on hydrology are important to study the ecology in the Tarim River basin.

Only recently, efforts have been made to evaluate and project the impact of climate change on hydrology in the Tarim River basin. These studies include research on the relationships of meteorological variables and streamflow based on the historical measurements (e.g., Chen et al., 2013; Xu et al., 2013) and use of the GCM outputs to drive a hydrologic model to study potential climate change on water resources (T. Liu et al., 2011; Z. Liu et al., 2010). The study of historical climate-hydrology relationships has limited applications on future water resources management, especially under the context of global climate change. Though GCMs have been widely used to study impacts of future climate change on hydrological systems and water resources, they are impeded by their inability to provide reliable information at the hydrological scales (F. Giorgi, 1990; Maraun et al., 2010). In particular, for mountainous regions, fine-scale information such as the altitude-dependent precipitation and temperature information, which is critical for hydrologic modeling, is not represented in GCMs (Seager & Vecchi, 2010). Therefore, recent studies tend to use the higher-resolution regional climate models (RCMs) to preserve the physical coherence between atmospheric and land surface variables (Anderson et

al., 2011; Bergstrom et al., 2001). As such, when evaluating the impact of climate change on water resources on a watershed scale, the use of RCMs instead of GCMs is preferable since RCMs have proven to provide more reliable results for impact study of climate change on regional water resources than GCM models (Buytaert et al., 2010; Elguindi et al., 2011). However, the raw RCM simulations may be still biased especially in the mountainous regions (Fowler et al., 2007; Murphy, 1999), which makes the use of RCM outputs as direct input for hydrological model challenging. As a result it is of significance to properly correct the RCM-simulated meteorological variables before they are used to drive a hydrological model, especially in an arid region where the hydrology is sensitive to climate changes.

Several bias correction methods have been developed to downscale meteorological variables from the RCMs, ranging from the simple scaling approach to sophisticated distribution mapping (Teutschbein & Seibert, 2012). And their applicability in the arid Tarim River basin has not been investigated; therefore, evaluating and finding the appropriate bias correction method is necessary to evaluate the impact of climate change on water resources.

This study evaluates performances of five precipitation bias correction methods and three temperature bias correction methods in downscaling RCM simulations and applied to the Kaidu River Basin, one of the most important headwaters of the Tarim River. These bias correction methods include the most frequently used bias correction methods. We compare their performances in downscaling precipitation and temperature and evaluate their impact on streamflow through hydrological modeling.

This chapter is constructed as follows: Section 4.2 briefly introduces the study area and data; Section 4.3 describes the bias correction methods for precipitation and temperature along with the hydrological model, sensitivity analysis method and result analysis strategy; Section 4.4 presents results and discussion, followed by conclusions in Section 4.5.

4.2 Study area and data

4.2.1 Study area and observed data

This study chooses the Kaidu River Basin as the study area, and the topography and climate conditions for this watershed are introduced in Section 3.2. The meteorological (Bayanbulak and Baluntai stations) and hydrological data (Dashankou station) are shown in Section 3.2.

The setup of the hydrological model could refer to Section 3.2 as the “simulation with lapse rates”.

4.2.2 Simulated meteorological variables from the RCM

GCM or RCM outputs are generally biased (Ahmed et al., 2013; Mehrotra & Sharma, 2012; Teutschbein & Seibert, 2012), and there is a need to correct these outputs before they are used for regional impact studies. The RCM outputs used in this study are based on the work done by Gao et al. (2013). In Gao et al. (2013), the RCM model (RegCM4.0) (Giorgi & Mearns, 1991) was driven by a global climate model BCC_CSM1.1 (Beijing Climate Center Climate System Model; Wu et al., 2013; Xin et al., 2013) at a horizontal resolution of 50 km over China.

The RCM outputs were validated with the observational data set (CN05.1) over China for the period from 1961 to 2005. The RCM outputs show reasonable simulation of temperature and precipitation in most parts of China except for some regions where our study area is located. For more details refer to Gao et al. (2013).

4.3 Methodology

Figure 4.1 shows the flow chart of the comparison procedure. First, the grid-based RCM simulation was downscaled to station scale using bias correction methods, and then the corrected meteorological data were compared to the observations at these two stations and to each other ("Meteorological data comparison" in Figure 4.1). These station-based meteorological data were then upscaled to watershed scale with the precipitation and temperature lapse rates before they were used to drive the hydrological model SWAT (Arnold et al., 1998). Finally, the simulated streamflow driven by the corrected and observed meteorological data were compared to observed streamflow and to each other ("Streamflow comparison" in Figure 4.1).

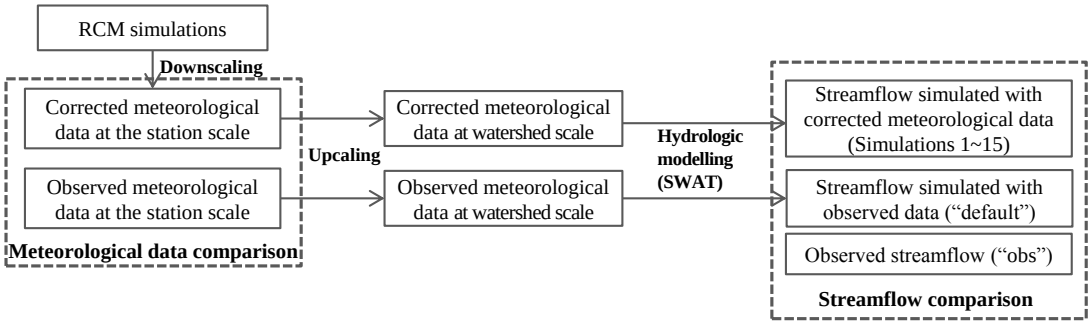

Figure 4.1 Flow chart of comparison procedure

4.3.1 Input sensitivity analysis

In this study, the SWAT model was firstly set up with available DEM (digital elevation

model), land use, soil, and observed climate data, and then model parameters were calibrated with the observed streamflow data at the Dashankou Station. The simulation results show: 1) model application with excellent performances for both the calibration (1986 ~ 1989) and validation (1990 ~ 2001) periods with daily NS ((Nash & Sutcliffe, 1970), see the definition in Equation 3-6) and R^2 values over 0.80, which is highly acceptable; 2) model parameters are reasonable and spatial patterns of precipitation and temperature are in agreement with other studies in the region (see more details in Chapter 3). Figure 4.2 shows a comparison of mean hydrographs of the observed (obs) and simulated flows (default). This calibrated model hence provides a basis for evaluation of the impact of different correction methods on streamflow.

To study the relative importance of the five meteorological variables, the Sobol' sensitivity analysis method (Sobol', 2001) was applied. The Sobol' method is based on the decomposition of the variance V of the objective function:

$$V = \sum_i V_i + \sum_i \sum_{j>i} V_{ij} + \cdots + V_{1,2,\cdots,n} \quad \text{(Equation 4-1)}$$

where

$$V_i = \mathrm{V}(\mu(Y|X_i))$$

$$V_{ij} = \mathrm{V}\left(\mu(Y|X_i, X_j)\right) - V_i - V_j$$

and so on. Herein, $V(.)$ denotes the variance operator, V is the total variance, and V_i and V_{ij} are main variance of X_i (the i^{th} factor of X) and partial variance of X_i and X_j. Here factors X are the changes applied to these five meteorological variables, respectively (see Table 4.1 for a list of these factors). In practice, normalized indices are often used as sensitivity measures:

$$S_i = \frac{\mathrm{V_i}}{\mathrm{V}}, 1 \le i \le n \quad \text{(Equation 4-2)}$$

$$S_{ij} = \frac{\mathrm{V_{ij}}}{\mathrm{V}}, 1 \le i < j \le n \quad \text{(Equation 4-3)}$$

$$S_{Ti} = S_i + \sum_j S_{ij} + \sum_j \sum_k S_{ijk} + \cdots + S_{1,2,\ldots,n}, 1 \le i \le n \quad \text{(Equation 4-4)}$$

where S_i, S_{ij} and S_{Ti} are the main effect of X_i, first order interaction between X_i and X_j, and total effect of X_i. S_{Ti} ranges from 0 to 1 and denotes the importance of the factor to model output. The larger S_{Ti}, the more important this factor is. The difference between S_{Ti} and S_i denotes the significance of the interaction of this factor with other factors. As a result, the larger this difference, the more significant the interaction is.

Table 4.1 Sensitivity indices of the five meteorological variables based on the Sobol' method

Factor[a]	Meaning	Factor Range	Main effect S_i (%)	Total effect S_{Ti} (%)
a__tmp	Additive change to temperature	[-5,5]	15.0	36.9
r__pcp	Relative change to precipitation	[-0.5,0.5]	44.0	74.0
r__hmd	Relative change to humidity	[-0.5,0.5]	0.0	0.0
r__slr	Relative change to solar radiation	[-0.5,0.5]	7.7	22.6
r__wnd	Relative change to wind speed	[-0.5,0.5]	0.3	0.9

[a] Here, '*a__*' or '*r__*' means an addictive or a relative change to the initial parameter values.

4.3.2 Bias correction methods

In this study, five bias correction methods were used for precipitation, and three for temperature. These methods are listed in Table 4.2. All these bias correction methods were conducted on a daily basis from 1975 to 2005.

Table 4.2 Bias correction methods for RCM-simulated precipitation and temperature.

Bias correction for precipitation	Bias correction for temperature
Linear scaling (LS)	Linear scaling (LS)
Local intensity scaling (LOCI)	Variance scaling (VARI)
Power transformation (PT)	Distribution mapping for temperature using Gaussian distribution (DM)
Distribution mapping for precipitation using gamma distribution (DM)	
Quantile mapping (QM)	

4.3.2.1 Linear scaling (LS) of precipitation and temperature

The LS method aims to perfectly match the monthly mean of corrected values with that of observed ones (Lenderink et al., 2007). It operates with monthly correction values based on the differences between observed and raw data (raw RCM-simulated data in this case). Precipitation is typically corrected with a multiplier and temperature with an additive term on a monthly

basis:

$$P_{cor,m,d} = P_{raw,m,d} \times \frac{\mu(P_{obs,m})}{\mu(P_{raw,m})} \quad \text{(Equation 4-5)}$$

$$T_{cor,m,d} = T_{raw,m,d} + \mu(T_{obs,m}) - \mu(T_{raw,m}) \quad \text{(Equation 4-6)}$$

where $P_{cor,m,d}$ and $T_{cor,m,d}$ are corrected precipitation and temperature on the d^{th} day of m^{th} month and $P_{raw,m,d}$ and $T_{raw,m,d}$ are the raw precipitation and temperature on the d^{th} day of m^{th} month. $\mu(.)$ represents the expectation operator (e.g., $\mu(P_{obs,m})$ represents the mean value of observed precipitation at given month *m*).

4.3.2.2 Local intensity scaling (LOCI) of precipitation

The LOCI method (Schmidli et al., 2006) corrects the wet-day frequencies and intensities and can effectively improve the raw data which have too many drizzle days (days with little precipitation). It normally involves two steps: firstly, a wet-day threshold for the m^{th} month $P_{thres,m}$ is determined from the raw precipitation series to ensure that the threshold exceedance matches the wet-day frequency of the observation; secondly, a scaling factor $s_m = \frac{\mu(P_{obs,m,d} | P_{obs,m,d} > 0)}{\mu(P_{raw,m,d} | P_{raw,m,d} > P_{thres,m})}$ is calculated and used to ensure that the mean of the corrected precipitation is equal to that of the observed precipitation:

$$P_{cor,m,d} = \begin{cases} 0, & if\ P_{raw,m,d} <= P_{thres,m} \\ P_{raw,m,d} \times S_m, & otherwise \end{cases} \quad \text{(Equation 4-7)}$$

4.3.2.3 Power transformation (PT) of precipitation

While the LS and LOCI account for the bias in the mean precipitation, it does not correct biases in the variance. The PT method uses an exponential form to further adjust the standard deviation of precipitation series. Since PT has the limitation in correcting the wet-day probability (Teutschbein & Seibert, 2012), which was also confirmed in our study (not shown), the LOCI method is applied to correct precipitation prior to the correction by PT method. Therefore, to implement this PT method, firstly, we estimate b_m, which minimizes:

$$f(b_m) = \frac{\sigma(P_{obs,m})}{\mu(P_{obs,m})} - \frac{\sigma(P_{LOCI,m}^{b_m})}{\mu(P_{LOCI,m}^{b_m})} \quad \text{(Equation 4-8)}$$

where b_m is the exponent for the m^{th} month, $\sigma(.)$ represents the standard deviation operator, and

$P_{LOCI,m}$ is the LOCI-corrected precipitation in the m^{th} month. If b_m is larger than 1, it indicates that the LOCI-corrected precipitation underestimates its coefficient of variance in month m.

After finding the optimal b_m, the parameter $s_m = \frac{\mu(P_{obs,m})}{\mu(P_{LOCI,m}^{b_m})}$ is then determined such that the mean of the corrected values corresponds to the observed mean. The corrected precipitation series are obtained based on the LOCI-corrected precipitation $P_{cor,m,d}$:

$$P_{cor,m,d} = s_m \times P_{LOCI,m,d}^{b_m} \quad \text{(Equation 4-9)}$$

4.3.2.4 Variance scaling (VARI) of temperature

The PT method is an effective method to correct both the mean and variance of precipitation, but it cannot be used to correct temperature time series, as temperature is known to be approximately normally distributed (Terink et al., 2010). VARI method was developed to correct both the mean and variance of normally distributed variables such as temperature (Terink et al., 2010; Teutschbein & Seibert, 2012). Temperature is normally corrected using the VARI method with Equation 4-10.

$$T_{cor,m,d} = [T_{raw,m,d} - \mu(T_{raw,m})] \times \frac{\sigma(T_{obs,m})}{\sigma(T_{raw,m})} + \mu(T_{obs,m}) \quad \text{(Equation 4-10)}$$

4.3.2.5 Distribution Mapping (DM) of precipitation and temperature

The DM method is to match the distribution function of the raw data to that of the observations. It is used to adjust mean, standard deviation and quantiles. Furthermore, it preserves the extremes (M. J. Themeßl et al., 2012). However, it also has its limitation due to the assumption that both the observed and raw meteorological variables follow the same proposed distribution, which may introduce potential new biases.

For precipitation, the gamma distribution (Thom, 1958) with shape parameter α and scale parameter β is often used for precipitation distribution and has been proven to be effective (e.g., Piani et al., 2010):

$$f_r(x|\alpha,\beta) = x^{\alpha-1} \times \frac{1}{\beta^{\alpha} \times \Gamma(\alpha)} \times e^{\frac{-x}{\beta}}; x \geq 0, \alpha, \beta > 0 \quad \text{(Equation 4-11)}$$

where $\Gamma(.)$ is the gamma function. Since the raw RCM-simulated precipitation contains a large number of drizzle days, which may substantially distort the raw precipitation distribution, the

correction is done on LOCI-corrected precipitation $P_{LOCI,m,d}$:

$$P_{cor,m,d} = F_r^{-1}\left(F_r\left(P_{LOCI,m,d}|\alpha_{LOCI,m},\beta_{LOCI,m}\right)|\alpha_{obs,m},\beta_{obs,m}\right) \quad \text{(Equation 4-12)}$$

where $F_r(.)$ and $F_r^{-1}(.)$ are the gamma CDF (cumulative distribution function) and its inverse. $\alpha_{LOCI,m}$ and $\beta_{LOCI,m}$ are the fitted gamma parameter for the LOCI-corrected precipitation in a given month *m*, and $\alpha_{obs,m}$ and $\beta_{obs,m}$ are these for observations.

For temperature, the Gaussian distribution (or normal distribution) with mean μ and standard deviation σ is usually assumed to fit temperature best (Teutschbein & Seibert, 2012):

$$f_N(x|\mu,\sigma) = \frac{1}{\sigma\times\sqrt{2\pi}} \times e^{\frac{-(x-\mu)^2}{2\sigma^2}}; x \in \mathbf{R} \quad \text{(Equation 4-13)}$$

And then similarly the corrected temperature can be expressed as

$$T_{cor,m,d} = F_N^{-1}\left(F_N\left(T_{raw,m,d}|\mu_{raw,m},\sigma_{raw,m}\right)|\mu_{obs,m},\sigma_{obs,m}\right) \quad \text{(Equation 4-14)}$$

where $F_N(.)$ and $F_N^{-1}(.)$ are the Gaussian CDF and its inverse, $\mu_{raw,m}$ and $\mu_{obs,m}$are the fitted and observed means for the raw and observed precipitation series at a given month *m*, and $\sigma_{raw,m}$ and $\sigma_{obs,m}$are the corresponding standard deviations, respectively.

4.3.2.6 Quantile Mapping (QM) of precipitation

The QM method is a non-parametric bias correction method and is generally applicable for all possible distributions of precipitation without any assumption on precipitation distribution. This approach originates from the empirical transformation (M. Themeßl et al., 2012) and was successfully implemented in the bias correction of RCM-simulated precipitation (J. Chen et al., 2013; Sun et al., 2011; M. Themeßl et al., 2012; Wilcke et al., 2013). It can effectively correct bias in the mean, standard deviation and wet-day frequency as well as quantiles.

For precipitation, the adjustment of precipitation using QM can be expressed in terms of the empirical CDF (*ecdf*) and its inverse ($ecdf^{-1}$):

$$P_{cor,m,d} = ecdf_{obs,m}^{-1}\left(ecdf_{raw,m}\left(P_{raw,m,d}\right)\right) \quad \text{(Equation 4-15)}$$

4.3.3 Performance evaluation

The performance evaluation of these correction methods is based on their abilities to

reproduce precipitation, temperature, and streamflow simulated with a hydrological model (SWAT) driven by bias-corrected RCM simulations. When evaluating the ability to reproduce streamflow, streamflow is firstly simulated by running the hydrological model driven by 15 different combinations of corrected precipitation, max/min temperature with different correction methods (these hydrologic simulations are then referred to as simulations 1-15, which are listed in Table 4.3) together with hydrologic simulations driven by observed meteorological data (default) and raw RCM simulation (raw). These 15 simulations were then compared with observed streamflows and default and raw.

The performance evaluation of precipitation, temperature and streamflow are as follows.

1) For corrected precipitation, frequency-based indices and time series performances are compared with observed precipitation data. The frequency-based indices include mean, median, standard deviation, 99th percentile, probability of wet days, and intensity of wet day while time-series-based metrics include NS, percent bias (P_{BIAS}), R^2 and mean absolute error (MAE), which is defined as follows:

$$MAE = \frac{\sum_{i=1}^{n}|Y_i^{obs} - Y_i^{sim}|}{n} \quad \text{(Equation 4-16)}$$

where Y_i^{obs} and Y_i^{sim} are the i^{th} observed and simulated variables, Y^{mean} is the mean of observed variables, and n is the total number of observations.

NS and P_{BIAS} indicate how well the simulation matches the observation, which are illustrated in Section 3.3. MAE demonstrates the average model prediction error with less sensitivity to large errors.

Table 4.3 Performances of simulated streamflows driven by raw RCM-simulated (raw) and 15 combinations of bias-corrected precipitation and temperature data (denoted as numbers from 1 to 15) compared to the simulation driven by observed climate (default) during the period 1986 ~ 2001. For simulations 1-15, solar radiation is corrected with the LS method.

Bias correction method			Daily				Monthly			
	Precipitation	Temperature	NS (-)	PBIAS (%)	R^2 (-)	MAE (m^3/s)	NS (-)	PBIAS (%)	R^2 (-)	MAE (m^3/s)
raw	raw	raw	-47.69	398.9	0.4	547.5	-56.34	399.4	0.6	524.6
1	LS	LS	-2.66	106.2	0.5	150.1	-3.09	106.4	0.7	140.2
2	LS	VARI	-2.43	103.5	0.5	145.4	-2.85	103.7	0.7	135.9
3	LS	DM	-2.43	103.5	0.5	145.4	-2.85	103.7	0.7	135.9
4	LOCI	LS	0.49	-8.0	0.5	56.0	0.70	-7.9	0.7	38.2

5	LOCI	VARI	0.50	-8.6	0.5	55.6	0.70	-8.6	0.7	38.1
6	LOCI	DM	0.50	-8.6	0.5	55.6	0.70	-8.6	0.7	38.1
7	PT	LS	0.38	-3.3	0.4	61.7	0.64	-3.3	0.7	41.4
8	PT	VARI	0.39	-4.1	0.5	61.3	0.65	-4.1	0.7	41.1
9	PT	DM	0.39	-4.1	0.5	61.3	0.65	-4.1	0.7	41.1
10	DM	LS	0.41	3.6	0.5	60.3	0.66	3.6	0.7	40.5
11	DM	VARI	0.42	2.8	0.5	59.5	0.67	2.9	0.7	40.0
12	DM	DM	0.42	2.8	0.5	59.5	0.67	2.9	0.7	40.0
13	QM	LS	0.39	-2.6	0.5	61.3	0.65	-2.6	0.7	40.9
14	QM	VARI	0.40	-3.4	0.5	60.8	0.65	-3.4	0.7	40.7
15	QM	DM	0.40	-3.4	0.5	60.8	0.65	-3.4	0.7	40.7

2) For corrected temperature, frequency-based indices and time series performances are compared with observed temperature data. The frequency-based indices include mean, median, standard deviation, and 10^{th} and 90^{th} percentiles while time-series-based metrics include NS, P_{BIAS}, R^2 and MAE.

3) For simulated streamflow driven by corrected RCM simulations, the frequency-based indices are visualized using a box plot, exceedance probability curve. Time-series-based metrics include NS, P_{BIAS}, R^2 and MAE.

4.4 Results and discussion

4.4.1. Initial streamflow simulation driven with raw RCM simulations and sensitivity analysis

To illustrate the necessity of bias correction in climate change impact on hydrology, we recalibrated SWAT using the raw RCM simulations while keeping all SWAT parameters in their reasonable ranges. The assumption is that if the recalibrated hydrological model driven by the raw RCM simulations performs well and model parameters are reasonable, then there is no need for bias correction. The streamflow simulated by the recalibrated model was plotted in Figure 4.2, and it systematically overestimates the observation with NS equals to -6.65. Therefore, it is necessary to correct the meteorological variables before they can be used for a hydrological impact study.

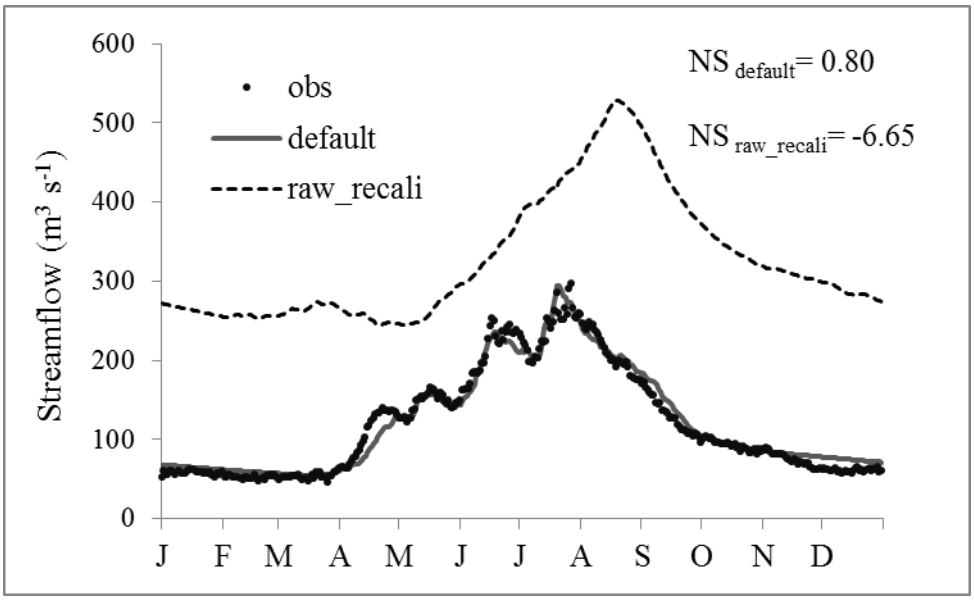

Figure 4.2 Mean annual hydrographs of observed streamflow (obs) and simulated streamflow using observed meteorological data (default) during the period of 1986 ~ 2001 at the Dashankou Station. The simulated streamflow using raw RCM-simulated meteorological data after recalibration (raw_recali) is also plotted. The NS values are for the daily continuous data and not for the mean hydrograph.

The Sobol' method was applied to study which meteorological variables should be corrected for hydrological modeling. Table 4.1 lists the sensitivity results for these five meteorological variables. As can be seen, precipitation is the most sensitive factor (the main effect S_i is 44.0% and total effect S_{Ti} is 74.0%), followed by temperature (S_i = 15.0% and S_{Ti} = 36.9%) and solar radiation (S_i = 7.7% and S_{Ti} = 22.6%), and the interactions between these factors are large. Relative humidity and wind speed are insensitive in this case. This means precipitation, temperature and solar radiation need to be bias corrected before being applied to hydrologic models, while relative humidity and wind speed over the region do not need any correction.

4.4.2 Evaluation of corrected precipitation and temperature

The bias correction was done on RCM-simulated precipitation, max/min temperature, and solar radiation (for solar radiation, the LS and VARI methods were used) for two meteorological stations Bayanbulak and Baluntai. Results show that (1) for solar radiation, there is no significant difference for different correction methods (there the results are not shown); and (2) similar results were obtained for minimum temperature and maximum temperature, and for Bayanbulak and Baluntai. Therefore, we only listed and discussed results for Bayanbulak, and

maximum temperature.

Table 4.4 Frequency-based statistics of daily observed (obs), raw RCM-simulated (raw) and bias-corrected precipitations at the Bayanbulak Station

	Mean (mm)	Median (mm)	Standard deviation (mm)	99th percentile (mm)	Probability of wet days (%)	Intensity of wet day (mm)
obs	0.73	0.0	2.4	12.4	32	2.3
raw	2.87	1.4	4.1	19.7	86	3.3
LS	0.73	0.2	1.5	7.6	73	1.0
LOCI	0.73	0.0	1.7	8.1	32	2.3
PT	0.73	0.0	2.4	11.4	32	2.3
DM	0.78	0.0	2.3	11.5	32	2.5
QM	0.73	0.0	2.4	12.4	32	2.3

Table 4.4 lists the frequency-based statistics of observed (obs), raw RCM-simulated (raw) and corrected (denoted by the corresponding correction method) precipitation data at the Bayanbulak Station. This station has a daily mean precipitation of 0.73 mm or annual mean of 266 mm and precipitation falls in 32% of the days in a year with a mean intensity of 2.3 mm. Compared to the observations, the raw RCM simulation deviates significantly from observation, with overestimation of all the statistics. All the bias correction methods improve the raw RCM-simulated precipitation; however, there are differences in their corrected statistics. LS method has a good estimation of the mean while it shows a large bias in other measures, e.g., it largely overestimated the probability of wet days (e.g., up to 41% overestimation) and underestimated the standard deviation (up to 0.9 mm underestimation). The LOCI method provides a good estimation in the mean, median, wet-day probability and wet-day intensity; however, there is a slight underestimation in the standard deviation and therefore the 99th percentile. Compared to LS and LOCI, the PT method performs well in all these metrics. The DM method has a slight overestimation of the mean and an underestimation of standard deviation. This means that precipitation does not follow the assumed gamma distribution. On the contrary, the QM method does not have this assumption and it provides an excellent estimation of these statistics. These results are consistent with previous studies (Graham et al., 2007; M. Themeßl et al., 2012; Themeßl et al., 2011; Wilcke et al., 2013) but are different from the research by Piani et al. (2010), who found that performance of DM method is unexpectedly well for the humid Europe region. This discrepancy can be partly attributed to the precipitation

regime for different regions since a better fit of the assumed distribution leads to a better performance of DM.

Table 4.5 Frequency-based statistics (unit: ℃) of daily observed (obs), raw RCM-simulated (raw) and bias-corrected maximum temperatures at the Bayanbulak Station

	Mean	Median	Standard deviation	10^{th} percentile	90^{th} percentile
obs	3.08	7.20	14.50	-18.70	19.20
raw	3.45	3.21	10.88	-10.34	17.90
LS	3.08	6.65	14.14	-17.33	19.40
VARI	3.08	6.85	14.50	-17.76	19.36
DM	3.08	6.85	14.50	-17.76	19.36

Table 4.5 lists the frequency-based statistics of observed (obs), raw RCM-simulated (raw) and corrected (denoted by the corresponding method) maximum temperature data at the Bayanbulak Station. The mean and standard deviation of obs are 3.1 and 14.5 ℃, with the 90^{th} percentile being 19.2 ℃. Analysis of the raw indicates deviation from obs, with an overestimation of the mean, and underestimations of the median, standard deviation, and 90^{th} percentile. All three correction methods correct biases in the raw and improve estimations of the statistics. LS has a correct estimation of mean but slight underestimations of the median and standard deviation, while VARI and DM have good estimations of all the frequency-based statistics. These results confirm the study by Teutschbein and Seibert (2012), i.e., the LS method does not adjust the standard deviation and the percentiles while the VARI and DM methods do.

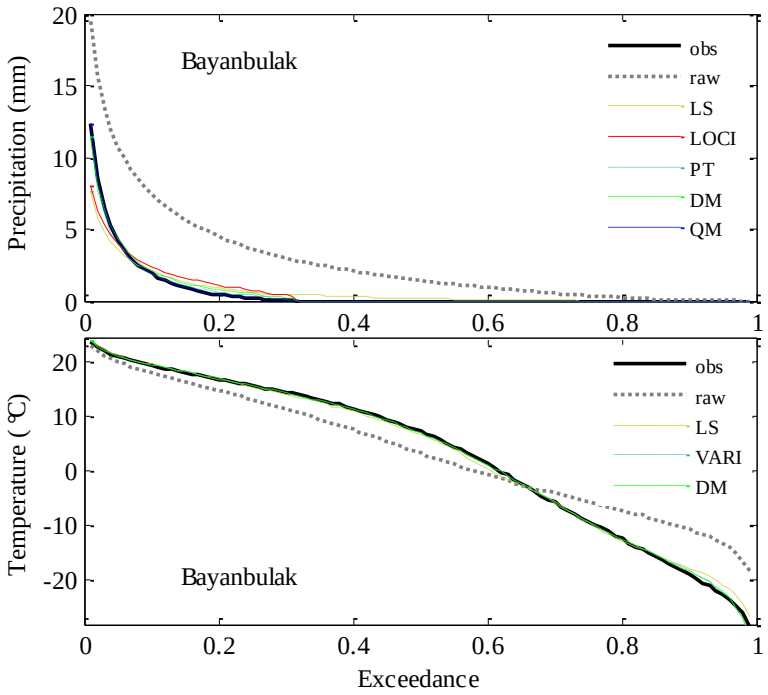

Figure 4.3 Exceedance probabilities of the observed (obs), raw, and bias-corrected precipitation (top) and temperature (bottom) at the Bayanbulak Station.

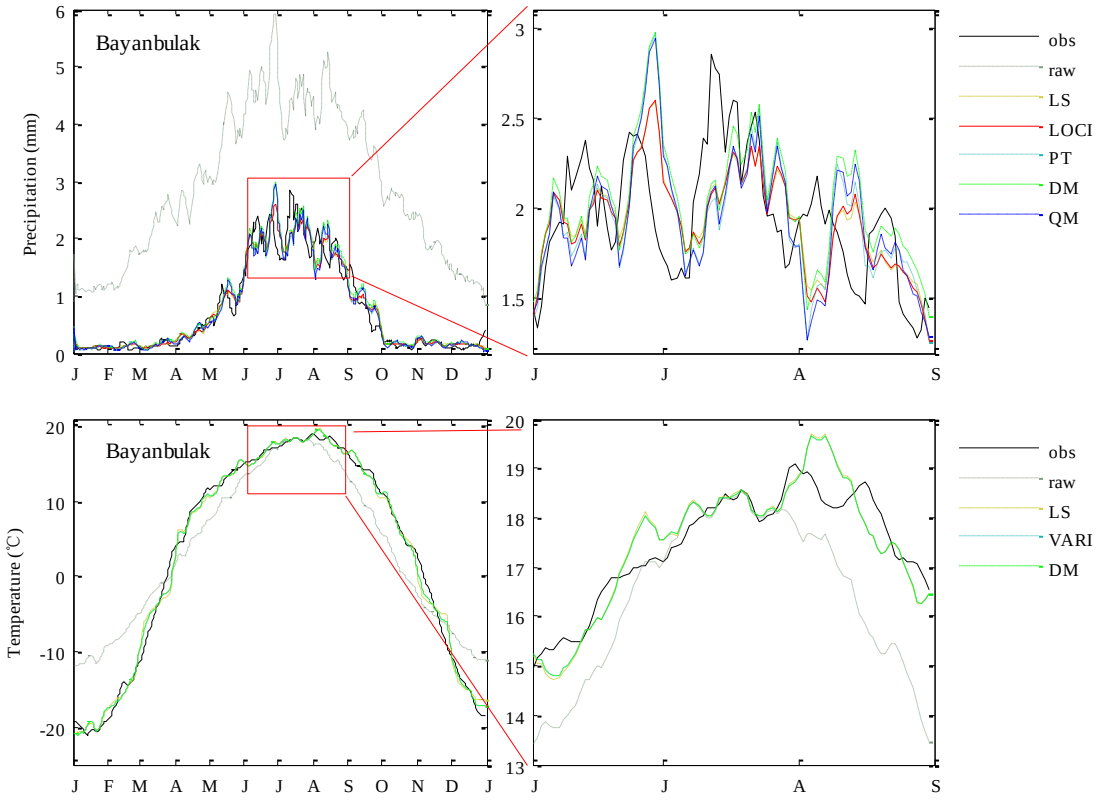

Figure 4.4 Daily mean precipitation and temperature of observed (obs), raw RCM-simulated (raw), and bias-corrected values at Bayanbulak Station, which were smoothed with the 7-day moving average method. The precipitation and temperature during May-August is amplified to inspect the performance of each correction method.

Figure 4.3 shows the exceedance probability curves of the observed and corrected precipitation and temperature. For precipitation, the raw RCM simulations are heavily biased (as also shown by statistics in Table 4.5). All correction methods effectively, but in different extent, correct biases in raw precipitation. The LS method underestimates the high precipitation with probabilities below 0.06 and overestimates the low precipitation with probabilities between 0.06 and 0.32. The overestimation of precipitation with probabilities between 0.32 and 0.73 indicates LS method has a very limited ability in reproducing dry day precipitation (below 0.1 mm). Similar to LS method, the LOCI method also overestimates the low precipitation with probabilities between 0.08 and 0.32 and underestimates the high intensities with probabilities below 0.08, which is in line with previous arguments by (Berg et al., 2012). However, unlike the LS method, the LOCI method performs well on the estimation of the dry days with precipitation below 0.1 mm. The PT, DM and QM methods well-adjust precipitation exceedance except that the DM method slightly overestimates the precipitation with probabilities between 0.12 and 0.28. For temperature, the raw temperature overestimates low temperature with probabilities above 0.65 and underestimates high temperature with probabilities below 0.65. All temperature correction methods adjust the biases in raw temperature and the corrected temperature has similar quantile values to the observation. They performed equally well and differences among these correction methods are negligible.

Time-series-based performances were evaluated and results are shown in Figure 4.5 and Table 4.6. For precipitation, all bias correction methods significantly improve the raw RCM simulations. However, as shown in the right plot of Figure 4.5, there is a systematic mismatch between observations and corrections which follow the pattern of the raw RCM-simulated precipitation, which indicates that all bias correction methods fail to correct the temporal pattern of precipitation. In addition, this mismatch differs between different methods, among which the differences are smaller for the LS and LOCI methods than for the PT, DM and QM methods. This resulted in a slightly better squared difference based measures (e.g., NS, R^2) for LS and LOCI than PT, DM and QM methods, as is indicated in Table 4.6. Similar to precipitation, all correction methods significantly improved the raw RCM-simulated temperature. Biases in raw temperature (e.g., 1.1 ℃ in spring, 1.0 ℃ in summer, 3.3 ℃ in autumn, and up to 7.6 ℃ in winter) were corrected. These three correction methods performed equally well and no significant differences exist in terms of the average daily temperature graphs.

Table 4.6 Time-series-based metrics of bias-corrected precipitation and temperature calculated on a monthly scale at the Bayanbulak Station

		NS (-)	PBIAS (%)	R^2 (-)	MAE (mm or ℃)
Precipitation	raw	-6.78	293.28	0.42	65.40
	LS	0.64	0.06	0.65	9.66
	LOCI	0.61	-0.71	0.64	10.14
	PT	0.42	-0.09	0.53	11.98
	DM	0.46	6.64	0.56	11.78
	QM	0.44	0.03	0.54	11.99
Temperature	raw	0.84	15.78	0.88	4.31
	LS	0.95	3.04	0.95	2.35
	VARI	0.94	4.78	0.94	2.52
	DM	0.94	4.74	0.94	2.52

Table 4.6 lists the time-series based metrics of corrected precipitation and temperature at the Bayanbulak Station. For precipitation, the performance of the raw RCM-simulated precipitation is very poor with NS = -6.78, PBIAS = 293.28% and MAE = 65.40 mm for monthly data, and the improvements of correction are obvious. The PBIAS values of the corrected precipitation are within $\pm 7\ \%$ and NS values approach 0.64. It is worth noting that the LS and LOCI methods perform better than the PT and QM methods in terms of time series performances. For temperature, although the raw RCM simulation obtains an acceptable NS value (0.84), it overestimates the observation with PBIAS = 15.78% and MAE = 4.31 ℃. The PBIAS values of the corrected temperatures are within $\pm 5\%$ and NS values are over 94% (better than that of the raw) for all three correction methods and there is no significant difference between these results, which indicates the corrected monthly temperature series are in good agreement with the observation.

4.4.3 Evaluation of streamflow simulations

Figure 4.5 compares the mean, median, first and third quantiles of daily observed streamflows (obs), simulated streamflows using observed meteorological inputs (“default”), raw RCM simulations (raw) and 15 combinations of corrected precipitation and corrected temperature (i.e., simulations 1-15). The overestimation of simulated streamflow using raw RCM simulations (i.e., raw) is obvious. Simulations 1-3 overestimate streamflow with 100%

overestimation of the mean streamflow while simulations 4-15 reproduce similar streamflows as the observation or simulation "default". As the major difference between simulations 1-3 and other simulations is that simulations 1-3 use the LS-corrected precipitation, which means precipitation corrected with the LS method has great bias in flow simulation in this study.

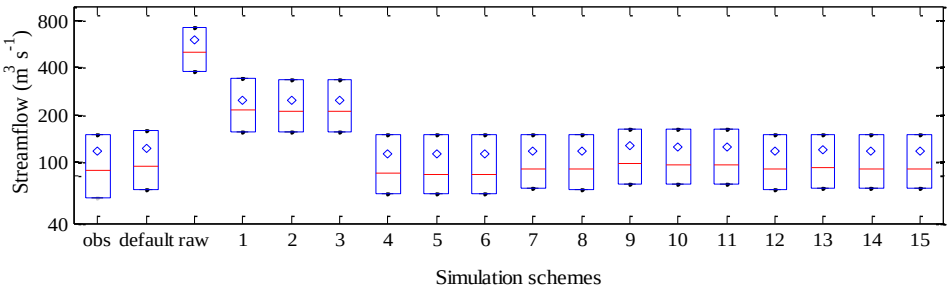

Figure 4.5 Box plots of observed (obs) and simulated daily streamflows using observed (default), raw RCM-simulated (raw) and corrected meteorological data (setup of simulations 1-15 are listed in Table 4.3). The mean values are shown with diamonds.

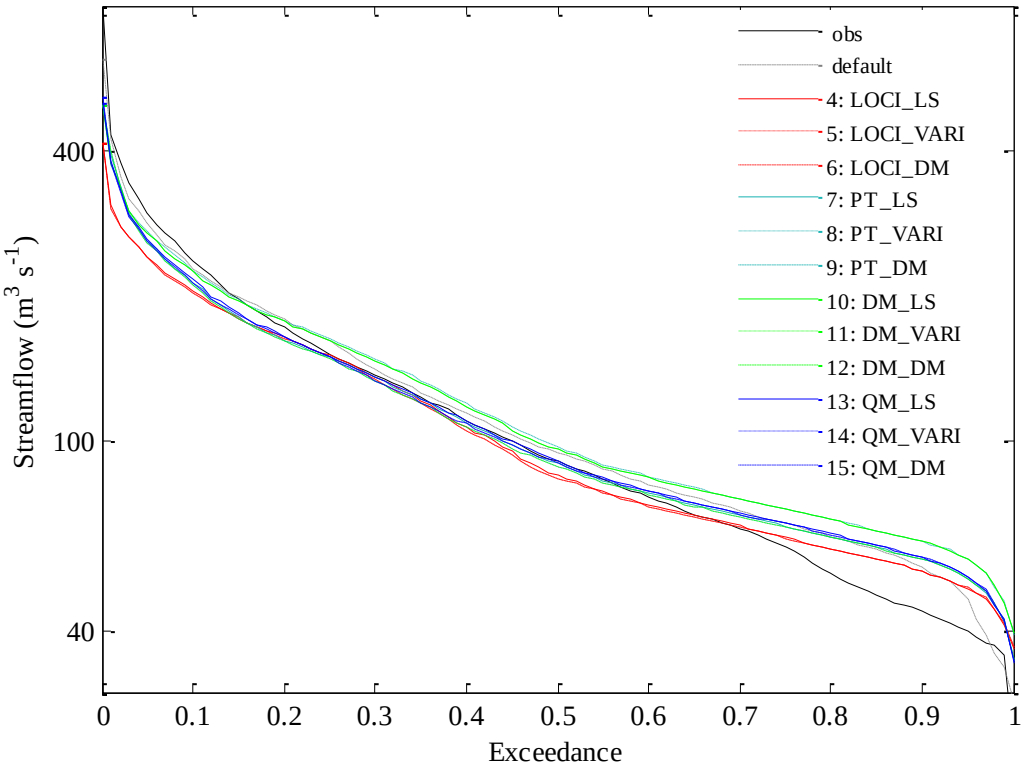

Figure 4. 6 Exceedance probability curves of observed (obs) and simulated streamflow driven by observed (default), and bias-corrected meteorological data (numbers from 4 to 15; see Table 4.3 for detailed setup of these simulations).

To investigate the performances of bias correction methods for different hydrological

seasons, we divided the streamflow into two different periods according to the hydrograph (Figure 4.2): the wet period is from April to September and the dry period is from October to March of the following year. It indicates that the performances of bias correction methods are, except for magnitudes, similar for both wet and dry periods (not shown), which demonstrates that the evaluation is robust and can provide useful information for both dry and wet seasons.

Figure 4.6 shows the exceedance probability curves (flow duration curves) of the observed streamflow (obs), and streamflows with simulation default and simulations 4-15. For plotting purpose, simulations raw and 1-3 are not shown. Generally, all simulations are in good agreement with the observation with probabilities between 0.12 and 0.72, and precipitation correction methods have more significant influence than temperature correction methods. This confirms the previous sensitivity results that precipitation is the most sensitive driving force in streamflow simulation. Similar to performances of bias-corrected precipitation, simulations with DM-corrected precipitation (i.e. simulations 10-12) and LOCI-corrected precipitation (i.e., simulations 4 to 6) deviate the observation the most, these are followed by the PT and QM methods. All simulations encounter the problem to correctly mimic the low flow part (i.e. probabilities larger than 0.7). This might be a systematic problem of the calibrated hydrologic model (as indicated by simulation default), e.g., the objective function of the hydrological modeling is not focused on baseflow. Differences among streamflows driven by different temperature but same precipitation are insignificant, which is different from the study of Teutschbein and Seibert (2012). This may be related to the watershed characteristic.

The performances of simulation raw, simulations 1-15 at daily and monthly time steps (simulation default is taken as reference), are summarized in Table 4.3. The raw is heavily biased with NS close to -56.3 and PBIAS as large as 399 % for monthly data. All the 15 simulations improve the statistics significantly. For simulations 1-3, whose precipitation series are corrected by the LS method, NS ranges from -3.09 to -2.85 for monthly streamflow and they substantially overestimate the streamflow with PBIAS over 100 %. For simulations 4-15, monthly NS values are over 0.60, which indicates they can reproduce satisfactory monthly streamflows in this watershed, and simulations with precipitation corrected by LOCI (simulations 4-6) have best NS and PBIAS values. However, these indices of are lower for daily streamflow (NS values range from 0.38 to 0.50), and this is related to the mismatch between corrected and observed precipitation time series (see top plot in Figure 4.4), which is intrinsic from the RCM model and cannot be improved through these correction methods.

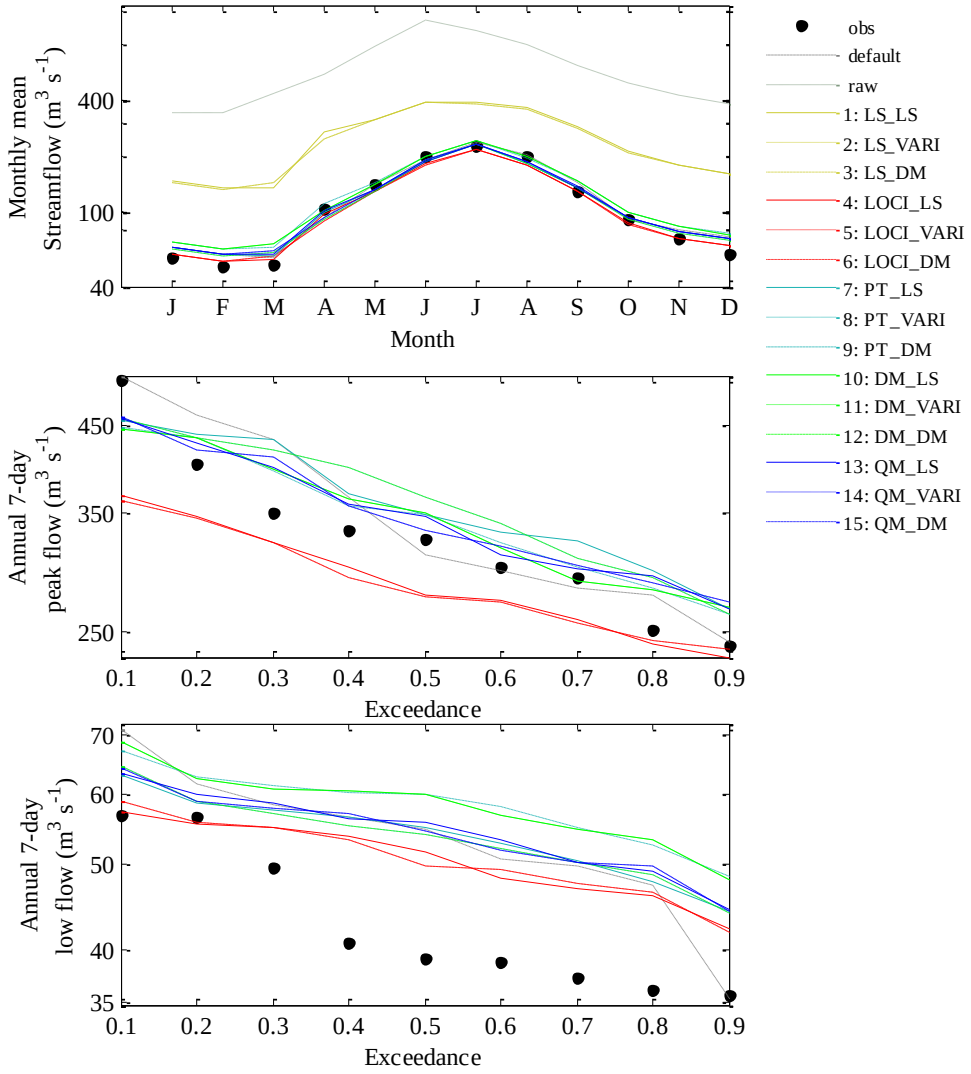

Figure 4.7 Monthly mean streamflow (top) and exceedance probability curves of annual 7-day peak flow (middle) and annual 7-day low flow (bottom) during 1986 ~ 2001 in the Kaidu River Basin (obs: observed streamflow; default: simulated with observed meteorological data; raw: simulated with RCM-simulated meteorological data; 1-15: simulated with corrected RCM meteorological data listed in Table 4.3).

It is worth noting that simulations 1-3 and simulations 4-6, whose precipitation is corrected by LS and LOCI, respectively, vary significantly. The difference between LS and LOCI is that LOCI introduces a threshold for precipitation on wet days to correct the wet-day probability while LS does not. That is a simple but quite pragmatic approach since the raw RCM-simulated precipitation usually has too many drizzle days (Teutschbein and Seibert, 2012). Obviously, wet-day probability is crucial to streamflow simulation when using elevation bands to account for spatial variation in SWAT (see more details in SWAT manual; http://www.brc.tamus.edu/).

Figure 4.7 shows the monthly mean streamflow and exceedance probability curves of

7-day peak flow and 7-day low flow. For the monthly mean streamflow, obviously the raw is heavily biased with deviations ranging from 282% to 426%. Simulations 1-3 also overestimate the observation and the default as discussed before, while simulations 4-15 reproduced good monthly mean streamflow. The annual peak flow and low flow are presented in Figure 4.7 to investigate the impact of bias correction methods on extreme flows. For the peak flow, the exceedance probabilities of the simulations 4-15 are close to the observation while raw and simulations 1-3 deviate significantly (not shown). It is worth noting that simulations 4, 5 and 6, which perform the best in terms of the NS values, underestimate the peak flow by 1% ~ 28%. The reason may be that the LOCI method adjusts all precipitation events in a certain month with a same scaling factor, which leads to the underestimation of the standard deviation and high precipitation intensity (Table 4.4), and finally results in an underestimation of the peak streamflow. For the low flow, all simulations overestimate the observation, but are in good agreement with the default, which can be attributed to the systematic deficit in the hydrological model. The DM method slightly overestimates both peak flow and low flow. Results show slightly better performance of the PT and QM methods than LOCI and DM in predicting extreme flood and low flow, which is consistent with previous studies in North America and Europe (J. Chen et al., 2013; Teutschbein & Seibert, 2012).

4.5 Conclusions

The work presented in this study compared the abilities of five precipitation and three temperature correction methods in downscaling RCM simulations. The downscaled meteorological data were then used to model hydrologic processes in an arid region in China. The evaluation of the correction methods includes their abilities to reproduce precipitation, temperature and streamflow using a hydrological model driven by corrected meteorological variables. Several conclusions can be drawn.

1. Sensitivity analysis shows precipitation is the most sensitive driving force in streamflow simulation, followed by temperature and solar radiation, while relative humidity and wind speed are not sensitive.

2. Raw RCM simulations are heavily biased from observed meteorological data, and this results in biases in the simulated streamflows which cannot be corrected through calibration of the hydrological model. However, all bias correction methods effectively improve precipitation, temperature, and streamflow simulations.

3. Different precipitation correction methods show a big difference in downscaled precipitations while different temperature correction methods show similar results in downscaled temperatures. For precipitation, the PT and QM methods performed equally best in

terms of the frequency-based indices; while the LOCI method performed best in terms of the time-series-based indices.

4. For simulated streamflow, precipitation correction methods have a more significant influence than temperature correction methods and their performances on streamflow simulations are consistent with these of corrected precipitation: i.e., the PT and QM methods performed equally best in correcting the flow duration curve and peak flow while the LOCI method performed best in terms of the time-series based indices. Note the LOCI and DM methods should be used with caution when analyzing drought or extreme streamflows because the LOCI method may underestimate the extreme precipitation and the DM method performs ineffectively when either simulated precipitation or observed precipitation does not follow the proposed distribution. Moreover, the LS method is not suitable in hydrological impact assessments where there is a large variation in precipitation distribution when few meteorological stations are used since LS fails to correct wet-day probability.

Generally, selection of the precipitation correction method is more important than selection of the temperature correction method to downscale GCM/RCM simulations and thereafter for streamflow simulations. This might be generally true for other regional studies as GCMs/RCMs normally tend to better represent the temperature field than the precipitation field. However, the selection of a precipitation correction method will be case dependent. The comparison procedure listed in Figure 2 can be applied for other cases.

References

Ahmed, K. F., Wang, G., Silander, J., Wilson, A. M., Allen, J. M., Horton, R., & Anyah, R. (2013). Statistical downscaling and bias correction of climate model outputs for climate change impact assessment in the US northeast. *Global and Planetary Change, 100*, 320-332.

Anderson, W. P., Jr., Storniolo, R. E., & Rice, J. S. (2011). Bank thermal storage as a sink of temperature surges in urbanized streams. *Journal of Hydrology, 409*(1-2), 525-537. doi:10.1016/j.jhydrol.2011.08.059

Arnell, N. W. (1992). Factors controlling the effects of climate change on river flow regimes in a humid temperate environment. *Journal of Hydrology, 132*(1–4), 321-342. doi:http://dx.doi.org/10.1016/0022-1694(92)90184-W

Arnold, J. G., Srinivasan, R., Muttiah, R. S., & Williams, J. (1998). Large area hydrologic modeling and assessment part I: Model development1. *JAWRA Journal of the American Water Resources Association, 34*(1), 73-89.

Berg, P., Feldmann, H., & Panitz, H. J. (2012). Bias correction of high resolution regional climate model data. *Journal of Hydrology, 448*, 80-92. doi:10.1016/j.jhydrol.2012.04.026

Bergstrom, S., Carlsson, B., Gardelin, M., Lindstrom, G., Pettersson, A., & Rummukainen, M. (2001). Climate change impacts on runoff in Sweden-assessments by global climate models, dynamical downscaling and hydrological modelling. *Climate research, 16*(2), 101-112.

Buytaert, W., Vuille, M., Dewulf, A., Urrutia, R., Karmalkar, A., & Celleri, R. (2010). Uncertainties

in climate change projections and regional downscaling in the tropical Andes: implications for water resources management. *Hydrology and Earth System Sciences, 14*(7), 1247-1258. doi:10.5194/hess-14-1247-2010

Chen, J., Brissette, F. P., Chaumont, D., & Braun, M. (2013). Finding appropriate bias correction methods in downscaling precipitation for hydrologic impact studies over North America. *Water Resources Research, 49*(7), 4187-4205. doi:10.1002/wrcr.20331

Chen, Y., Xu, C., Chen, Y., Li, W., & Liu, J. (2010). Response of glacial-lake outburst floods to climate change in the Yarkant River basin on northern slope of Karakoram Mountains, China. *Quaternary International, 226*(1), 75-81.

Chen, Z., Chen, Y., & Li, B. (2013). Quantifying the effects of climate variability and human activities on runoff for Kaidu River Basin in arid region of northwest China. *Theoretical and applied climatology, 111*(3-4), 537-545.

Elguindi, N., Somot, S., Déqué, M., & Ludwig, W. (2011). Climate change evolution of the hydrological balance of the Mediterranean, Black and Caspian Seas: impact of climate model resolution. *Climate dynamics, 36*(1-2), 205-228.

Fowler, H. J., Ekström, M., Blenkinsop, S., & Smith, A. P. (2007). Estimating change in extreme European precipitation using a multimodel ensemble. *Journal of Geophysical Research, 112*, D18.

Gao, X., Wang, M., & Giorgi, F. (2013). Climate change over China in the 21st century as simu-lated by BCC_CSM1. 1-RegCM4. 0. *Atmos. Oceanic Sci. Lett, 6*, 381-386.

Giorgi, F. (1990). Simulation of regional climate using a limited area model nested in a general circulation model. *Journal of Climate 3*(9), 941-963.

Giorgi, F., & Mearns, L. O. (1991). Approaches to the simulation of regional climate change: a review. *Reviews of Geophysics, 29*(2), 191-216.

Graham, L. P., Andréasson, J., & Carlsson, B. (2007). Assessing climate change impacts on hydrology from an ensemble of regional climate models, model scales and linking methods–a case study on the Lule River basin. *Climatic Change, 81*(1), 293-307.

Lenderink, G., Buishand, A., & Deursen, W. v. (2007). Estimates of future discharges of the river Rhine using two scenario methodologies: direct versus delta approach. *Hydrology and Earth System Sciences, 11*(3), 1145-1159.

Li, B., Chen, Y., & Shi, X. (2012). Why does the temperature rise faster in the arid region of northwest China? *Journal of Geophysical Research, 117*(D16115).

Liu, T., Willems, P., Pan, X. L., Bao, A. M., Chen, X., Veroustraete, F., & Dong, Q. H. (2011). Climate change impact on water resource extremes in a headwater region of the Tarim basin in China. *Hydrology and Earth System Sciences, 15*(11), 3511-3527. doi:10.5194/hess-15-3511-2011

Liu, Z., Xu, Z., Huang, J., Charles, S. P., & Fu, G. (2010). Impacts of climate change on hydrological processes in the headwater catchment of the Tarim River basin, China. *Hydrological Processes, 24*(2), 196-208. doi:10.1002/hyp.7493

Maraun, D., Wetterhall, F., Ireson, A. M., Chandler, R. E., Kendon, E. J., Widmann, M., Thiele-Eich, I. (2010). Precipitation downscaling under climate change: Recent developments to bridge the gap between dynamical models and the end user. *Reviews of Geophysics, 48*(3), RG3003. doi:10.1029/2009RG000314

Mehrotra, R., & Sharma, A. (2012). An improved standardization procedure to remove systematic

low frequency variability biases in GCM simulations. *Water Resources Research, 48*(12), W12601. doi:10.1029/2012WR012446

Murphy, J. (1999). An evaluation of statistical and dynamical techniques for downscaling local climate. *Journal of Climate, 12*(8), 2256-2284.

Nash, J. E., & Sutcliffe, J. (1970). River flow forecasting through conceptual models part I—A discussion of principles. *Journal of hydrology, 10*(3), 282-290.

Piani, C., Haerter, J. O., & Coppola, E. (2010). Statistical bias correction for daily precipitation in regional climate models over Europe. *Theoretical and Applied Climatology, 99*(1-2), 187-192. doi:10.1007/s00704-009-0134-9

Schmidli, J., Frei, C., & Vidale, P. L. (2006). Downscaling from GC precipitation: A benchmark for dynamical and statistical downscaling methods. *International Journal of Climatology, 26*(5), 679-689. doi:10.1002/joc.1287

Seager, R., & Vecchi, G. A. (2010). Greenhouse warming and the 21st century hydroclimate of southwestern North America. *Proceedings of the National Academy of Sciences of the United States of America, 107*(50), 21277-21282. doi:10.1073/pnas.0910856107

Shen, Y., & Chen, Y. (2010). Global perspective on hydrology, water balance, and water resources management in arid basins. *Hydrological Processes, 24*(2), 129-135.

Sobol', I. M. (2001). Global sensitivity indices for nonlinear mathematical models and their Monte Carlo estimates. *Mathematics and Computers in Simulation, 55*(1-3), 271-280. doi:10.1016/s0378-4754(00)00270-6

Sun, F., Roderick, M. L., Lim, W. H., & Farquhar, G. D. (2011). Hydroclimatic projections for the Murray-Darling Basin based on an ensemble derived from Intergovernmental Panel on Climate Change AR4 climate models. *Water Resources Research, 47*, W00G02. doi:10.1029/2010wr009829

Terink, W., Hurkmans, R., Torfs, P., & Uijlenhoet, R. (2010). Evaluation of a bias correction method applied to downscaled precipitation and temperature reanalysis data for the Rhine basin. *Hydrology & Earth System Sciences, 14*(1), 687-703.

Teutschbein, C., & Seibert, J. (2012). Bias correction of regional climate model simulations for hydrological climate-change impact studies: Review and evaluation of different methods. *Journal of Hydrology, 456*, 12-29. doi:10.1016/j.jhydrol.2012.05.052

Themeßl, M., Gobiet, A., & Heinrich, G. (2012). Empirical-statistical downscaling and error correction of regional climate models and its impact on the climate change signal. *Climatic Change, 112*(2), 449-468. doi:10.1007/s10584-011-0224-4

Themeßl, M. J., Gobiet, A., & Heinrich, G. (2012). Empirical-statistical downscaling and error correction of regional climate models and its impact on the climate change signal. *Climatic Change, 112*(2), 449-468.

Themeßl, M. J., Gobiet, A., & Leuprecht, A. (2011). Empirical‐statistical downscaling and error correction of daily precipitation from regional climate models. *International Journal of Climatology, 31*(10), 1530-1544.

Thom, H. C. (1958). A note on the gamma distribution. *Monthly Weather Review, 86*(4), 117-122.

Wang, H., Chen, Y., Li, W., & Deng, H. (2013). Runoff responses to climate change in arid region of northwestern China during 1960–2010. *Chinese Geographical Science, 23*(3), 286-300.

Wilcke, R. A. I., Mendlik, T., & Gobiet, A. (2013). Multi-variable error correction of regional climate models. *Climatic Change, 120*(4), 871-887.

Wu, T., Li, W., Ji, J., Xin, X., Li, L., Wang, Z., Wei, M. (2013). Global carbon budgets simulated by the Beijing Climate Center Climate System Model for the last century. *Journal of Geophysical Research: Atmospheres*, *118*(10), 4326-4347.

Xin, X., Wu, T., Li, J., Wang, Z., Li, W., & Wu, F. (2013). How well does BCC_CSM1. 1 reproduce the 20th century climate change over China. *Atmos. Oceanic Sci. Lett*, *6*(1), 21-26.

Xu, C., Chen, Y., Chen, Y., Zhao, R., & Ding, H. (2013). Responses of Surface Runoff to Climate Change and Human Activities in the Arid Region of Central Asia: A Case Study in the Tarim River Basin, China. *Environmental management*, *51*(4), 926-938.

5 Impact of future climate change on hydrological processes in the Kaidu River Basin

Modified from:

Fang, G., Yang, J., Chen, Y., Zhang, S., Deng, H., Liu, H., & De Maeyer, P. (2015). Climate Change Impact on the Hydrology of a Typical Watershed in the Tianshan Mountains. Advances in Meteorology, 2015, 1-10. doi:10.1155/2015/960471.

To study the impact of future climatic changes on hydrological processes in the Kaidu River Basin, two sets of future climatic data were used to force a well-calibrated hydrologic model: one is bias-corrected RCM (Regional Climate Model) outputs for RCP4.5 and RCP8.5 future emission scenarios, and the other is simple climate change (SCC) with absolute temperature change of -1 ~ 6 ℃ and relative precipitation change of -20% ~ 60%. Results show: 1) temperature is likely to increase by 2.2 ℃ and 4.6 ℃ by the end of the 21st century under RCP4.5 and RCP8.5, respectively, while precipitation will increase by 2% ~ 24%, with a significant rise in the dry season and small change in the wet season; 2) flow will change by -1% ~ 20%, while evapotranspiration will increase by 2% ~ 24% ; 3) flow increases almost linearly with precipitation while its response to temperature depends on the magnitude of temperature change and flow decreases significantly for temperature increase greater than 2 ℃; 4) similar results were obtained for simulations with RCM outputs and with SCC for mild climate change conditions while results were significantly different for intense climate change conditions.

Keywords: climate change; uncertainty analysis; hydrologic modeling; Tarim River

5.1 Introduction

The Tianshan Mountains, regarded as "Water tower of Central Asia" (Sorg et al., 2012), are located in the innermost center of the Eurasian continent. The long distance to the surrounding oceans causes a dry climate, especially for the surrounding basins. Rivers starting in the mountainous regions provide agricultural and domestic water for the surrounding basins and oases. With its distinctive topographic and landscape features, the Tianshan Mountains show a unique energy balance and hydrologic cycle and are expected to be sensitive to climate change (Li et al., 2015; Liu et al., 2010).

Many reports show a widespread climatic and hydrologic change in the Tianshan Mountains during the past few decades (Shi et al., 2007). For example, temperature demonstrated a significant rising trend (significant level is smaller than 0.001) at a rate of 0.33 ~ 0.34 ℃/decade during 1960 ~ 2010, higher than China (0.25 ℃/decade) and the entire globe (0.13 ℃/decade) (B. Li et al., 2012; S. Wang et al., 2011); precipitation increased substantially in most regions especially for the middle and high latitudes; glacier area decreased by 11.5% and the thickness of snowpack has also decreased (Aizen et al., 1997). Pan evaporation and wind speed have also changed (Li et al., 2013). The annual runoff increased as well, e.g. for the Urumqi River, the Kaidu River and the Aksu River (Wang et al., 2013; Ye et al., 2005).

Future changes in the streamflow and watershed hydrology have become increasingly important to water resource management in the Tianshan Mountains. However, only a limited number of studies currently focus on impact of future climate change on hydrology, e.g., Sorg et al. (2012) indicated that the total runoff is likely to remain stable or even increase slightly in the near future but it will decrease at the end of the 21st century for Central Asia. There are also researches demonstrating that the annual runoff will decrease to some extent in the first half of the 21st century (T. Liu et al., 2011; Z. Liu et al., 2010). Previous studies seldom address implications of climate change on the hydrologic cycle and hydrological components (e.g., ET, surface flow and groundwater). To complement these studies, this paper aims at understanding the future hydrological system and assessing the responses of the hydrologic system to climate change.

In the present study, two sets of climatic data, i.e. RCM outputs and SCC data, are used to force SWAT (Arnold et al., 1998) and are applied to the Kaidu River Basin, a typical watershed on the south slope of the Tianshan Mountains, to assess future changes of the hydrologic cycle and the hydrological effects of changes in climate variables. Questions that are addressed include the followings: 1) How will the future climate and hydrology change in this region? 2) What is the effect of climate change on the hydrologic cycling? 3) What is the difference

between simulations with RCM outputs and SCC? Understanding these issues will enable to assess the future hydrological change and its unique hydro-meteorological processes better.

5.2 Study area and data

The study area is the Kaidu River Basin, which is illustrated in detail in Section 3.2. As one of the headwaters of the Tarim River, it provides water resources for agricultural activity and ecological environment of the oasis in the lower reaches. This oasis, with a population of over 1.15 million, is stressed by lack of water and water resources are the main factor constricting the development (Chen et al., 2013). Therefore, projecting the impact of future climate change on water resources is urgent to the sustainable development of this region.

The daily observed meteorological data (including precipitation, maximum/minimum temperature, wind speed and relative humidity of two meteorological stations Bayanbulak and Baluntai) from 1970 to 2005 are from the China Meteorological Data Sharing Service System (http://www.cma.gov.cn/2011qxfw/2011qsjgx/). The observed streamflow data at the Dashankou hydrologic station are used to calibrate the hydrological model.

5.3 Methodology

5.3.1 Hydrologic model and uncertainty analysis method

In this study, the distributed hydrological model SWAT was used to analyze the hydrological processes, and used to predict future hydrological response to climate change.

GLUE (Generalized Likelihood Uncertainty Estimation) (Beven & Binley, 1992) is an uncertainty analysis technique, in which the parameter uncertainty accounts for all sources of uncertainty, such as input uncertainty, structure uncertainty, parameter uncertainty and response uncertainty (Yang et al., 2008). In GLUE, the parameter uncertainty is described as a set of discrete “behavioral” parameter sets with corresponding “likelihood weights”.

The procedure of a GLUE analysis consists of three steps. Firstly, after the definition of the “generalized likelihood measure”, $L(\theta)$, a large number of parameter sets are randomly sampled from the prior distribution and each parameter set is assessed as either “behavioral” or “non-behavioral” by comparing its value of $L(\theta)$ to the threshold value. Secondly, each behavioral parameter set is given a “likelihood weight” and we gave them equal weights in this study. Finally, prediction uncertainty is represented by 5% and 95% quantiles of the cumulative distribution of the behavior parameter sets.

Two indices are used to quantify the quality of the uncertainty performance. Those indices are the percentage of measurements bracketed by the 95% prediction uncertainty band (P-factor)

and width of band (R-factor, calculated by the average width of the band divided by the standard deviation of the corresponding measured variable).

5.3.2 Regional climate model

The RCM outputs used in this study are based on the work done by Gao et al. (2013), which is illustrated in Section 4.2.2. After the RCM model was validated with the observational dataset over China for the period period, it was used to predict the future climate change under the new emission scenarios (RCP4.5 and RCP8.5). The RCM validation shows reasonable simulations of temperature and precipitation were obtained over most parts of China and compared to the BCC_CSM1.1 model, marked improvement of the RCM was achieved in reproducing present day precipitation and temperature. For more details refer to Gao et al. (2013).

5.3.3 Bias correction methods

Five precipitation and three temperature correction methods were selected to bias-correct the raw RCM outputs. Precipitation correction methods include linear scaling, local intensity scaling, power transformation, distribution mapping and quantile mapping. Temperature correction methods include linear scaling, variance scaling and distribution mapping. They are combined into 15 schemes to evaluate their performances in simulating streamflow. It turns out that the precipitation correction methods have more significant influence than the temperature correction methods on streamflow simulation, and the power transformation and quantile mapping perform best in terms of frequency based statistics. Thereafter, the quantile mapping method (for precipitation) and the distribution mapping (for temperature) are selected to correct the raw RCM outputs for the future period (more details see Section 4).

5.3.4 SCC data description and analysis procedures

In the following section, temperature and precipitation are denoted as T and P and the absolute and relative change are represented by Δ and δ. For example, ΔT refers to an absolute temperature change and δP a relative precipitation change. The hydrological processes analyzed in this study include streamflow, surface runoff, subsurface runoff and evapotranspiration, which are denoted as Q, R_s, R_{ss} and ET and their relative changes are described as δQ, δR_s, δR_{ss} and δET, respectively.

The SCC was constructed to represent a wide range of changes in climatic variables and how these changes might translate in streamflow and other hydrological components and also to analyze the differences between simulations with RCM outputs and SCC. For SCC, perturbations of the corrected RCM simulated P and T from 1986 ~ 2005 (control period) are set, i.e., for T, an additive change (Δ) is used: ΔT= -1, 0, 1, 2, 3, 4, 5, 6 °C. For P, a relative change (δ)

is used: δP = -20%, -10%, 0, 10%, 20%, 30%, 40%, 50% and 60%. They are put into 81 SCC scenarios, with ΔT= 0 and δP = 0% being the climate for control period.

By investigating the transient evolution of climate change in the corrected RCM outputs on decadal scales, five periods (each spanning 20 years) are defined: 1986~2005 (control period) and 2020~2039, 2040~ 2059, 2060~2079 and 2080~2099. Due to the intra-annual characteristics of the hydrometeorology in the Kaidu River Basin, the wet season (from April to September) and dry season (from October to March next year) are defined based on the intra-annual distribution of P and Q, e.g., P and Q in the wet season account for 88% and 73% of their annual amounts. The climatic and hydrological changes are classified into three categories, i.e. a significant change, small change and insignificant change, to clearly demonstrate the changing magnitude according to the values of relative change for precipitation and hydrological components and absolute change of temperature. These categories are presented in Table 5.1.

Table 5.1 Classification of magnitude for climatic and hydrological changes. δ and Δ represent relative change and absolute change.

	Precipitation & Hydrological components (%)	Temperature (℃)
Significant change	$\|\delta\| \geq 20$	$\|\Delta\| \geq 2$
Small change	$10 \leq \|\delta\| < 20$	$1 \leq \|\Delta\| < 2$
Insignificant change	$\|\delta\| < 10$	$\|\Delta\| < 1$

5.4 Results and discussion

5.4.1 Validation of the hydrological model and the bias correction methods

Performance of the hydrological model forced by observed meteorological data and the 95% prediction uncertainty bands are shown in Figure 5.1. The simulated streamflow agrees quite well with the observation for both calibration period (1986 ~ 1989) and validation period (1990 ~ 2002). For the uncertainty analysis, NS is used as L(θ) and 0.70 as threshold value with 10,000 initial parameter sets, 288 sets were selected as behavioral points. The results show that most of the observations are bracketed by the 95% prediction uncertainty band (P-factor are 87% and 80% for calibration and validation periods with R-factor being 1.18 and 1.19, respectively). The lower P-factor for the validation period can be partly attributed to operation

of hydropower station since 1991 which leads to great fluctuation in winter streamflow. Statistics of model efficiency (Table 5.2) indicate excellent performances for both calibration and validation periods, with "NS"s and "R^2"s over 0.80, which is highly acceptable according to (Moriasi et al., 2007). Concerning the monthly streamflow, the "NS" is 0.89 during 1986 ~ 2005 and it indicates that the SWAT model captured the natural monthly streamflow variability adequately.

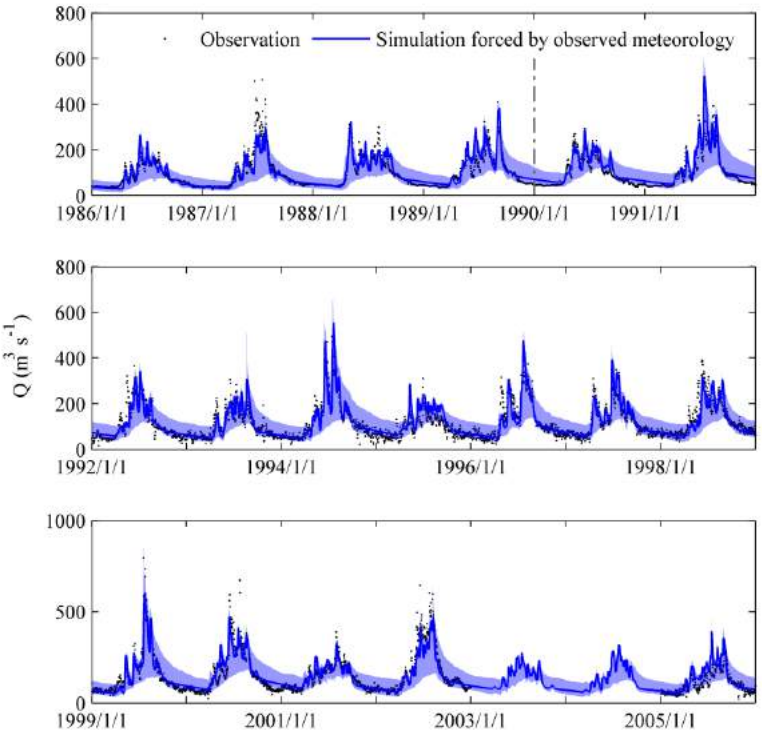

Figure 5.1 Time series of daily observed streamflows (dots) and simulated streamflows forced by observed meteorological data (blue line) for calibration period (1986 – 1989) and validation period (1990 – 2005) with 95% prediction uncertainty bands (blue shaded area).

Table 5.2 Statistics of bias-corrected RCM outputs and SWAT simulated streamflows forced by the observed climate variables and bias-corrected RCM outputs.

Statistics	*NS*	*PBIAS*	R^2
"RCM simulated precipitation with bias correction" [a]			
Validation period 1990~2005 (daily) [b]	-0.57	-6.80%	0.00
Validation period 1990~2005 (monthly)	0.57	-6.80%	0.60
"RCM simulated maximum temperature with bias correction" [a]			
Validation period 1990~2005 (daily)	0.77	3.80%	0.80
Validation period 1990~2005 (monthly)	0.95	4.00%	0.90
"Streamflow simulated with observed meteorological data"			
Calibration period 1986~1989 (daily)	0.80	0.01%	0.80

First validation period 1990~2002 (daily)	0.81	2.94%	0.81
Second validation period 1986~2005 (monthly)	0.89	2.86%	0.90
"Streamflow simulated with bias-corrected RCM outputs"			
Validation period 1990~2002 (daily)	0.46	-6.98%	0.47
Validation period 1986~2005 (monthly)	0.62	-7.85%	0.63

[a] Bias correction methods used are quantile mapping for precipitation and distribution mapping for temperature.

[b] "daily" or "month" in the brackets means the time step used to calculate the statistics.

The performances of bias-corrected RCM outputs (compared to observed meteorological data) are listed in Table 5.2. The "NS"s are -0.57 (0.57) and 0.77 (0.95) for daily (monthly) precipitation and temperature for 1990 ~ 2005, respectively. And the statistics of the streamflow simulated with the bias-corrected RCM outputs shows acceptable results with "NS"s equal to 0.46 and 0.62 and PBIAS within 10% for daily and monthly streamflows.

5.4.2 RCM projected hydrometeorologic changes

5.4.2.1 Changes in temperature and precipitation

Temperature is highly likely to increase in the future, with a basin warming of 1.0 ~ 2.2 ℃ and 1.6 ~ 4.6 ℃ under RCP4.5 and RCP8.5 in the 21st century (Table 5.3). Temperature increases continuously under both scenarios but the magnitude is larger under RCP8.5 (Figure 5.2).

Table 5.3 RCM projected precipitation change (δP), temperature change (ΔT) and streamflow change (δQ) for the 21st century under RCP4.5 and RCP8.5 compared to the control period (1986~2005)

		2020~2039	2040~2059	2060~2079	2080~2099
	δP (%)	4.0	2.0	11.0	16.0
RCP4.5	ΔT (℃)	1.0	1.6	2.0	2.2
	δQ (%)	6.0	-1.0	10.0	18.0
	δP (%)	7.0	15.0	19.0	24.0
RCP8.5	ΔT (℃)	1.6	2.3	3.3	4.6
	δQ (%)	4.0	16.0	20.0	15.0

Precipitation shows an overall increasing trend in the 21st century with an annual increase of 2% ~ 16% and 7% ~ 24% under RCP4.5 and RCP8.5, which confirms the previous arguments of Sorg et al. (2012). However, precipitation change varies substantially among seasons (Figure 5.2). Normally, a small increase in the wet season (-2% ~ 16%) and a significant increase during dry season (18% ~ 78%) are projected. Note that the relative increase (not the absolute increment) of precipitation for the dry season is much bigger than for the wet season, which is in line with the climate changes in other regions, e.g. the semi-arid Colorado River Basin (Christensen & Lettenmaier, 2007) and the wet Ganges–Brahmaputra–Meghna basin (Masood et al., 2015).

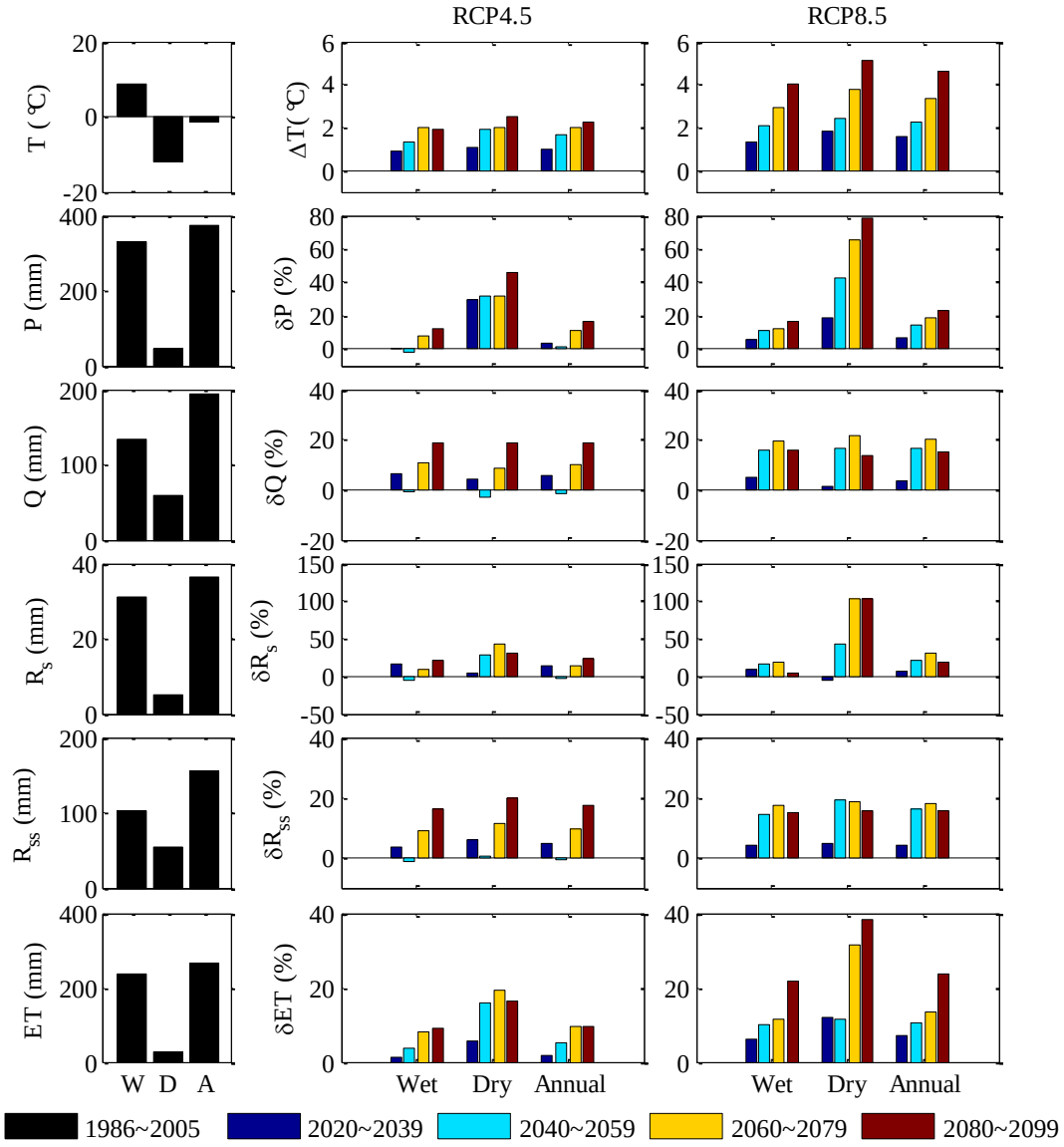

Figure 5.2 Summary of future climate inputs (P and T) and simulated hydrologic components (Q, R_s, R_{ss} and ET) under RCP4.5 and RCP8.5, compared to their values in the control period (1986~2005). All these hydrometeorologic factors are presented in terms of wet season, dry season

and annual values.

5.4.2.2 Changes in the hydrological cycle

The changes in precipitation and temperature cause changes in potential streamflow. The average annual streamflow rises by -1% ~ 18% and 4 ~ 20% under the RCP 4.5 and RCP8.5 in the 21st century, based on the average annual streamflow of 194 mm for the control period (1986 ~ 2005) (Table 5.3). Note that the streamflow stopped increasing in 2080 ~ 2099 (end 21st century) under RCP8.5 despite the rise in precipitation, which confirms the finding of Sorg et al. (2012) and may aggravate water scarcity in this region.

Figure 5.2 also shows the projected changes in surface runoff (R_s), subsurface runoff (R_{ss}) and evapotranspiration (ET) under RCP4.5 and RCP8.5. Overall, changes of hydrologic components are bigger for RCP8.5 than for RCP4.5. The annual change of R_s is insignificant (<5%) but with obvious seasonal variability, e.g., changes of R_s range from -22% to 2% for the wet season and 4% ~ 78% for the dry season under RCP8.5. The annual R_{ss} changes -0.7% ~17% and 4% ~18% for RCP4.5 and RCP8.5, which is consistent with the changes of Q. ET increases continuously in the 21st century with average increases of 2% ~ 10% and 7% ~ 24% under RCP4.5 and RCP8.5.

5.4.3 Response of hydrological cycle to climate change

The response of the hydrological cycle to climate change is estimated by running the hydrological model forced by SCC. The responses of Q, R_s, R_{ss} and ET to climate change are demonstrated with response surfaces in Figure 5.3.Q is positively related to P and negatively related to T. The relationship of δQ and δP is almost linear with the streamflow elasticity (δQ/δP) being about 1.0 when $\Delta T < 2°C$, i.e., a 1% change in the mean annual precipitation results in a 1% change in the mean annual streamflow. δQ/δP is lower than that for other arid regions, e.g., 2.0 ~ 3.5 for Australia (Chiew et al., 2006). The possible reasons are: 1) the Kaidu River Basin, located in the south slope of the Tianshan Mountains with a high average altitude (2,995 m), is characterized by a cold climate (average annual temperature is −4.1°C for the Bayanbulak Station) and accordingly there is a low amount of energy available for ET, which results in a relatively high runoff coefficient (Q/P=0.51) and consequently a low streamflow elasticity; 2) the streamflow is also influenced by temperature dominated snowmelt (snowfall accounts for about 17% of watershed precipitation), which reduces the dependence of streamflow on precipitation and therefore results in a low streamflow elasticity (Chiew et al., 2006).

The response of Q to ΔT depends on the magnitude of ΔT. Q decreases slightly when 0 <

ΔT ≤2.0 ℃ while it decreases dramatically when ΔT ＞ 2.0 ℃ for both wet and dry season. For example, when ΔT = 2.0 °C, a 40% precipitation increase results in an average value of Q being 240 mm (23% increase compared to the average streamflow of 194 mm) but when ΔT = 4.0 °C, the same precipitation increase only generates an average Q of 180mm (about 7% decrease) (Figure 5.3).

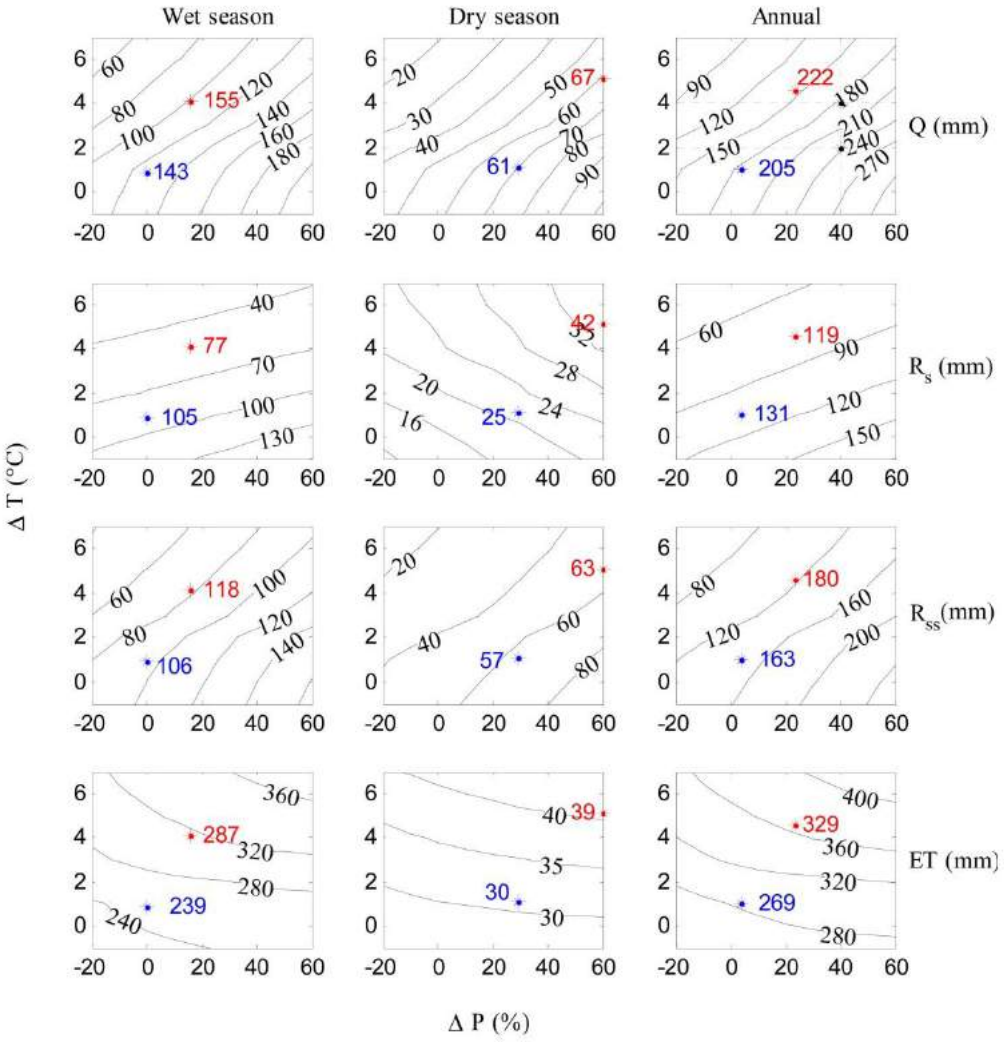

Figure 5.3 Response surfaces of streamflow (Q), surface runoff (R_s), subsurface runoff (R_{ss}) and evapotranspiration (ET) to climate change. The simulations with RCM outputs for 2020 ~ 2039 under RCP4.5 and for 2080 ~ 2099 under RCP8.5 (their corresponding meteorological changes are listed in Table 3) are indicated using blue and red stars with labels.

The responses of R_s, R_{ss} and ET to climate change are also demonstrated in Figure 5.3. For

R_s, the responses of R_s to ΔT are quite different for the wet and dry seasons: the higher the ΔT, the lower R_s for the wet season but the higher R_s for the dry season. Since R_s in the dry season only accounts for 13% of the annual R_s, the response of annual R_s is consistent with that of the wet season. For R_{ss}, the responses of R_{ss} to ΔT and δP are similar to the responses of Q due to the dominant role of groundwater recharge in water yield in the Kaidu River Basin. For ET, it is mainly influenced by ΔT with temperature sensitivity ($\delta ET/\Delta T$) being 7.3%/°C. To verify this result, we firstly investigated basin scale energy and water budget using the Budyko method (Budyko, 1974; Jones et al., 2012). It is shown that ET is mainly energy limited rather than water limited (average ET/P = 0.67 and PET/P = 0.88). Secondly, the high determinate coefficient $R^2 = 0.75$ (significant level is smaller than 0.01) between the mean annual T and ET also indicates that ET has a strong correlation with T. This is consistent with previous studies, which have shown that a significant variation in ET is expected to follow changes in air temperature (Abbaspour et al., 2009; Setegn et al., 2011).

In addition, simulations with RCM outputs are shown in Figure 5.3 to analyze the differences between simulations of these two data sets. Two typical periods of RCM simulations are selected, i.e. 2020 ~ 2039 under RCP4.5 and 2080 ~ 2099 under RCP8.5, to represent mild and intense climate change scenarios (shown as blue and red stars in Figure 5.3). It is indicated that the simulations of hydrological components with RCM outputs for 2020 ~ 2039 under RCP4.5 (mild climate change) are close to these of the nearby contour lines (simulations with SCC), which suggests similar results of Q, R_s, R_{ss} and ET are obtained for RCM outputs and for SCC under mild climate change scenarios. However, for 2080 ~ 2099 under RCP8.5 with δP = 24%, $\Delta T = 4.6$°C, the simulated values of Q, R_s, R_{ss} and ET deviate from the simulations of SCC. There are two possible reasons: 1) changes of other meteorological inputs, i.e., solar radiation, wind speed and humidity, are slightly smaller for 2020 ~2039 under RCP4.5 than those for 2080 ~ 2099 under RCP8.5 (-0.8%, 2.6%, 0.9% compared to -2.2%, 4.1%, 1.4%); 2) for 2080 ~ 2099 under RCP8.5, precipitation increases 24% with great seasonal variation, which may alter the hydrological regime, e.g., precipitation increases 139% for March, April and May while it decreases -0.1% for June, July and August. Since changes of solar radiation, wind speed and humidity are within $\pm 5\%$, the second reason, i.e., the shift of the precipitation temporal distribution contributes a lot to the deviation of simulations with RCM outputs from simulations with SCC.

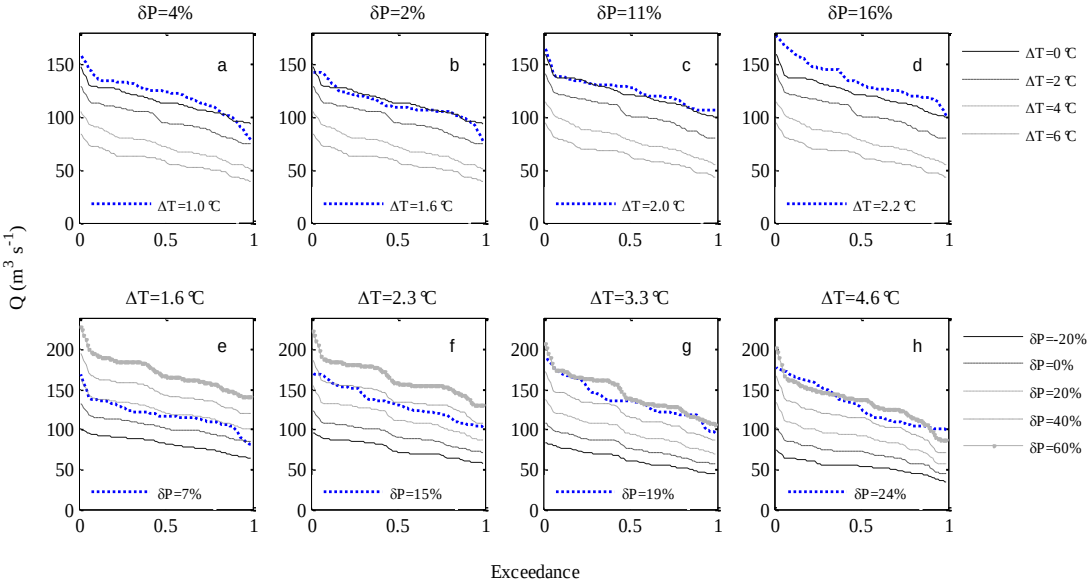

Figure 5.4 Exceedance probability curves of average annual streamflow (Q) in response to temperature change and precipitation change based on SCC with each plot either with fixed precipitation change (a ~ d) and fixed temperature change (e ~ h). Dotted blue line in each plot denotes exceedance probability curves of average annual streamflow for the simulation with RCM outputs given fixed δP and ΔT as summarized in Table 5.3

Further, the exceedance probability curves of the annual runoff in response to climate change are demonstrated in Figure 5.4. The exceedance probability curves are almost parallel when ΔT ranging from 0 ~ 6 °C. However, the responses of Q to δP are not the same for each exceedance probability: high sensitivity of Q with probabilities less than 0.1 and low sensitivity of the Q with probabilities larger than 0.9. A comparison of the simulations with RCM outputs (four future periods under RCP4.5 and RCP8.5) and with SCC (same changes in T or P with the corresponding RCM outputs) indicates that differences between simulation with RCM outputs and SCC are becoming greater as climate change getting more intense, e.g., the simulation with RCM for 2080 ~ 2099 under RCP8.5 overestimates the corresponding simulations with SCC (Figure 5.4h), which collaborates the conclusion that under intense climate change scenarios the simulated hydrology with RCM deviates from that simulated with SCC.

The contributions of hydrologic components to water yield are displayed by De Finetti diagram in Figure 5.5. For the control period, the averages of R_s, R_{ss} and ET are 0.22, 0.28 and 0.50. For SCC, as ΔT increases from 0 to 6°C, the contribution of ET increases rapidly from 0.49 to 0.73 and the contributions of R_s and R_{ss} decrease from 0.22 to 0.11 and from 0.29 to 0.16. ΔT has a more significant influence on the proportion change than δP. As δP changes from -20%

to 60%, ET decreases from 0.71 to 0.58 and R_s and R_{ss} increase from 0.13 to 0.15 and from 0.16 to 0.27. For simulations with RCM outputs, proportions of hydrological components don't change significantly under RCP4.5, while the proportion of ET shows a significant increase under RCP8.5.

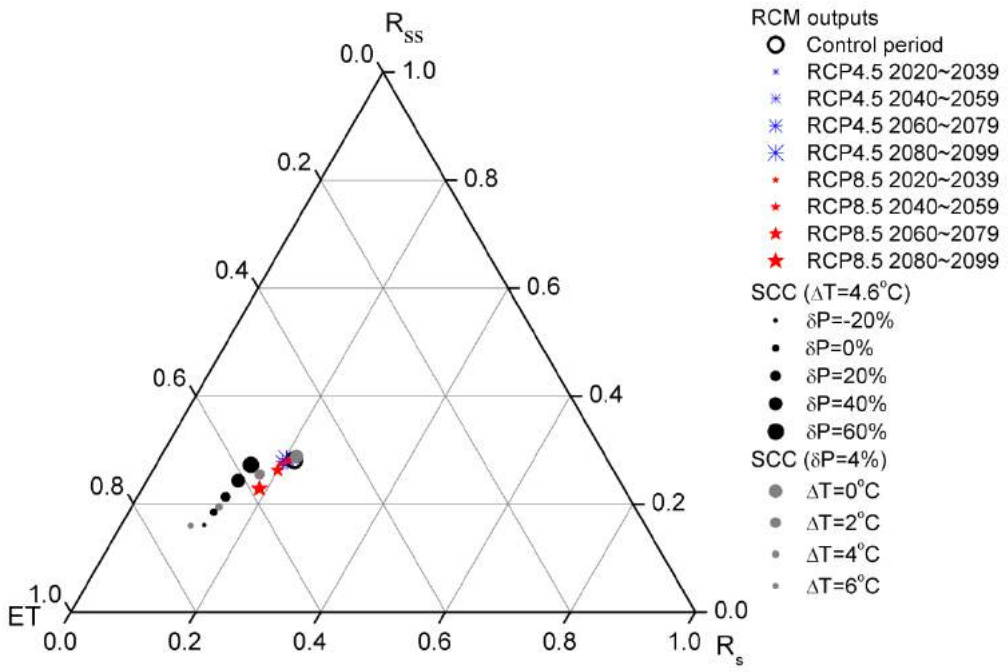

Figure 5.5 De Finetti diagram (ternary plot) of evapotranspiration (ET), surface runoff (R_s) and subsurface runoff (R_{ss}) for SCC (shown as dots) and RCM outputs (shown as stars, details of the projected changes in RCM outputs can refer to Table 5.3).

5.4.4 Sources of uncertainty and other considerations

There are uncertainties in estimating climate change impact on hydrology. As indicated by previous studies (Hagemann et al., 2013), the sources of uncertainty may rise from climate models, emission scenarios, downscaling and the hydrological model.

For hydrological modeling itself, the effect of future climate in any specific catchment is difficult to project due to the possibility that the hydrological system may not be stationary with complex feedbacks (Silberstein et al., 2012). For example, the same land cover and soil data were used for both control period and future climate change period, which may not well represent the land surface under the future climate changes. Effects of land cover change on streamflows and other components of the hydrological cycle are not considered.

Though uncertainty in hydrologic modeling was quantified with the GLUE method, it only accounts for part of the total uncertainty in climate change impact studies (Kingston & Taylor,

2010). Uncertainties associated with the climate model and downscaling were not considered here although two emission scenarios were included. Any uncertainty associated with them may cause the results to deviate from reality. However, we are dedicated to pursuing a thorough investigation of the response of the hydrological cycle to future climate change for this region and we believe this study is an important first step in achieving this goal.

5.5 Conclusions

This study assessed the implications of climate change on hydrology in a typical watershed in the Tianshan Mountains with two sets of climatic data, i.e., RCM outputs and SCC, loosely coupled to a hydrological model (SWAT). Major conclusions can be summarized as follows:

1. The hydrological model shows excellent performance with "NS"s over 0.8 for the daily streamflow for both calibration and validation period. And the selected bias correction methods were effective in downscaling RCM outputs, with "NS"s being 0.57 and 0.95 regarding monthly precipitation and temperature. The simulated streamflow using the bias corrected RCM outputs could reproduce the observed streamflow with "NS" equals to 0.62.
2. T increases 1.0 ℃ ~ 2.2 ℃ and 1.6 ℃ ~ 4.6 ℃ under RCP4.5 and RCP8.5 in the 21st century. For P, it shows an overall increasing trend (2% ~ 24%) with significant increase for the dry season (18% ~ 78%) and relatively small change for the wet season (-2% ~ 16%) under two emission scenarios. The projected Q shows an overall increasing trend (-1% ~ 18% and 4 ~ 20% for RCP4.5 and RCP8.5) in the 21st century.
3. Q increases almost linearly with P while the response of Q to T depends on the magnitude of ΔT and Q decreases significantly when ΔT is greater than 2°C.
4. Similar responses of Q, R_s, R_{ss} and ET to P and T are obtained for the RCM outputs and for SCC under mild climate change scenarios. However, for intense climate change scenarios, simulations of Q, R_s, R_{ss} and ET with RCM outputs (e.g. for 2080 ~ 2099 under RCP8.5) deviate from simulations with SCC.
5. ΔT has more significant influence on the proportion change of each hydrologic component than δP does. As ΔT increases from 0 to 6°C, the contribution of ET increases rapidly from 0.49 to 0.73 and R_s, R_{ss} decrease by 0.11 and 0.13. As δP changes from -20% to 60%, ET, R_s and R_{ss} change -0.13, 0.02 and 0.11 as a result.

It is valuable to quantify the future responses of hydrology to climate change in the Tianshan Mountains. This study will provide useful information for water resource management and will serve as a basis for further climate change impact studies.

References

Abbaspour, K. C., Faramarzi, M., Ghasemi, S. S., & Yang, H. (2009). Assessing the impact of climate change on water resources in Iran. *Water resources research*, *45*(10).

Aizen, V. B., Aizen, E. M., Melack, J. M., & Dozier, J. (1997). Climatic and hydrologic changes in the Tien Shan, central Asia. *Journal of Climate, 10*(6), 1393-1404.

Arnold, J. G., Srinivasan, R., Muttiah, R. S., & Williams, J. (1998). Large area hydrologic modeling and assessment part I: Model development1. *JAWRA Journal of the American Water Resources Association, 34*(1), 73-89.

Beven, K., & Binley, A. (1992). The future of distributed models -model calibration and uncertainty prediction. *Hydrological Processes, 6*(3), 279-298. doi:10.1002/hyp.3360060305

Budyko, M. I. (1974). *Climate and Life*. New York: Academic Press.

Chen, Y., Du, Q., & Chen, Y. (2013). *Sustainable water use in the Bosten Lake Basin*. Beijing: Science press.

Chiew, F. H., Peel, M. C., McMahon, T. A., & Siriwardena, L. (2006). *Precipitation elasticity of streamflow in catchments across the world*. Paper presented at the Climate Variability and Change—Hydrological Impacts Proceedings of the Fifth FRIEND World Conference Havana, Cuba.

Christensen, N. S., & Lettenmaier, D. P. (2007). A multimodel ensemble approach to assessment of climate change impacts on the hydrology and water resources of the Colorado River Basin. *Hydrology and Earth System Sciences Discussions, 11*(4), 1417-1434.

Gao, X., Wang, M., & Giorgi, F. (2013). Climate change over China in the 21st century as simu-lated by BCC_CSM1. 1-RegCM4. 0. *Atmos. Oceanic Sci. Lett, 6*, 381-386.

Hagemann, S., Chen, C., Clark, D. B., Folwell, S., Gosling, S. N., Haddeland, I., Wiltshire, A. J. (2013). Climate change impact on available water resources obtained using multiple global climate and hydrology models. *Earth System Dynamics, 4*(1), 129-144. doi:10.5194/esd-4-129-2013

Jones, J. A., Creed, I. F., Hatcher, K. L., Warren, R. J., Adams, M. B., Benson, M. H., Covich, A. (2012). Ecosystem processes and human influences regulate streamflow response to climate change at long-term ecological research sites. *BioScience, 62*(4), 390-404.

Kingston, D. G., & Taylor, R. G. (2010). Sources of uncertainty in climate change impacts on river discharge and groundwater in a headwater catchment of the Upper Nile Basin, Uganda. *Hydrology and Earth System Sciences, 14*(7), 1297-1308. doi:10.5194/hess-14-1297-2010

Li, B., Chen, Y., & Shi, X. (2012). Why does the temperature rise faster in the arid region of northwest China? *Journal of Geophysical Research, 117*(D16115).

Li, Z., Chen, Y., Li, W., Deng, H., & Fang, G. (2015). Potential impacts of climate change on vegetation dynamics in Central Asia. *Journal of Geophysical Research: Atmospheres*.

Li, Z., Chen, Y., Shen, Y., Liu, Y., & Zhang, S. (2013). Analysis of changing pan evaporation in the arid region of Northwest China. *Water Resources Research, 49*(4), 2205-2212.

Liu, T., Willems, P., Pan, X. L., Bao, A. M., Chen, X., Veroustraete, F., & Dong, Q. H. (2011). Climate change impact on water resource extremes in a headwater region of the Tarim basin in China. *Hydrology and Earth System Sciences, 15*(11), 3511-3527. doi:10.5194/hess-15-3511-2011

Liu, Z., Xu, Z., Huang, J., Charles, S. P., & Fu, G. (2010). Impacts of climate change on hydrological processes in the headwater catchment of the Tarim River basin, China. *Hydrological Processes, 24*(2), 196-208. doi:10.1002/hyp.7493

Masood, M., Yeh, P.-F., Hanasaki, N., & Takeuchi, K. (2015). Model study of the impacts of future climate change on the hydrology of Ganges–Brahmaputra–Meghna basin. *Hydrology and Earth*

System Sciences, 19(2), 747-770.

Moriasi, D. N., Arnold, J. G., Van Liew, M. W., Bingner, R. L., Harmel, R. D., & Veith, T. L. (2007). Model evaluation guidelines for systematic quantification of accuracy in watershed simulations. *Transactions of the ASABE, 50*(3), 885-900.

Setegn, S. G., Rayner, D., Melesse, A. M., Dargahi, B., & Srinivasan, R. (2011). Impact of climate change on the hydroclimatology of Lake Tana Basin, Ethiopia. *Water Resources Research, 47*(4), W04511. doi:10.1029/2010WR009248

Shi, Y., Shen, Y., Kang, E., Li, D., Ding, Y., Zhang, G., & Hu, R. (2007). Recent and future climate change in northwest China. *Climatic change, 80*(3-4), 379-393.

Silberstein, R. P., Aryal, S. K., Durrant, J., Pearcey, M., Braccia, M., Charles, S. P., McFarlane, D. J. (2012). Climate change and runoff in south-western Australia. *Journal of Hydrology, 475*, 441-455. doi:10.1016/j.jhydrol.2012.02.009

Sorg, A., Bolch, T., Stoffel, M., Solomina, O., & Beniston, M. (2012). Climate change impacts on glaciers and runoff in Tien Shan (Central Asia). *Nature Climate Change, 2*(10), 725-731.

Wang, H., Chen, Y., Li, W., & Deng, H. (2013). Runoff responses to climate change in arid region of northwestern China during 1960–2010. *Chinese Geographical Science, 23*(3), 286-300.

Wang, S., Zhang, M., Li, Z., Wang, F., Li, H., Li, Y., & Huang, X. (2011). Glacier area variation and climate change in the Chinese Tianshan Mountains since 1960. *Journal of Geographical Sciences, 21*(2), 263-273.

Yang, J., Reichert, P., Abbaspour, K., Xia, J., & Yang, H. (2008). Comparing uncertainty analysis techniques for a SWAT application to the Chaohe Basin in China. *Journal of Hydrology, 358*(1), 1-23.

Ye, B., Yang, D., Jiao, K., Han, T., Jin, Z., Yang, H., & Li, Z. (2005). The Urumqi River source glacier No. 1, Tianshan, China: changes over the past 45 years. *Geophysical Research Letters, 32*(21).

6 General discussion

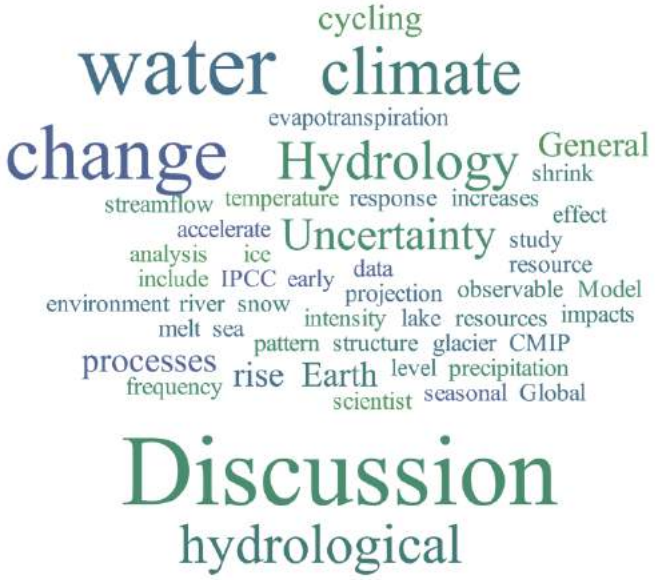

Over the last decades, climate change impact study has become the focus for governments and scientists. This dissertation has investigated the climate change impact on the hydrological processes in the Kaidu River Basin located in the south slope of the Tianshan Mountains.

This chapter summarizes and discusses the results obtained from this dissertation. Comments will be given on the results obtained in the previous chapters, including the general methodology, Comparison is made between our and other studies. Besides, the limitations of this study are also addressed , of which we discuss some valuable aspects concerning climate change impacts and try to shed some light on future work.

In the first section, the topics and related results are discussed. In the following two sections, the limitations of this dissertation are considered and also some future work is proposed.

6.1 Summary and discussion on research questions

This topic is inspired - not only by the unique geomorphological feature of Central Asia - but also by the great demand of water resources in some parts for use in agriculture, urban development and ecosystem management (Li et al., 2011). To study the impacts of climate change on hydrological cycling, we use a cascade of RCM, downscaling methods and one hydrological model to account for changes of hydrological processes. Following this objective, four research questions are addressed in each chapters. In Table 6.1, an overview of the topics and main results of the chapters is given.

- RQ1: How will the climate change in the 21st century for the mountainous regions of Central Asia?
- RQ2: What are the major hydrologic processes and influential factors in hydrologic modelling in the Kaidu River Basin?
- RQ3: How can we effectively downscale the climatic projections from climate models and apply them to the hydrological modeling?
- RQ4: How will the hydrological processes change in the 21st century in the Kaidu River Basin?

Table 6.1 Overview of the main methodology and the results of each chapter

Chaper	RQ	Topics and methodology	Main results
Ch2: Projected climate changes for the mountainous regions of Central Asia in the 21st century	RQ1	▪ State-of-the-art GCM ensemble in the CMIP5 project ▪ Using the BMA to better account for the ensemble information of precipitaiton and tempeature	▪ mean annual temperature will rise considerably by 0.031 °C/a and 0.054 °C/a, precipitation will increase by 0.09 and 0.11 mm/a, and snowfall will dramatically decrease by -0.12 and -0.20 mm/a under RCP4.5 and RCP8.5, respectively; ▪ Snowfall fraction declines
Ch3: Hydrological modeling of the Kaidu River basin	RQ2	▪ State-of-the-art hydrological modeling using SWAT ▪ Quantifying the contribution of meteoroligcla input to streamflow modeling ▪ Indentify the critical hydrological processes	▪ Meteorological input account for 64% of model uncertainty ▪ Groundwater process is most important hydrological processes in the Kaidu River Basin
Ch4: Comparing bias correction methods in downscaling meteorological variables for a hydrologic impact study	RQ3	▪ Verification of the necessity of bias correction on downscaling climatic variables ▪ Comparison of the start-of-the-art bias correction methods in downscaling meteorological variables and its impact to hydrological modeling	▪ Bias correction methods could improve the raw climate simulations ▪ Linear regression method is not suitable to correct precipitation, while Local intensity scaling, Power transformation (PT), Distribution mapping for precipitation using gamma distribution (DM) and Quantile mapping (QM) is effective while Local intensity scaling (LOCI) slightly underestimates the extreme precipitation and streamflow. ▪ Bias correction methods for temperature works well
Ch5: Impact of climate change on hydrological processes in the Kaidu River Basin	RQ4	▪ One-way coupling of the state-of-the-art RCM and a hydrological model ▪ Response of hydrological processes to climate change	▪ Temperature is likely to increase by 2.2 °C and 4.6 °C by the end of the 21st century under RCP4.5 and RCP8.5, respectively, while precipitation will increase by 2% ~ 24%, with a significant rise in the dry season and small change in the wet season ▪ Flow will change by -1% ~ 20%, while evapotranspiration will increase by 2% ~ 24% ▪ Flow increases almost linearly with precipitation under mile climate change scenarios

RQ1: How will the climate change in the 21st century for the mountainous regions of Central Asia?

Climate change in Central Asia has gone through a lot of concerns during the past few decades. However, due to the scarce data, the climatic changes of the mountainous regions of Central Asia (MCA) have not been well investigated. (Aizen et al., 1997) concluded that the average rising rates in air temperature and precipitation were 0.01 ℃/a and 1.2 mm/a, and the snow cover area has decreased with the maximum snow thickness and snow duration decreasing by 10 cm and 9 days for the second half of the 20th century the Tianshan mountains. The past climate change in the MCA is comparable with that in the Andes ranges, where a warming rate is approximately 0.05-0.20 ℃/decade (Vuille et al., 2003). The future climate change is quite important concerning to high sensitivity of hydrological processes to climate change. In Chapter 2, we have estimated the climate change in the 21st century for the mountainous regions of the Central Asia (MCA) using a 21-GCM simulation ensemble from CMIP5. To better interpret the climate change and reduce uncertainty, an improved BMA technique was applied to combine the ensemble information of competing GCMs.

We examined changes in precipitation, temperature and snowfall. In our study, the BMA was used to incorporate competing information from each GCM model. An effective BMA technique improved by (Sloughter et al., 2007), which is suitable to simulate the gamma distribution, was applied. The BMA effectiveness in the combination of multi climate predictions, is proved by (Najafi & Moradkhani, 2015; Raftery et al., 2005).

Results show that temperature is very likely to increase under RCP4.5 and RCP8.5 and precipitation is also expected to augment for the larger part of the MCA. Worth noticing is that the snowfall will decline dramatically (especially for the southwest part).

The temperature change in the mountainous regions of Central Asia is likely to rise faster (0.054 ℃/a under RCP8.5) than the global average (0.037 ℃/a), which means that the study area is a hot spot in climate change studies (IPCC, 2013). Concerning precipitation, the increasing rate is 0.09 and 0.11 mm/a under RCP4.5 and RCP4.5. Snowfall will decline dramatically by 26.4% from 72 mm to 53 mm under RCP8.5. Snowfall fraction will decrease from 0.58 in the control period to 0.43 in 2070-2099 under RCP8.5. The results agree with the previous studies. For example, annual snowfall is projected to decrease across much of the Northern Hemisphere during the twenty-first century, with increases projected at higher latitudes (Krasting et al., 2013). For the western and central part of Europe, a strong decrease in the number of Hellmann days and mean Hellmann-day-snowfall is expected with a reduction rate reaching −30% per degree warming, except the high Alps and parts of Scandinavia (de Vries et al., 2014).

Though it is showing an overall increasing tendency of precipitation, considerable uncertainties exist in not only the magnitude but also in the changing direction. The high uncertainty is predictable, since uncertainties in the precipitation prediction is much higher than in temperature prediction. Buytaert et al. (2010) indicated that the uncertainties even exceeded the predicted precipitation change, and Giorgi and Coppola (2010) found a significant correlation between change and bias in about 30% of the cases analyzed, which means that a performance-based selection of models in producing climate change scenarios can affect the estimation. The great uncertainty is also a stimulation for searching a better manner to extract information for ensemble data. Here in our study, the BMA technique can be viewed as an effective way to provide the more accurate information for policy-makers from simulation ensemble.

Climate change exerts a great impact on water storage in the MCA. The increased temperature and shift in precipitation form will definitely alter the current status of the solid water storage and change the water supply conditions. The influence of climate change on the runoff and the hydrologic processes certainly needs to be investigated further.

RQ2: What are the major hydrologic processes and influential factors in hydrologic modeling in the Kaidu River Basin?

A distributed hydrological model was established in the Kaidu River Basin and excellent modeling results have been achieved. A combined sensitivity analysis shows that the meteorological input contributes up to 64 % of the model uncertainty and that the groundwater flow is the most important hydrologic process, which accounts to 80% of the model uncertainty when fixing the meteorological input. The groundwater–stream water interaction is fatally important in the Kaidu River Basin.

Normally, the parameter sensitivity analysis was used to screen out the unimportant parameters and to indicate which parameter is sensitive and therefore needs to be calibrated (Yang et al., 2008). For example, some studies demonstrated that CN2 in SWAT is the most sensitive parameter (Saha et al., 2014; Van Griensven et al., 2006), while it is not so sensitive in the Kaidu River Basin due to the special features of this watershed (See details in Chapter 3). In this study, the sensitivity analysis was also applied to quantify the uncertainties caused by parameters. This is the first time to apply the quantitative sensitivity analysis method to quantify input uncertainty in hydrological modeling, to our best knowledge. The meteorological inputs are most important in the hydrological modeling, therefore, some hydrologists are dedicated to search for more reliable data (e.g. remote sensing data, enhanced observations). For example, Mango et al. (2011) concluded that adding remote sensing data significantly improved the

simulation performance.

The hydrological modeling has developed rapidly due to the development of the computer and hydrological theory. Currently, the regional and global hydrological models have also been developed, besides the catchment hydrological models. Bierkens (2015) reviewed the development of the global hydrological models. The regional hydrological model has also been used in many studies (Bormann & Diekkrüger, 2003). Regarding the catchment hydrological modeling, Pechlivanidis et al. (2011) reviewed the catchment scale hydrological modeling, the related calibration approaches and the uncertainty analysis procedures. However, it has always been a challenging task in the distributed hydrological modeling in data scarce regions. The bottleneck is the meteorological interpolation based on few meteorological stations, especially in the mountainous region. Ly et al. (2013) reviewed the application of certain methods and geostatistical approaches used in the interpolation of rainfall. And it is important to improve the quality of rainfall data and ultimately, the quality of hydrological modeling.

Though model performance was excellent in terms of the stream flow simulation, however, several deficiencies should be discussed. First of all, the glacier processes (glacier melting and accumulation) have not been included in this study, given that the glacier area is about 1.6% in the Kaidu River Basin according to the Chinese Glacier Inventory (Guo et al., 2014). This may affect the calibration and the validation of the hydrological model to some extent. Secondly, the calibrated parameters may be inaccurate, due to the lack of validation data of the underlying surface and the great heterogeneity.

RQ3: How can we effectively downscale the climatic projections from climate models and apply them to the hydrological modeling?

To effectively cope with this issue, we firstly used a RCM model to simulate the high resolution climate in this region and then, downscale them to station scale. The following was the bias correction of the most important meteorological variables. As a result, very good simulations for both the climatic and watershed hydrologic conditions were achieved for some of the bias correction methods.

There are many different approaches concerning downscaling, e.g., dynamic downscaling and statistical downscaling. And the latter, including SDSM, has been widely employed and investigated due to its less computation burden (Wilby et al., 1998). However, these procedures heavily rely on the locally observed atmospheric predictor and are not suitable in this region, since few climate stations are available. Moreover, the spatially interpolated dataset and the climate reanalysis dataset e.g. ERA-interim, NCEP/NCAR, GPCC, MERRA, CFSR have so far been unable to fill this gap, as they fail to reveal the accurate estimation of the station data (Hu &

Zhang, 2014; Wright et al., 2009). Therefore, the combination of the RCM and bias correction methods was applied in this region in order to create a better representation of the current and future climate and to serve the impact study of climate change.

Each bias correction method has its pros and cons. In Chapter 4, we have evaluated the applicability and performance of several widely used bias correction methods, based on their performances in reproducing the meteorological and hydrological conditions. The evaluation metrics generally have a great impact on the assessment of different models or methods. Thereafter, two different kinds of evaluation systems are used: frequency based metrics and time series based metrics. Based on these two evaluation metrics, all the temperature bias correction methods obtained similar results, which is not discussed in detail here. Only the precipitation bias corrections are being dealt with. The LS method is not suitable in bias correcting the RCM simulated precipitation, though it could perfectly reproduce the total amount of the monthly value. When using it to force the SWAT model, it overestimated the stream flow due to the overestimating of the wet-day frequency. In addition, it has also underestimated the extreme precipitation and the extreme stream flow as a consequence. The results correspond with the conclusions of (Teutschbein & Seibert, 2012). On the contrary, the LOCI method (with the adjustment of the wet-day frequency) achieved a much better performance.

The QM method outperformed the DM method, which demonstrates a slight overestimation of the mean and has the assumption that the observed and simulated precipitation follow the gamma distribution. These are supported by previous studies (Graham et al., 2007; Themeßl et al., 2011; Wilcke et al., 2013). That is the reason why the QM method (i.e., BCSD) is most widely applied in the climate change impact studies (Salathe et al., 2007; Sun et al., 2011; Wood et al., 2004). Moreover, some improvements of the QM method have been made gradually made. For example, incorporating and adjusting the model cumulative distribution functions for the projection period on the basis of the difference between the model and the observation for the training period (Li et al., 2010).

A major drawback of the bias correction method is the lack of connection for different stations and variables. In addition, all the bias correction methods failed to correct the time series of both precipitation and temperature. For example, the major problem in the crop yield simulation are the unrealistically long dry spells during the growing season (Ines & Hansen, 2006).

In addition, this case study deals with an arid area in China based on a specific RCM and hydrologic model, but the methodology and some results can be applied to other areas and models as well.

RQ4: How will the hydrological processes change in the 21st century in the Kaidu River Basin?

We have examined the changes in hydrological processes for the Kaidu River Basin using two sets of future climatic data to force a well-calibrated hydrologic model: one is the bias-corrected RCM outputs under RCP4.5 and the RCP8.5 future emission scenarios and the other is the simple climate change (SCC) with an absolute temperature change of -1 ~ 6 ℃ and a relative precipitation change of -20% ~ 60%. The first dataset was used to predict future hydrological processes and the second one to evaluate the sensitivity of hydrological processes to climate change. The combination of these two datasets help to comprehensively understand the future hydrologic regime in the Kaidu River Basin.

The assessment of the climate change impact on the hydrologic processes has been exerted for most parts of the world (IPCC, 2013). According to IPCC5, the general conclusions include: 1) For each degree of global warming, approximately 7% of the global population is expected to be exposed to a decrease of at least 20% (multi-model mean) of renewable water resources; 2) The renewable surface water and groundwater resources are projected to reduce in most dry subtropical regions but increase at high latitudes; 3) The climate change has altered the observed stream flow seasonality (e.g. forwarded snowmelt discharge, increased winter flows and reduced summer low flows) in snow-recharged regions. However, studies of the observed climate changes and their impacts are still inadequate for many areas, particularly in North, Central and West Asia (high confidence) (IPCC, 2013).

Concerning temperature, precipitation and stream flow variation, our results are consistent with previous studies. As to the responses of the hydrological processes to climate change, we concluded that flow increases almost linearly with precipitation while its response to temperature is depending on the magnitude of temperature change and that flow decreases significantly for a temperature rise greater than 2 ℃. This critical threshold of warming is also the aim of the Paris climate conference in 2015. Our study has demonstrated that snowmelt will be pushed forward causing the spring stream flow to increase. This is highly beneficial because the Boston Lake is at its lowest water table and the Yanqi Basin is demanding irrigation water of the growing season. An accelerated melting peak may thus alleviate a shortage in spring irrigation water and causing a summer drought.

Results should be treated with caution, however, because a large proportion of the climate models experience difficulty simulating the interannual precipitation variation (Annamalai et al., 2007; S. Yang et al., 2008), despite the recent progresses in improving the resolution of the anticipated spatial and temporal changes in precipitation (Immerzeel et al., 2010).

Another drawback of this case study is that the glacier melt and accumulation processes have not yet been taken into account, which will influence the hydrological processes in the future. Glacier retreats were observed in the Tianshan Mountains (Kaldybayev et al., 2016) and it will affect the hydrologic regime in the future, especially with the continuous warming (Immerzeel et al., 2010). Future glacier variation was not considered in this study.

6.2 Critical reflection

This dissertation studied the hydrologic cycle in the Kaidu River Basin and the climate change impact on the hydrological processes. In this section, some critical aspects are being presented concerning the current methodology and results for each chapter.

Chapter 2: Several drawbacks existed in the projection of future climate change in the mountainous regions of Central Asia. Firstly, the resolutions of all the GCM models are too low to represent the complex mountain topography. There is a smoothing effect of GCM simulation, e.g. for BCC-CSM1.1-m (resolution is 1.12 °× 1.12 °), the GCM outputs for this grid are the average value over this big grid. The topographical effect cannot exactly be depicted. Secondly, though the BMA method is applied to better account for the reliable climate in the future, the BMA itself induces new uncertainty in the climatic projections.

Chapter 3: In this case, the critical problem for hydrological modeling is that it failed to account for the effect of glacier melt and accumulation. In addition, the strong interaction of surface and groundwater with the scarce meteorological and hydrological data makes the hydrological modeling a challenging project. The calibrated parameters, e.g. the soil hydrologic properties, cannot be fully validated, especially considering its heterogeneity. Therefore, it should be used carefully when applying these parameters for Prediction in Ungauged Basins (PUB).

Chapter 4: The climate variables are downscaled directly to station scale using different bias correction methods. However, there is an assumption that the climate remains stable when using this strategy to downscale future climate, which may not be satisfied. Additionally, the conclusion we made that the precipitation bias correction methods had a greater significance on the simulated stream flow may be case-sensitive. The reason may be that the temperature sensitivity is lower than the precipitation and maybe because temperature itself is easier to be corrected. The selection of the appropriate bias correction should occur according to the research objective (the focus of a certain study), e.g. flood, drought, seasonal patterns, etc.

Chapter 5: Firstly, only one RCM is used in projecting the future hydrological processes, which resulted in the error amplification as stated before. Secondly, we have utilized one way coupling of the RCM simulated climate and hydrological model, which ignores the feedback of

the hydrological cycle to the atmosphere. Thirdly, similar to the deficiency in Chapter 3, glacier processes have not yet been considered in this case. The simulated stream flow has a high dependence on the hydrological model and the only forcing is the climate data and the climate change induced changes in the underlying surface or building reservoirs and electricity plants have not been considered yet.

6.3 Some recommendations for future work

Every dissertation is subject to some limitations, there are no exceptions for this one. In this section, we try to shed some light on the potential direction and improvement of the current study. Several actions are being proposed, concentrating on the following topics.

6.3.1 Future work on climate change detection

We need to figure out urgently how the climate will change with high confidence in the future, especially in the mountainous regions of Central Asia. It is suggested to reduce the uncertainty sources in the climate models and to improve the spatial resolution, especially the development of the regional climate models.

6.3.2 Future work on hydrological modeling

Concerning hydrological modeling, it is suggested to collect more field data, such as the fluxes, actual evaporation, soil water infiltration, etc. , though it may be time consuming and requiring a lot of money. An alternative way may be the use of isotope observations. It is easy to obtain and it is able to trace the hydrologic cycle. At last, different kinds of models should be used in order to understand the hydrological processes.

6.3.3 Future work on impact evaluation and uncertainty analysis

Considering the rapid development of the current studies on the climate change impact, it is suggested to take the impact of human activities into account as suggested in the next IPCC assessment. Furthermore, the climate extremes (and the extreme hydrological events) should also be looked at closely, since the extreme events will exert much severe disaster to human society and ecosystem.

As to the uncertainty quantification, previous studies generally take into account several models, downscaling methods and hydrological models (the numbers are determined by the available quantity) and ignore the potential uncertainties, besides these selected models. Therefore, it is important to find a way to fully account for the uncertainties, which were not/have not been included in the chosen models. It should also be noted that reducing the uncertainty is much important than quantifying uncertainty to policy makers.

References

Aizen, V. B., Aizen, E. M., Melack, J. M., & Dozier, J. (1997). Climatic and hydrologic changes in the Tien Shan, central Asia. *Journal of Climate, 10*(6), 1393-1404.

Annamalai, H., Hamilton, K., & Sperber, K. R. (2007). The South Asian summer monsoon and its relationship with ENSO in the IPCC AR4 simulations. *Journal of Climate, 20*(6), 1071-1092.

Bierkens, M. F. P. (2015). Global hydrology 2015: State, trends, and directions. *Water Resources Research, 51*(7), 4923-4947. doi:10.1002/2015WR017173

Bormann, H., & Diekkrüger, B. (2003). Possibilities and limitations of regional hydrological models applied within an environmental change study in Benin (West Africa). *Physics and Chemistry of the Earth, Parts A/B/C, 28*(33), 1323-1332.

Buytaert, W., Vuille, M., Dewulf, A., Urrutia, R., Karmalkar, A., & Celleri, R. (2010). Uncertainties in climate change projections and regional downscaling in the tropical Andes: implications for water resources management. *Hydrology and Earth System Sciences, 14*(7), 1247-1258. doi:10.5194/hess-14-1247-2010

de Vries, H., Lenderink, G., & van Meijgaard, E. (2014). Future snowfall in western and central Europe projected with a high-resolution regional climate model ensemble. *Geophysical Research Letters, 41*(12), 4294-4299. doi:10.1002/2014GL059724

Giorgi, F., & Coppola, E. (2010). Does the model regional bias affect the projected regional climate change? An analysis of global model projections. *Climatic Change, 100*(3-4), 787-795. doi:10.1007/s10584-010-9864-z

Graham, L. P., Andréasson, J., & Carlsson, B. (2007). Assessing climate change impacts on hydrology from an ensemble of regional climate models, model scales and linking methods–a case study on the Lule River basin. *Climatic Change, 81*(1), 293-307.

Guo, W., Xu, J., Liu, S., Shangguan, D., Wu, L., Yao, X., Wang, Y. (2014). The Second Glacier Inventory Dataset of China (Version 1.0). *Cold and Arid Regions Science Data Center at Lanzhou*. doi:10.3972/glacier.001.2013.db

doi:10.3972/glacier.001.2013.db

Hu, Z., & Zhang, C. (2014). *Evaluation of Reanalysis, Spatially-interpolated and Remote-sensing derived Precipitation Datasets over Central Asia.* Paper presented at the EGU General Assembly Conference Abstracts.

Immerzeel, W. W., Van Beek, L. P., & Bierkens, M. F. (2010). Climate change will affect the Asian water towers. *Science, 328*(5984), 1382-1385.

Ines, A. V., & Hansen, J. W. (2006). Bias correction of daily GCM rainfall for crop simulation studies. *Agricultural and forest meteorology, 138*(1), 44-53.

IPCC. (2013). The Physical Science Basis. Working Group I Contribution to the Fifth Assessment Report of the Intergovernmental Panel on Climate Change. *Cambridge, United Kingdom and New York, USA*.

Kaldybayev, A., Chen, Y., & Vilesov, E. (2016). Glacier change in the Karatal river basin, Zhetysu (Dzhungar) Alatau, Kazakhstan. *Annals of Glaciology, 57*(71), 11.

Krasting, J. P., Broccoli, A. J., Dixon, K. W., & Lanzante, J. R. (2013). Future Changes in Northern Hemisphere Snowfall. *Journal of Climate, 26*(20), 7813-7828. doi:10.1175/JCLI-D-12-00832.1

Li, H., Sheffield, J., & Wood, E. F. (2010). Bias correction of monthly precipitation and temperature fields from Intergovernmental Panel on Climate Change AR4 models using equidistant quantile

matching. *Journal of Geophysical Research: Atmospheres (1984–2012), 115*(D10).

Li, L., Luo, G., Chen, X., Li, Y., Xu, G., Xu, H., & Bai, J. (2011). Modelling evapotranspiration in a Central Asian desert ecosystem. *Ecological Modelling, 222*(20), 3680-3691.

Ly, S., Charles, C., & Degré, A. (2013). Different methods for spatial interpolation of rainfall data for operational hydrology and hydrological modeling at watershed scale: A review. *Biotechnologie, Agronomie, Société et Environnement = Biotechnology, Agronomy, Society and Environment [= BASE], 17*(2).

Mango, L. M., Melesse, A. M., McClain, M. E., Gann, D., & Setegn, S. G. (2011). Land use and climate change impacts on the hydrology of the upper Mara River Basin, Kenya: results of a modeling study to support better resource management. *Hydrology and Earth System Sciences, 15*(7), 2245-2258. doi:10.5194/hess-15-2245-2011

Najafi, M. R., & Moradkhani, H. (2015). Multi-model ensemble analysis of runoff extremes for climate change impact assessments. *Journal of Hydrology, 525*(0), 352-361. doi:http://dx.doi.org/10.1016/j.jhydrol.2015.03.045

Pechlivanidis, I., Jackson, B., McIntyre, N., & Wheater, H. (2011). Catchment scale hydrological modelling: a review of model types, calibration approaches and uncertainty analysis methods in the context of recent developments in technology and applications. *Global NEST Journal, 13*(3), 193-214.

Raftery, A. E., Gneiting, T., Balabdaoui, F., & Polakowski, M. (2005). Using Bayesian model averaging to calibrate forecast ensembles. *Monthly Weather Review, 133*(5), 1155-1174.

Saha, P., Zeleke, K., & Hafeez, M. (2014). Streamflow modeling in a fluctuant climate using SWAT: Yass River catchment in south eastern Australia. *Environmental Earth Sciences, 71*(12), 5241-5254. doi:10.1007/s12665-013-2926-6

Salathe, E. P., Mote, P. W., & Wiley, M. W. (2007). Review of scenario selection and downscaling methods for the assessment of climate change impacts on hydrology in the United States Pacific Northwest. *International Journal of Climatology, 27*(12), 1611-1621.

Sloughter, J. M. L., Raftery, A. E., Gneiting, T., & Fraley, C. (2007). Probabilistic quantitative precipitation forecasting using Bayesian model averaging. *Monthly Weather Review, 135*(9), 3209-3220.

Sun, F., Roderick, M. L., Lim, W. H., & Farquhar, G. D. (2011). Hydroclimatic projections for the Murray-Darling Basin based on an ensemble derived from Intergovernmental Panel on Climate Change AR4 climate models. *Water Resources Research, 47*, W00G02. doi:10.1029/2010wr009829

Teutschbein, C., & Seibert, J. (2012). Bias correction of regional climate model simulations for hydrological climate-change impact studies: Review and evaluation of different methods. *Journal of Hydrology, 456*, 12-29. doi:10.1016/j.jhydrol.2012.05.052

Themeßl, M. J., Gobiet, A., & Leuprecht, A. (2011). Empirical - statistical downscaling and error correction of daily precipitation from regional climate models. *International Journal of Climatology, 31*(10), 1530-1544.

Van Griensven, A., Meixner, T., Grunwald, S., Bishop, T., Diluzio, M., & Srinivasan, R. (2006). A global sensitivity analysis tool for the parameters of multi-variable catchment models. *Journal of Hydrology, 324*(1), 10-23.

Vuille, M., Bradley, R. S., Werner, M., & Keimig, F. (2003). 20th century climate change in the tropical Andes: observations and model results *Climate Variability and Change in High*

Elevation Regions: Past, Present & Future (pp. 75-99): Springer.

Wilcke, R. A. I., Mendlik, T., & Gobiet, A. (2013). Multi-variable error correction of regional climate models. *Climatic Change, 120*(4), 871-887.

Wood, A. W., Leung, L. R., Sridhar, V., & Lettenmaier, D. (2004). Hydrologic implications of dynamical and statistical approaches to downscaling climate model outputs. *Climatic change, 62*(1-3), 189-216.

Wright, C., De Beurs, K., Akhmadieva, Z., Groisman, P. Y., & Henebry, G. (2009). Reanalysis data underestimate significant changes in growing season weather in Kazakhstan. *Environmental Research Letters, 4*(4), 045020.

Yang, J., Reichert, P., Abbaspour, K., Xia, J., & Yang, H. (2008). Comparing uncertainty analysis techniques for a SWAT application to the Chaohe Basin in China. *Journal of Hydrology, 358*(1), 1-23.

Yang, S., Zhang, Z., Kousky, V. E., Higgins, R. W., Yoo, S.-H., Liang, J., & Fan, Y. (2008). Simulations and seasonal prediction of the Asian summer monsoon in the NCEP Climate Forecast System. *Journal of Climate, 21*(15), 3755-3775.

7 General conclusion

This dissertation involves several methodologies to interpret the climate change impact on hydrological processes. Through all the chapters, a comprehensive evaluation of the climate change impact on hydrologic processes has been concluded. From top to bottom, we have applied a cascade which comprises the RCM models, downscaling and bias correction, and hydrological model in order to investigate the climate change impact in the Kaidu River Basin.

The future climate in the Mountainous regions of Central Asia was analyzed. Temperature will increase significantly and at the same time, a slight augmentation is expected in precipitation. The precipitation form are also shifting from snowfall towards rainfall. The decreased snowfall fraction will exert a great impact on the snow/glacier covered area and the snow/glacier melting. We should be careful that the climate change in the study area (increasing temperature, increasing precipitation, and substantially reducing snowfall will change the hydrologic regime (e.g., temporal and spatial distribution of floods and droughts) in the near future, as well as its greater variation in the far future.

By investigating the sensitivities in the hydrological processes, we have concluded that the meteorological input contributes to 64 % of the model uncertainty in the Kaidu River Basin by implementing a combined sensitivity analysis approach. This suggests that the highly spatial resolution meteorological data (e.g. satellite data) should be used for hydrologic modeling in this area.

A very practical method was proposed in the statistical downscaling of the RCM outputs when assessing the impact of climate change on the hydrological processes. Since the performance of the bias correction methods has been case sensitive, it is suggested to apply the proposed comparison procedure for other studies.

In the 21st century, the stream flow shows an overall increasing trend (-1% ~ 18% and 4 ~ 20% for RCP4.5 and RCP8.5) with the snow melting season pushing forward, which is quite beneficial to the irrigation farms in the lower reaches of the Kaidu River Basin. However, special caution should be exercised in the low flow during summer.

This study synthetically evaluated the impact of climate change on the hydrologic processes in the Kaidu River Basin. Although this method is not new, to our best knowledge, it is the first time that future climate in the mountainous regions of Central Asia has been analyzed with GCM simulation ensemble, the contribution of meteorological variables has been quantified in hydrological modeling, several bias correction methods has been compared in downscaling RCM outputs in this region. A good prediction of future hydrological processes will provide a basis for decision-makers.

Summary

Global climate change has created social, economic and ecological problems, which have been a great concern for scientists, the public and government in recent decades. The arid and semi-arid regions are sensitive to climate change. The arid region in Central Asia is one of the most important arid areas in the world, where water originates from the mountains. Climate change impact on hydrological processes in this region has become a scientific hot spot. In this study, we investigated future climate change in the mountainous regions of Central Asia (MCA), studied the hydrological processes in a typical watershed of the Kaidu River Basin, discussed and compared different bias correction methods in downscaling the outputs of climate models and finally, analyzed the future hydrological processes in the Kaidu River Basin.

1. We estimated and predicted future climate change in the MCA based on an ensemble of 21 General Circulation Models (GCMs) from the Coupled Model Intercomparison Project Phase 5 (CMIP5) by using the Bayesian Model Averaging (BMA) technique. The results showed: (1) BMA outperforms the simple ensemble analysis and the BMA mean matches all three observed climate variables (i.e. temperature, precipitation, snowfall); (2) At the end of 21st century, generally, mean annual temperature will rise considerably by 5.0 ℃, mean annual precipitation will increase by 5.9% from 186 mm to 197 mm, and mean annual snowfall will dramatically decrease by 26.4% from 72 mm to 53 mm under RCP8.5 compared to those in the control period (1976-2005); (3) Precipitation is increasing in the North Tianshan area, while it is decreasing in the Amu Darya region and snowfall shows a significant decrease in the western part of the Tianshan. The snowfall fraction (S/P) will also decrease from 0.58 to 0.43; (4) Snowfall shows a high sensitivity to temperature in autumn and spring of -25.9 ~ -1.5%/℃, while a low sensitivity during winter (about -8.6 ~ 3.8%/℃). In winter, the temperature has a positive impact on snowfall for 56% of grids. The climate change in the MCA is featured by an increasing temperature and precipitation but a decreasing snowfall, which poses a potential flood risk and which may cause a loss of solid water storage in the MCA and seasonal shifts in the runoff.

2. We analyzed the hydrological processes and quantified the contribution of the meteorological input to the model output by coupling the Morris method and the SDP method (State-Dependent Parameter method) and by applying a distributed

hydrologic model of SWAT (Soil and Water Assessment Tool). (1) The meteorological input contributes up to 64 % of model uncertainty due to the scarcity of the observed meteorological data, especially in the alpine region; (2) The groundwater flow is the most important hydrological process in this watershed; (3) The model calibration is robust with the Nash–Sutcliffe coefficients ("NS"s) and "R^2"s over 0.80 for both the calibration and the validation period (considering the length of the validation period is five times larger than the calibration period). The significance is obvious when compared to the simulation without considering the effect of spatial variation in the meteorological input (NS = 0.80 and NS = 0.47 for "with lapse rates" and "without lapse rates", respectively). An accurate meteorological input is of great importance to the distributed hydrological model, especially in the mountainous regions.

3. We have compared five precipitation and three temperature correction methods in downscaling RCM (Regional Climate Model) simulations applied to the Kaidu River Basin. The implemented precipitation correction methods include linear scaling (LS), local intensity scaling (LOCI), power transformation (PT), distribution mapping (DM) and quantile mapping (QM), while the temperature correction methods include LS, variance scaling (VARI) and DM. (1) Streamflows are sensitive to precipitation, temperature and solar radiation but not to relative humidity and wind speed; (2) The raw RCM simulations are heavily biased from the observed meteorological data and their use for simulations results in large biases from the observed streamflow and all bias correction methods improved these simulations effectively; (3) Concerning precipitation: the PT and QM methods performed equally best in correcting the frequency-based indices (e.g. standard deviation, percentile values), while the LOCI method gained better results in terms of the time-series-based indices (e.g. NS, R^2); (4) For temperature: all correction methods performed equally well in correcting the raw temperature; and (5) As to the simulated streamflow, the precipitation correction methods have a more significant influence than the temperature correction methods and the streamflow simulation performances are consistent with those of the corrected precipitation. The case study concerns an arid area in China (based on a specific RCM and hydrological model) but the methodology and some results can also be applied to other areas and models.

4. We assessed the impact of future climatic changes on hydrological processes in the Kaidu River Basin by using two sets of future climate data to force a well-calibrated hydrologic model. The future climatic data are bias-corrected RCM outputs for RCP4.5 and RCP8.5 and simple climate change (SCC) with an absolute

temperature change of -1 ~ 6 ℃ and a relative precipitation change of -20 ~ 60%. (1) The temperature is likely to increase by 2.2 and 4.6 ℃ by the end of the 21st century under RCP4.5 and RCP8.5 respectively, while precipitation will increase by 2 ~ 24%, with a considerable rise in the dry season and a small change in the wet season; (2) The flow will change by -1 ~ 20%, while the evapotranspiration will increase by 2 ~ 24%; (3) The flow increases almost linearly with precipitation, while its response to temperature depends on the temperature change magnitude and it decreases significantly for a temperature increase larger than 2 ℃; (4) Similar results have been obtained for simulations with RCM outputs and with SCC for mild climate change conditions, while the outcome was substantially different regarding intense climate change conditions.

This dissertation evaluated the climate change impact on the hydrological processes synthetically. The innovations are as follows. Firstly, the future climate was predicted using BMA technique to incorporate information of different GCMs. Secondly, for the first time the contribution of meteorological inputs in hydrological modeling was quantified. Thirdly, different bias correction methods were compared in the Kaidu River Basin and the evaluation procedure could be used in other watersheds and models. However, every dissertation has its limitations, and this work was no exception. Firstly, the glacier processes were not included in the hydrological modeling, which could introduce some biases in the future predictions. Secondly, there may be great uncertainty in the hydrological modeling due to the scarce data.

Samenvatting (Dutch Summary)

Sociale, economische en ecologische problemen ontstaan door globale klimaatverandering vormen een grote zorg voor wetenschappers, de overheid en de mensheid de laatste decennia.

De aride en semi-aride gebieden zijn gevoelig voor klimaatverandering. De aride regio in Centraal-Azië is één van de meest belangrijk droge gebieden ter wereld waar het water afkomstig is van de bergen. De watercyclus en de impact van de klimaatverandering op hydrologische processen in deze streek werden een wetenschappelijke hotspot.

In deze verhandeling onderzochten we de toekomstige klimaatverandering in bergzones van Centraal-Azië (MCA), bestudeerden we de hydrologische processen in een typisch stroombekken van het Kaidu Rivier Bassin, discussieerden we over en vergeleken we de verschillende afwijkende correctiemethodes ter verkleining van de output van de klimaatmodellen en uiteindelijk analyseerden we de toekomstige watercyclus in de Kaidu Rivier Bassin.

1. De geschatte en voorspelde toekomstige klimaatverandering in de MCA, gebaseerd op een een geheel van 21 Algemene Circulatie Modellen (GCM's) van de Coupled Model Intercomparison Project Phase 5 (CMIP5) door gebruik te maken van de Bayesian Model Averaging (BMA) techniek. De resultaten toonden aan dat : 1) BMA overtreft de eenvoudige analyse van het ensemble en het gemiddeld BMA komt overeen met al de 3 waargenomen klimaatvariabelen (d.w.z. temperatuur, neerslag, sneeuwval); 2) Over het algemeen zal op het einde van de 21ste eeuw de gemiddelde jaartemperatuur aanzienlijk stijgen met 5,0 ℃, de neerslag zal voor het hele gebied stijgen met 5,9 % van 186 mm naar 197 mm en de gemiddelde jaarlijkse sneeuwval zal dramatisch terugvallen met 26,4 %, van 72 mm tot 53mm onder RCP8.5 in vergelijking met deze in de referentieperiode (1976-2005); 3) De neerslag stijgt in de Noord-Tianshan (regio) terwijl het vermindert in de Amu Darya streek en de sneeuwval toont een belangrijke dalende trend in het westelijk deel van de Tianshan. De sneeuwvalfractie (S/P) daalt eveneens van 0.58 tot 0.43; 4) De sneeuwval toont een grote gevoeligheid ten overstaan van de temperatuur in de herfst en de lente van -25.9 ~ -1.5%/ ℃, terwijl een lage sensitiviteit in de winter (ongeveer -8.6 ~ 3.8%/ ℃). In de winter heeft de temperatuur een positieve invloed op de sneeuwval voor 56 % van de cellen. De klimaatverandering in de MCA is gekenmerkt door een stijgende temperatuur en neerslag maar ook door een teruggedrongen sneeuwval, wat een potentieel risico inhoudt voor overstroming en een verlies van solide wateropslag in de MCA en seizoensgebonden verschuivingen in de waterafvoer kan veroorzaken.

2. Door de Morris methode en de SDP methode (State-Dependent Parameter Method) te koppelen en een verspreid hydrologisch SWAT (Soil and Water Assessment Tool) model toe te passen, werden de hydrologische cycli geanalyseerd en het aandeel van de meteorologische inbreng in het output model gekwantificeerd. 1) De meteorologische inbreng draagt bij tot 64% van de modelonduidelijkheid door de schaarste aan waargenomen meteorologische gegevens, vooral in de alpiene regio; 2) De doorstroming van het grondwater is het meest belangrijke hydrologische proces in dit stroomgebied. 3) De modelcalibratie is krachtig/stabiel met de Nash-Sutcliffe coëfficiënten ("NS"s) en "R^2"s voor meer dan 0.80 voor zowel de kalibratie- als de validatieperiode (met de lengte van de validatieperiode vijf keer hoger dan voor de kalibratieperiode). Het belang hiervan is duidelijk wanneer we vergelijken met de simulatie zonder hierbij de invloed van de ruimtelijke variant in de meteorologische input te beschouwen (NS = 0.80 en NS = 0.47 respectievelijk voor met en zonder terugvalgraad verticale temperatuurgradiënt). Een accurate meteorologische inbreng is van groot belang voor het verspreid hydrologisch model, vooral in de bergstreken.

3. We vergeleken 5 neerslag correctiemethodes en 3 temperatuur correctiemethodes bij het verkleinen van de RCM simulaties (Regional Climate Model), toegepast op de Kaidu Rivierbassin. De toegepaste neerslagcorrectiemethodes omvatten zowel een lineaire schaling (LS), een plaatselijke intensiteitsschaling (LOCI), krachttransformatie (PT), distribution mapping (DM) en quantile mapping (QM), terwijl de temperatuur correctie-methodes LS, variance scaling (VARI) en DM inhouden. 1) Waterstromen zijn gevoelig aan neerslag, temperatuur en zonnestraling maar niet aan relatieve vochtigheid en windsnelheid; 2) Ruwe RCM-simulaties zijn erg vertekend door de waargenomen meteorologische gegevens en het gebruik hiervan voor stroomsimulaties resulteert in grote afwijkingen van de waargenomen stromingen en alle correctiemethodes verbeterden deze simulaties effectief. 3) Wat de neerslag betreft, de PT en QM methodes presteerden even goed in het verbeteren van de frequentie-gebaseerde indexen (vb. standaarddeviatie, percentielwaarden), terwijl de LOCI- methode het beter deed in termen van tijdsseries- gebaseerde indices (vb. NS, R^2); 4) Alle correctiemethodes waren even succesvol bij het verbeteren van de ruwe temperatuurgegevens; en 5) Wat de gesimuleerde stroming betreft: de neerslagcorrectiemethodes hebben een meer significante invloed dan de temperatuurcorrectiemethodes en de prestaties van de stroomsimulaties zijn consistent met deze van de gecorrigeerde neerslag. De case studie betreft een aride streek in China (gebaseerd op een specifiek RCM en hydrologisch model) maar de methodologie en enkele resultaten kunnen eveneens toegepast worden op andere gebieden en modellen.

4. We kunnen de impact van toekomstige klimaatveranderingen op de

hydrologische processen in het Kaidu Rivier Bassin evalueren door twee sets van toekomstige klimatologische gegevens te gebruiken om een goed gekalibreerd hydrologisch model te forceren. De klimaatgegevens in de toekomst zullen gecorrigeerde RCM outputs zijn voor RCP4.5 en RCP8.5 en een eenvoudige klimaatverandering (SCC)met een absolute temperatuurverandering van -1 ~ 6 ℃ en een relatieve neerslag-verandering van -20% ~ 60%. 1) De temperatuur heeft de neiging om te stijgen met 2.2 ℃ en 4.6 ℃ tegen het eind van de 21ste eeuw onder RCP4.5 en RCP8.5 respectievelijk, terwijl de neerslag zal toenemen met 2% ~ 24% met een belangrijke stijging in het droge seizoen en een kleine wijziging in het natte seizoen; 2) De doorstroming zal veranderen met -1% ~ 20%, terwijl de evapotranspiratie zal vermeerderen met 2% ~ 24%; 3) De waterstroom stijgt bijna lineair met de neerslag terwijl de reactie ervan op de temperatuur afhangt van de omvang van de temperatuurwijziging en de stroming duidelijk afneemt voor een temperatuurtoename van meer dan 2 ℃; 4) Gelijkaardige resultaten werden verkregen voor simulaties met RCM-outputs en met SCC voor milde klimaatwijzigingsvoorwaarden, terwijl de resultaten erg verschillend waren voor intense klimaatveranderingsvoorwaarden.

Huidig proefschrift evalueert de impact van klimaatsverandering op de hydrologisch processen. De vernieuwingen zijn de volgende. Eerst en vooral, werd het toekomstige klimaat voorspeld gebruik makend van de BMA techniek om alzo informatie uit verschillende GCMs te gebruiken. Ten tweede, werden voor de eerste maal de bijdrage van meteorologische input in hydrologische modellen gekwantificeerd. Ten derde werden verschillende foutcorrectiemethodes vergeleken in de Kaidu River Basin en deze evaluatieprocedure kan ook toegepast worden bij andere waterbekkens en modellen.

Hoe dan ook, elk proefschrift houdt haar beperkingen in, ook huidig. Ten eerste werden gletsjerprocessen niet mede beschouwd bij de hydrologische modelering, wat bepaalde fouten kan genereren in de voorspellingen. Ten tweede is er mogelijks een grote onzekerheid in de hydrologische modelering te wijten aan de schaarse data.

摘要 (Chinese summary)

近年来，由气候变化引起的全球社会、经济和生态环境等问题已经受到科学界、社会公众和各国政府的广泛关注。亚洲中部干旱区是世界重要干旱区之一，山区是水源的主要形成区，水资源系统脆弱，对气候变化响应极其敏感。其水资源的形成特征、对气候变化的响应以及未来趋势预测等成为水资源研究领域的热点问题。基于此，本研究开展中亚山区的未来气候变化预测分析，并以开都河流域为典型研究区，分析了其水文过程演变特征，重点对比了不同的气候校正方法在气候模式降解中的应用效果，从而更好的预测开都河流域未来水文过程变化特征，探讨其不确定性。

1、利用贝叶斯模型平均（Bayesian model averaging method, BMA）技术，对耦合模式比较计划第五阶段（Coupled Model Intercomparison Project Phase 5, CMIP5）21 个大气环流模式（General Circulation Model, GCM）未来中亚山区 21 世纪的气候变化预测结果进行了分析。结果表明：1）BMA 优于简单的 GCM 结果集合，BMA 得到的三个气候变量（即温度，降水，降雪）与观测值一致；2）到 21 世纪末（2070-2099），在 RCP8.5 下，气温将升高 5.0 ℃，降水从 1976-2005 年的 186 mm 增加到 197 mm，增加量为 5.9%，而降雪将下降 26.4%，从 72 mm 下降到 53 mm；3）降水在北天山增加，而在阿姆河地区减少；降雪在天山西部地区显著减少。同时，平均降雪占降水的比例（S/P）从当前控制期（1976-2005）的 0.58 下降到 21 世纪末（2070-2099）的 0.43（RCP8.5）；4）降雪对温度的敏感性在春秋季节较高，而在冬季较低，在高山边缘区降雪对温度最为敏感。气候变化整体上表现为温度升高，降水增加和降雪量减少，这将导致潜在的洪水风险，以及固体水资源的流失和径流的季节变化。

2、通过结合 Morris 和 SDP（State-Dependent Parameter method）敏感性分析方法，应用 SWAT（Soil and Water Assessment Tool）分布式水文模型分析开都河流域水文过程，并量化气象输入对水文模拟的贡

献。结果如下：1）由于在高寒山区观测气象数据稀少，气象输入占了模型不确定性的比例很大(64%)；2）地下水过程是该流域最重要的水文过程；3）构建的流域水文模型达到很好的模拟效果，在率定期和验证期日径流的 Nash–Sutcliffe 效率系数（NS）和 R^2 都达到 0.80 以上。4）当不考虑气象要素随高程变化时，率定的水文模型效率系数只有 NS = 0.47（考虑气象要素随高程变化时 NS = 0.80），表明气象要素空间变化对分布式水文模型非常重要，尤其是在山区气象资料稀少地区。

3、比较分析了 5 种降水校正方法和 3 种温度校正方法在区域气候模式（Regional Climate Model, RCM）降尺度中的应用效果。降水校正方法包括线性缩放(Linear Scaling, LS)，局部比例缩放(Local Intensity Scaling, LOCI)、幂转换(Power Transformation, PT)、利用 Gamma 分布的概率分布形式转化(Distribution Mapping, DM)和分位数校正(Quantile Mapping, QM)，温度校正方法的包括 LS、方差比例变换(VARIance scaling, VARI)和利用 Gaussian 分布的概率分布形式转化(DM)。结果表明：1）相对于观测气候，原始的 RCM 模拟存在严重偏差，从而导致了用原始 RCM 驱动的水文模拟也存在严重偏差；2）所有的偏差校正方法均可有效提高模拟效果；3）对于降水，基于频率的指标（如，标准偏差，百分位数值），PT 和 QM 方法表现最好，而基于时间序列的指标（如 NS，R^2），LOCI 方法表现最好；4）对于温度，所有的校正方法校正效果均较好，各校正方法差别不大；5）对于模拟径流，降水校正方法比温度校正方法对径流模拟的影响更为显著。虽然这种降尺度方法是基于特定的 RCM 和水文模型，应用于干旱区的特定流域，但是这种分析方法和一些结论可以应用到其他地区和模型。

4、采用两套气象数据驱动率定好的水文模型，评估了开都河流域 21 世纪水文过程对气候变化的响应。两套数据分别是 RCM 预测的未来气候数据和简单气候变化（Simple Climate Change, SCC），即相对于 1986-2005 年，温度绝对变化量设置为-1～6 ℃，降水相对变化设置为-20％～60％。结果表明：1）相对于 1986-2005 年，在 RCP4.5 和 RCP8.5 下，21 世纪末开都河流域温度将升高 2.2 ℃ 和 4.6 ℃，降水将增加 2％

～24％（干季显著上升和雨季降水变化很小）；2）相对于 1986-2005 年模拟的多年平均径流量（36.1 $m^3 \times 10^8$），径流变化-1％～20％。蒸散发量将增加 2％～24％；3）径流几乎随降水增加呈线性增加，而径流对温度的响应则依赖于温度变化幅度，当温度增加大于 2℃，径流显著降低；4）在温和的气候变化条件下，RCM 的模拟结果与简单气候变化情景类似，而在剧烈的气候变化条件下，二者的模拟结果差别较大。

本论文综合评估了开都河流域气候变化对水文过程的影响，利用 BMA 方法整合多个 GCM 信息预测了未来中亚山区气候变化，在水文过程分析方面，第一次定量评估气象输入对水文模拟的贡献，并提出了在资料稀缺的山区，偏差校正方法的应用流程，第一次比较了不同降水和气温校正方法在中亚山区的应用。本论文的不足可归结为 1）没有考虑冰川融水过程，这可能导致气候变化评估中的偏差；2）开都河流域地形复杂，气象和水文站点稀少，水文模拟存在很大的不确定性。

Curriculum Vitae (Bibliography)

Gonghuan Fang was born in Taian (China) on the 20th of February, 1989. In 2011, she graduated in Resources, Environmental and Urban/Rural Planning at the Shandong Normal University and started her academic education at the Xinjiang Institute of Ecology and Geography, University of Chinese Academy of Sciences. In 2013, she was recommended to transfer from a master student to a PhD student in University of Chinese Academy of Sciences and started to pursue her doctorate at Ghent University.

From September 2011 until June 2016, Gonghuan has worked at the Xinjiang institute of Ecology and Geography on two major projects. One is the National Basic Research Program of China "Impact of climate change on hydrologic cycle and security research on water resources in the arid regions of Northwest China" (2011-2014). And the other is the National Thousand Youth Talents Plan "Impact of climate change on water resources in the Tarim River Basin" (2013~2016).

Gonghuan has already contributed to several international conferences and she is also the author of a number of papers, which were published in leading international journals in the field of physical geography.

This dissertation presents a work on evaluating the impact of climate variability on hydrological processes in the Kaidu River Basin. A serie of techniques is applied including BMA for incorporating competing model predictions, sensitivity analysis approach for analyzing hydrological processes, bias correction methods for downscaling the climate model predictions, etc. The future hydrological processes are calculated and analyzed. The conclusions could serve water resources management and flood analysis, and can be used in other regions and models.